2007

Development of rational design methodology for spiral reinforcement in prestressed concrete piles in regions of high seismicity

Ann-Marie Fouad Fanous
Iowa State University

Development of rational design methodology for spiral reinforcement in prestressed concrete piles in regions of high seismicity

by

Ann-Marie Fouad Fanous

A thesis submitted to the graduate faculty

in partial fulfillment of the requirements for the degree of

MASTER OF SCIENCE

Major: Civil Engineering (Structural Engineering)

Program of Study Committee:
Sri Sritharan, Co-major Professor
Muhannad Suleiman, Co-major Professor
Lester Schmerr

Iowa State University

Ames, Iowa

2007

UMI Number: 1447471

ProQuest Information and Learning Company
300 North Zeeb Road
P.O. Box 1346
Ann Arbor, MI 48106-1346

TABLE OF CONTENTS

LIST OF FIGURES

LIST OF TABLES

CHAPTER 1. INTRODUCTION

1.1 Historical Background

Pile foundations date back to 12,000 years ago when Neolithic inhabitants of Switzerland drove wooden poles into the soft bottom of lakes in order to build their homes on them (Prakash and Sharma, 1990). Timber piles supported Venice in the marshy delta and protected early Italians from the invaders of Eastern Europe, while allowing them to be close to their source of livelihood. Simply put, pile foundations make it possible to construct structures in areas where the soil conditions are less than favorable for the design of shallow foundations (Prakash and Sharma, 1990).

1.2 Pile Types

Piles, in general, are divided into two categories: displacement or non-displacement piles, depending on the amount of soil displaced during installation. Non-displacement piles refer to the small effect in the state of stress in the pile's surrounding soil during the placement of the pile, whereas displacement piles refer to the lateral movement of the soil surrounding the pile during the installation of the pile (Das, 2004). Examples of displacement piles include driven concrete and closed-ended steel pipe piles, while H-shaped steel piles are commonly classified as non-displacement piles.

Several different materials have been used in pile design practice. These are timber piles, steel piles, and concrete piles. Until the late nineteenth and early twentieth centuries, timber piles were the only pile types used for deep foundations. This was due to their vertical load carrying capacity combined with lightness, as well as their durability and ease

of cutting and handling. Steel and concrete piles replaced timber piles for the mere fact that these materials could be fabricated into units that were capable of sustaining compressive, bending, and tensile stresses far beyond the timber piles. Steel piles typically serve as non-displacement piles and have been used for pile foundations due to the ease of fabrication and handling, their ability to endure hard driving, and their low strength to weight ratio.

The benefits of concrete piles include their ability to sustain high load-carrying capacity on land and offshore, as well as their durability within most soil and immersion conditions. The concrete piles could also be cast in numerous structural forms (Tomlinson, 1994). Concrete is readily available at a low cost, and it is more suitable in a corrosive environment. Concrete pile foundations may be classified into three major categories: cast-in-place concrete piles, composite concrete piles, and precast concrete piles. With cast-in-place displacement piles, the concrete is placed in a hole formed in the ground by boring, jetting, or coring a hole, or by driving a shell or casing into the ground. A rebar cage is lowered into the hole, shell, or casing and then filled with concrete. Some of the major advantages of cast-in-place concrete piles are that

- they can support extremely large loads;
- they are designed for ultimate loads because they are not subjected to driving and lifting stresses; and
- the predetermination of the pile's length is not critical.

Composite concrete piles can be composed of either concrete-steel sections or concrete filled steel pipes. In the case of concrete-steel sections, a standard steel member is

encased in concrete to protect the steel member in regions most vulnerable to deterioration. The significant advantages of the concrete-steel composite piles are that

- they can be provided at considerable lengths at a relatively low cost; and
- they are well suited for marine structures in which the upper section of the pile is subjected to a corrosive environment.

Some of the advantages of the concrete filled steel pipes are

- they are easy to control during installation;
- they can be treated as non-displacement piles during an open-end installation;
- open-end pipe is best against obstruction;
- they have high load capacities (i.e., 200 tons); and
- they are easy to splice (Bowles, 1996).

1.3 Precast Concrete Piles

Precast concrete piles are the third category of concrete piles. They are cast, cured and stored before they are installed. The most common method of installation for precast piles is driving and therefore the piles must be designed to endure service loads as well as handling and driving forces. Precast piles are further subdivided into two main categories: reinforced precast concrete piles and precast, prestressed concrete piles (Prakash and Sharma, 1990).

The reinforced precast concrete piles consist of an internal reinforcing cage of longitudinal bars and spiral or hoop reinforcement. These piles are used primarily for moderately deep foundations in an aquatic or marine environment. Some of the advantages of reinforced precast piles are

- they can be prefabricated under controlled conditions to maintain good quality construction;
- they can be used for land structures in areas where hard driving is necessary; and
- good corrosion resistance can be attained because the cured concrete provides a high quality moisture barrier.

In precast, prestressed concrete piles, prestressed tendons replace the typical longitudinal reinforcement with spiral reinforcement encasing the tendons. In addition to the advantages listed above for precast concrete piles, the precast, prestressed piles offer the following benefits:

- there is less potential for cracking during driving;
- there is further reduction to corrosion due to reduced crack width resulting from pre-compression; and
- they can usually be made lighter, longer, and more durable due to the concrete being placed under continuous compression through prestressing.

1.4 Seismic Design Approach

Precast, prestressed pile foundations are used to support bridges, buildings, and wharf structures. In the United States, high seismic regions such as California, Washington, South Carolina, and Alaska adopt certain standards for the design of foundations so that satisfactory performance of structures can be achieved when they are subjected to earthquake motions. As described by Paulay and Priestley (1992) and Priestley et al. (1996), the seismic design philosophy adopted in these regions generally follows the capacity design principles. These principles, as stated by Priestley et al. (1996), include:

- under design-level earthquakes, the structure is allowed to respond inelastically through flexural yielding;
- locations of plastic hinges are pre-selected and detailed carefully to ensure that the structure can develop a ductile response; and
- suitable strength margins are provided to ensure that undesirable mechanisms of inelastic responses cannot occur.

Thus, the seismic design philosophy promotes the notion that the foundation elements, including piles, should be inhibited from experiencing inelastic actions by forcing the plastic hinging to occur in the structure at or above the ground surface. An exception is made when bridge columns are extended into the ground as drilled shafts, in which case in-ground plastic hinges are allowed to form in the foundation shafts under seismic loading. However, preventing inelastic actions to piles that support footings is not always practicable since the moment gradient in the pile is influenced by local variations in soil stiffness along the pile length (Priestley et al. 1996). The extent of inelastic action that can potentially occur in piles during an actual earthquake is not well understood because earthquake reconnaissance efforts typically do not investigate this issue unless evidence for pile failure is seen at a particular site. Precast, prestressed piles have been widely used in the design of foundations for bridges, buildings, and wharf structures in high seismic regions. The subsequent sections provide more specific details of the seismic design approach for the aforementioned structures.

1.4.1 Bridges

In the United States, the Seismic Design Criteria (SDC, 2006) published by the California Department of Transportation (Caltrans, 2006)), the South Carolina Department of Transportation Seismic Design Specifications (SCDOT, 2001), and the Washington seismic design criteria (AASHTO, 2004) include special provisions for seismic design. Outside of the US, three specifications that are considered in seismic design provisions are the: 1) Specifications for Highway Bridges published by the Japan Road Association (JRA, 1996), 2) New Zealand Concrete Structure Standards (NZS, 2006), and 3) Canadian Highway Bridge Design Code (CAN/CSA, 1998).

The seismic design of bridges is typically specified for the design of ordinary bridges, as defined in Appendix A. Consistent with the capacity design philosophy, the foundation of bridges are required to be designed to resist the overstrength column capacity M_o and the corresponding overstrength shear V_o. The overstrength moment, M_o, applies a 20% overstrength magnifier to the plastic moment capacity of the pile to account for the material strength variations between the pile and the adjacent members as well as the pile moment capacities that may be greater than the idealized plastic moment capacity. The overstrength shear is then found based on the overstrength flexural moment. The type of soil surrounding the pile will greatly affect the design of the pile foundation. Foundations in competent soil can be analyzed and designed using a simple model that is based on assumptions consistent with observed response of similar foundations during past earthquakes. Caltrans (2006) provides indicators that a soil is capable of producing competent foundation performance which include the following:

- Standard penetration, upper layer (0-10 ft [0-3 m]) $N = 20$ (Granular soils)

- Standard penetration, lower layer (10-30 ft [3-9 m]) $N = 30$ (Granular soils)
- Undrained shear strength, $s_u > 1500$ psf (72 KPa) (Cohesive soils)
- Shear wave velocity, $v_s > 600$ ft/s (180 m/s)
- Low potential for liquefaction, lateral spreading, or scour

where N = The uncorrected blow count from the Standard Test Method for Penetration Test and Split- Barrel Sampling of Soil

Pile foundations located in marginal soils may contain considerable lateral displacements because the pile caps within the marginal soils may not govern the lateral stiffness of the foundation. Marginal defines the range on soil that cannot readily be classified as either competent or poor, where poor soil is traditionally characterized as having a standard penetration, N<10. The course of action for bridges in marginal soil will be determined on a project-by-project basis. If a soil is classified as marginal, the bridge engineer and foundation designer shall jointly select the appropriate foundation type, determine the impact of the soil structure interaction, and determine the analytical sophistication required to reasonably capture the dynamic response of the foundation as well as the overall dynamic response of the bridge. Although the type of soil surrounding the pile will greatly affect the design of the pile foundation, it is consistently noted that no information on the expected level of lateral displacement of the pile foundation was provided in any of the seismic design criterion considered.

Given the nature of the project, several seismic design criteria were investigated to determine the given requirements for the minimum transverse reinforcement or minimum ductility capacity. Chapter 2 reports several design equations used in the design of precast, prestressed piles and displays the vast discrepancy between the equations being used.

Thorough research of the seismic design criteria in regions with high seismic activity indicated that no specific requirements for the minimum transverse reinforcement or minimum ductility capacity of the piles were provided (i.e., SDC, 2006; SCDOT, 2001; JRA, 1996; and CAN/CSA, 1998). In Washington, however, detailing requirements for the spiral reinforcement in the plastic hinge region for precast, prestressed piles are as follows:

For piles not greater than 24.0 inches in diameter:

- spiral wire should be W3.9 or greater;
- spiral reinforcement at the ends of piles having a pitch of 3.0 inches for approximately 16 turns;
- the top 6.0 inches of pile having five turns of additional spiral winding at 1.0 inch pitch; and
- for the remainder of the pile, the strands should be enclosed with spiral reinforcement with not more than 6.0 inch pitch.

For piles greater than 24.0 inches in diameter:

- spiral wire should be W4.0 or greater;
- spiral reinforcement at the ends of piles having a pitch of 2.0 inches for approximately 16 turns;
- the top 6.0 inches of pile having five turns of additional spiral winding at 1.5 inch pitch; and
- for the remainder of the pile, the strands enclosed with spiral reinforcement with not more than 4.0 inch pitch.

1.4.2 Buildings

In the United States, the ACI 318 Building Code (ACI, 2005) and the ASCE Minimum Design Loads for Buildings and Other Structures (ASCE 7, 2005) include special provisions for seismic design for buildings. Outside of the US, three high seismic regions are considered for the seismic design specifications of buildings: 1) The National Building Code of Canada (2005); 2) The Building Standard Law in Japan (2004); and 3) New Zealand Concrete Structure Standards (NZS, 2006).

The seismic design of buildings is typically specified for buildings in high risk levels. A risk level is defined as the seismic performance or the design category of a building. Specifications regarding such risk levels are provided in Appendix C. From the investigated codes, it is evident that the design for inelastic actions within the pile is not accounted for. In relation to this project, particular requirements of the transverse reinforcement within a pile foundation of a building structure are provided by the ACI 318 Building Code (ACI, 2005), the ASCE Minimum Design Loads for Buildings and Other Structures, (ASCE, 2005), and the New Zealand Concrete Structure Standards (NZS, 2006).

According to the Notes on ACI 318-05 Building Code Requirements for Structural Concrete (PCA, 2005), when a pile is expected to experience tension forces from an earthquake, a suitable load path is required to transfer these tension forces from the longitudinal reinforcement of the column through the pile cap, to the reinforcement of the pile foundation. With this knowledge, the code calls for continuous reinforcement, fully detailed, over the length resisting the tensile forces. Thus, the requirement of the transverse reinforcement within a pile foundation of a building structure indicates that the:

1. transverse reinforcement is essential at the top of the pile for at least five times the member's cross-sectional dimension, but not less than six feet below the bottom of the pile cap; and
2. for precast concrete driven piles, the length of the transverse reinforcement shall be sufficient to account for potential variations in the elevation in pile tips.

In the ASCE 7 (2005) design criteria are placed on the plastic hinge regions for precast, prestressed piles in high seismic regions. These criteria are as follows:

1. Length of ductile region: where the total pile length in the soil is 35 ft or less, the ductile pile region shall be taken as the entire length of the pile. Where the pile length exceeds 35 ft, the ductile pile region shall be taken as the greater of 35 ft or the distance from the underside of the pile cap to the point of zero curvature plus three times the least pile dimension.
2. Spiral spacing: in the ductile pile region, the center to center spacing of the spirals or hoop reinforcement shall not exceed one-fifth of the least pile dimension, six times the diameter of the longitudinal strand, or 8 in, whichever is smaller.
3. Splicing: spiral reinforcement shall be spliced by lapping one full turn, by welding, or by the use of a mechanical connector. Where spiral reinforcement is lap spliced, the ends of the spiral shall terminate in a seismic hook in accordance with ACI 318, except that the bend shall not be less than 135°.
4. Volumetric ratio of transverse reinforcement:
    a. where the transverse reinforcement consists of spirals or circular hoops, the required amount of the volumetric ratio of spiral transverse

reinforcement in the ductile pile region is permitted to be obtained by providing an inner and an outer spiral.

b. Where transverse reinforcement consists of rectangular hoops and cross ties, the total cross-sectional area of lateral transverse reinforcement in the ductile region, the hoops and cross ties shall be equivalent to deformed bars not less than a number three in size. Rectangular hoop ends shall terminate at a corner with seismic hooks.

c. Outside of the ductile pile region, the spiral or hoop reinforcement with a volumetric ratio not less than one-half of that required for transverse confinement reinforcement shall be provided.

Both the ACI code (2005) and the ASCE 7 (2005) provide equations for the amount of transverse reinforcement required in the ductile regions of the pile. Chapter 2 reports these design equations, along with several other design equations used in the design of precast, prestressed piles.

1.4.3 Wharfs

Wharf structures serve as an accommodation to the import and export industry, and represent a large economic investment. However, when subjected to earthquake damage, the associated economic loss will be very significant. Figure 1.1 portrays a normal section through a typical wharf structure and displays the three main components of it.

1. A rock dike consisting of a quarry run rock placed along the water's edge, which serves to retain the backlands earth fill and also as an anchor to the wharf piles.

Riprap protection and concrete ratproofing is placed on the surface of the quarry run material;

2. A concrete deck that extends the berthing face into the deeper water; and
3. Vertical precast, prestressed concrete piles, which are designed to support the deck loads and resist lateral seismic forces (Birdy and Dodd, 1999).

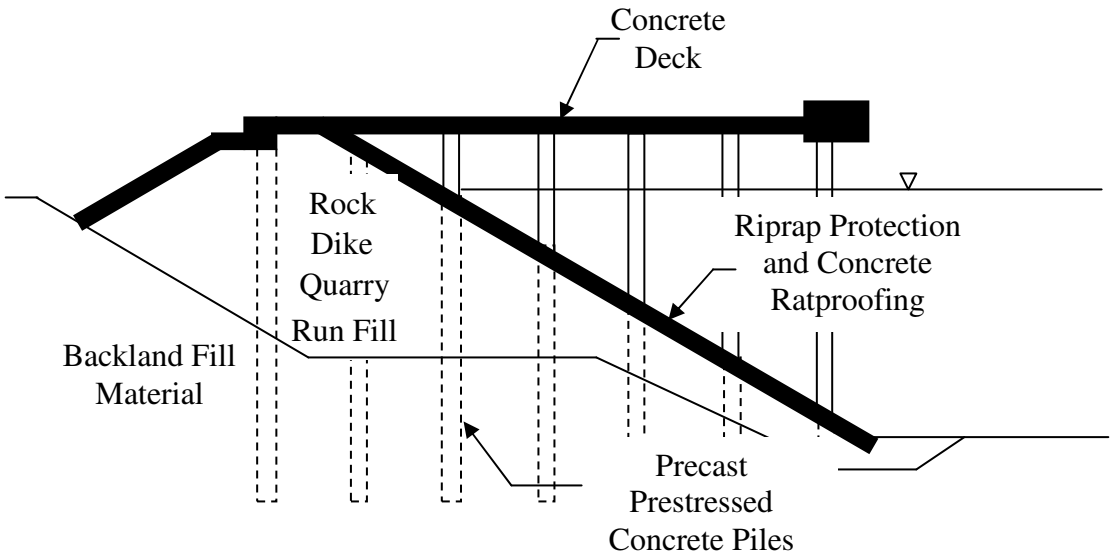

Figure 1.1. Typical section through a wharf structure (Birdy and Dodd, 1999)

The pile foundations are driven into the ground-composed of quarry run material, riprap protection, and backland fill material. The piles are driven directly through the riprap material in order to avoid tilting of the pile foundations. In the process of driving the precast, prestressed piles, high compressive stresses generally develop at the pile head and the pile end, and thus these regions require spiral confinement with a very tight pitch. The precast, prestressed pile foundations supporting the wharf structures ought to be designed as a ductile frame with plastic hinges forming in the piles under seismic actions. Adequate performance of the pile foundations of a wharf structure depend greatly on careful detailing of the pile-to-

superstructure connection as well as the P-delta effects, confinement reinforcement, and axial load ratios. At the pile head, the prestressing strands may extend into the superstructure in order to further provide continuity. Sufficient development length must be supplied in order to avoid the strands pulling out of the superstructure before the flexural capacity of the pile head is reached, (Birdy and Dodd, 1999), although this length was not specified.

This spiral reinforcement will also contribute to considerable shear resistance. The details of the design of precast, prestressed pile foundation for a wharf structure are comparable to the AASHTO LRFD Bridge Design Specifications (see section 1.4.1.3) (Birdy and Dodd, 1999). Specific codes have been established by the Port of Los Angeles (POLA, 2004) and the Marine Oil Terminal Engineering and Maintenance Standards (MOTEMS, 2005) of California for the design of wharf structures. These codes, however, do not specify requirements for the minimum amount of transverse reinforcement or minimum ductility capacity of the piles.

1.5 Scope of Research

Section 1.4 reviews the published seismic design criteria as well as current codes and standards and reveals that none of the investigated criterion accounts for the inelastic behavior of the pile foundation during a seismic event. For example, during a seismic event, the pile foundation may experience moments that will induce cracks along the length of the pile. These cracks will result in a reduction in the moment of inertia of the pile cross section. In the current study, a methodology is developed that accounts for the variation of the moment of inertia of the pile as the deformation of the pile takes place. The main objective of this project is to develop design equations to determine the minimum

transverse reinforcement necessary to achieve target ductility over a given range of axial loads in prestressed concrete piles used in high seismic regions. The research will establish the minimum target ductility in a manner consistent with the ductility requirements of current codes.

The current seismic design philosophy emphasizes that inelastic action in the foundation elements including piles should be inhibited by forcing plastic hinging to occur at the column base. However, preventing all inelastic action in piles is not always practicable since the moment gradient in the pile is influenced by variations in soil stiffness along the pile length. The extent of inelastic action that occurs in piles during an actual earthquake is not well understood. Given this uncertainty, the project will focus on the following:

1. determine an appropriate curvature demand through a literature review;
2. establish an equation that will supply the minimum amount of transverse reinforcement for a prestressed concrete pile, while providing the necessary curvature capacity beyond that established as the potential maximum curvature demand;
3. embed a curvature ductility factor within the developed equation in order to aid designers in providing an economically appropriate amount of transverse reinforcement;
4. using the developed equation, determine permissible lateral displacements that the prestressed piles will be able to withstand in different soil conditions; and
5. formulate recommendations suitable for the design of confinement reinforcement for precast prestressed piles in seismic regions.

1.6 Report Layout

The remainder of this report includes a thorough description of the procedures of this project. The chapters to follow include a detailed literature review including discussion on the expected curvature demand, a complete description of the development of the proposed equation and the analysis done with the equation on specific piles, an extensive account of the previously analyzed piles evaluated in certain soil conditions, and the conclusions and recommendations upon the completion of the project.

CHAPTER 2. LITERATURE REVIEW

2.1 Introduction

Precast, prestressed piles have been widely used in the design of foundations in structures built on different environmental conditions including those built on poor soil conditions and heavy marine environments. These structures, as well as the precast, prestressed piles, are subjected to variety of loads including lateral loads induced by wind, waves, and earthquakes. Given the focus of this report, this chapter is dedicated to current seismic design practice adopted for precast, prestressed concrete piles, the reported curvature demands and curvature capacities for these piles designed for seismic regions, and discussion on the design of transverse reinforcement for precast, prestressed piles.

2.2 Current Seismic Design Practice

A variety of prestressed precast concrete piles are standardized by the precast industry. The cross sections of these piles may be square and solid, square and hollow, octagonal and solid, octagonal and hollow, circular and solid or circular and hollow; some examples are illustrated in Figure 2.1.

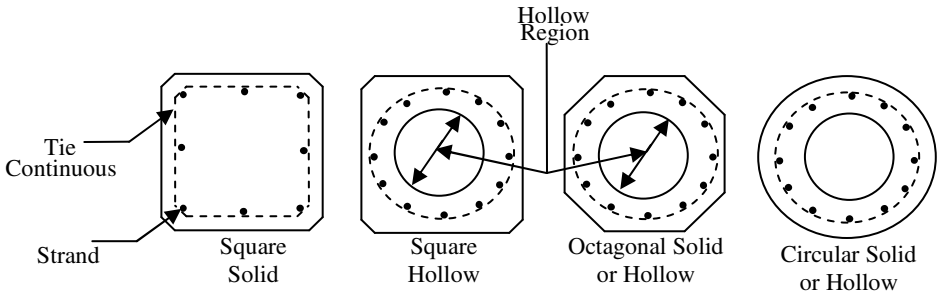

Figure 2.1. Cross sections of prestressed concrete piles (PCI, 1999)

Of the different cross sections, the precast, prestressed piles with solid square cross sections and solid octagonal cross sections are the most commonly used types in design practice in seismic regions (Arulmoli, 2006). This is due to the fact that the square piles types are easier to cast, while the octagonal piles minimize the impact of spalling on the moment-curvature response of these piles. Given the typical length requirements, it is convenient to cast the precast, prestressed piles in a horizontal position rather than in a vertical position. With the piles being cast horizontally, the square piles, in particular, provide an ease to the casting process. The most common sizes utilized in current seismic design practice are 12-inch, 14-inch, and 16-inch square piles, and 16-inch and 24-inch octagonal piles. Figures 2.2, 2.3, and 2.4 provide typical details of the standard piles used for bridge foundations in seismic regions by the California Department of Transportation (Caltrans).

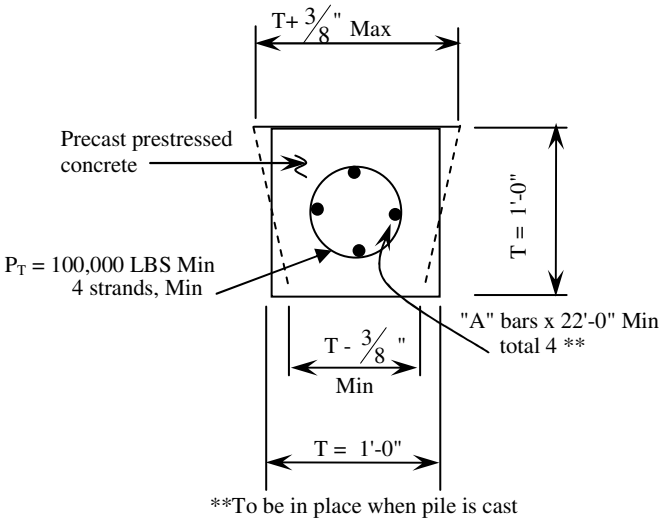

Figure 2.2. Detail of a 12-inch precast, prestressed concrete square cross-section used by Caltrans (2006)

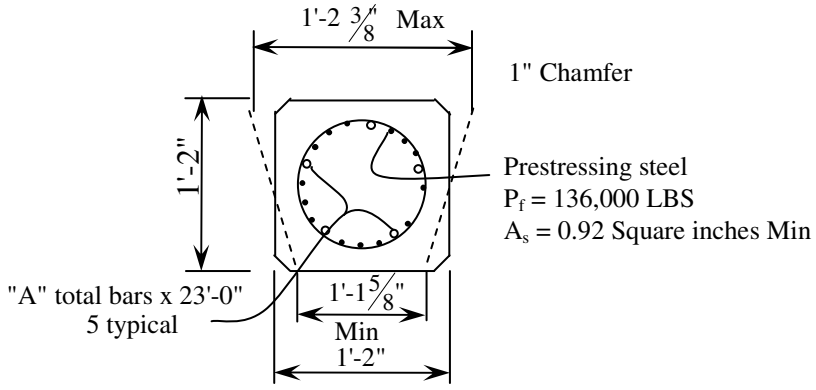

Figure 2.3. Detail of a 14-inch precast, prestressed concrete square cross-section used by Caltrans (2006)

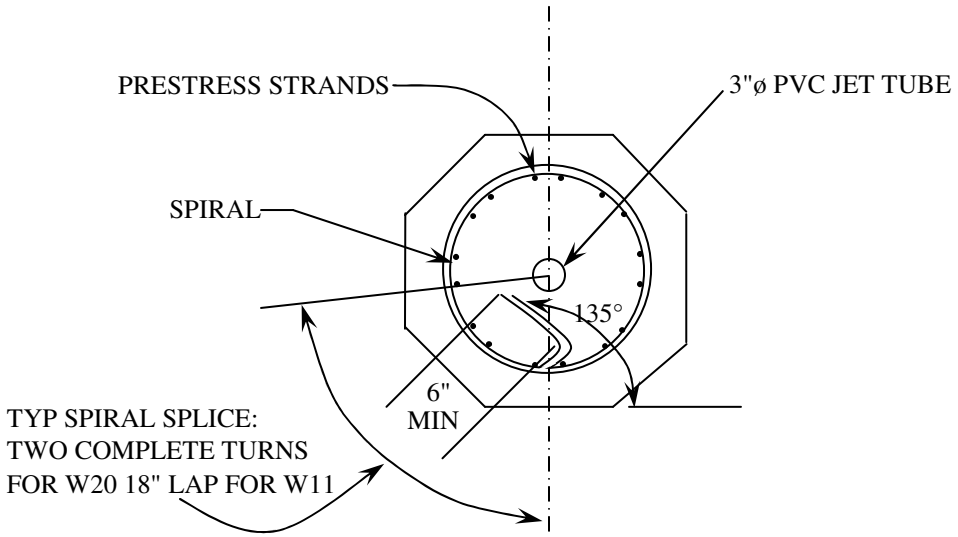

Figure 2.4. Detail of a 24- precast, prestressed concrete square cross-section used by POLA (2003)

In the design of precast, prestressed concrete piles, several reinforcement types may be utilized and specified in terms of reinforcement ratios. Such ratios include: the longitudinal mild steel reinforcement ratio (ρ_l), longitudinal prestressed reinforcement ratio (ρ_p), and volumetric ratio of the confinement reinforcement (ρ_s). The ratio of the mild steel reinforcement and the ratio of the prestressed steel are defined as the total area of longitudinal reinforcement with respect to the total area of the cross section of the pile. The

volumetric ratio of the confinement reinforcement is specified by several different codes and is more thoroughly discussed in Section 2.4. These code-specified ratios are largely empirical in nature and are not based on satisfying a specific curvature demand, thus leading to significant differences in the reinforcement requirements. Therefore, the following section is dedicated to establishing a possible curvature demand for piles based on previous studies including field investigations, site surveys, and analytical studies.

2.3 Curvature Demand

Despite the advancements in seismic design over the past decades, strict limitations have been placed on the use of precast, prestressed concrete piles in high seismic regions (Banerjee et al., 1987). For example, ATC 3-06 (1978) states that "*precast concrete piles shall not be used to resist flexure caused by earthquake motions unless it can be shown that they will be stressed to below the elastic limit under the maximum soil deformations that would occur during an earthquake*." This implies that the piles should not be subjected to any inelastic actions. In contrary, ACI 318 (2005) specifies requirements on the transverse reinforcement in the confinement region of precast concrete piles. These requirements are stated in Chapter 1 of this report.

These requirements were set primarily due to a lack of understanding of the curvature demands that the precast, prestressed piles would be subjected to during moderate to large earthquakes (Banerjee et al., 1987). Investigating this lack of understanding is of paramount importance in this study because it will establish the expected curvature demand for the precast, prestressed piles used in seismic regions so that the appropriate confinement reinforcement can be satisfactorily quantified for the plastic regions of these piles.

Two critical curvatures of a pile are the maximum curvature demand and curvature capacity. The first term refers to the maximum curvature that the pile section may experience when the foundation is subjected to an earthquake input motion. This curvature value establishes the maximum curvature that the pile may ever experience during its lifetime. The curvature capacity, on the other hand, establishes the potential curvature that a pile section can sustain without compromising its ability to sustain the combined axial and flexural actions.

Under ideal circumstances, upon the occurrence of an earthquake, whether a small, medium, or large event, the curvature that a pile undergoes along its length should be recorded. Such field data is of significant importance as the curvature that the pile must be able to resist in a major earthquake is not well understood. In the absence of such critical information on the maximum possible curvature demand for piles in seismic regions, the determination of confinement reinforcement for the plastic hinge region in concrete piles becomes very challenging. Therefore, through an extensive investigation of literature on reported curvature demands and curvature capacity of piles used in seismic regions, a tentative upper limit for the curvature demand is established in this chapter after providing an overview of curvature ductility and how it relates to the curvature demand and curvature capacity of a pile.

Although the curvature demands established from subjecting piles to earthquake loading or investigation of piles subjected to major earthquakes would be more useful, it is noted that such data is seldom found in the literature. Consequently, the capacity of piles found in the literature is useful for establishing the maximum possible curvature demand in

recognition that widespread damage to piles and the corresponding curvature has not been reported following major seismic events around the world.

2.3.1 Overview of Curvature Ductility

The curvature demands on piles depend on the axial load, moment demand, material properties, pile fixity as well as the strength and stiffness of the soil surrounding the top portion of the pile (Priestley et al. 1996 and Song et al. 2004). In regions of the pile where the curvature demand is high, adequate section ductility must be ensured through a satisfactory pile design procedure. Curvature ductility of a pile may be used to define its ability to undergo large amplitude cyclic lateral deformations by undergoing post-elastic strains in specific regions, without a significant reduction in its lateral load carrying capacity (Joen and Park, 1990). These critical regions, termed plastic hinges, are therefore detailed for experiencing inelastic flexural actions (Paulay and Priestley, 1992). Figure 2.5 portrays the potential locations of the plastic hinges for piles with different head fixity conditions.

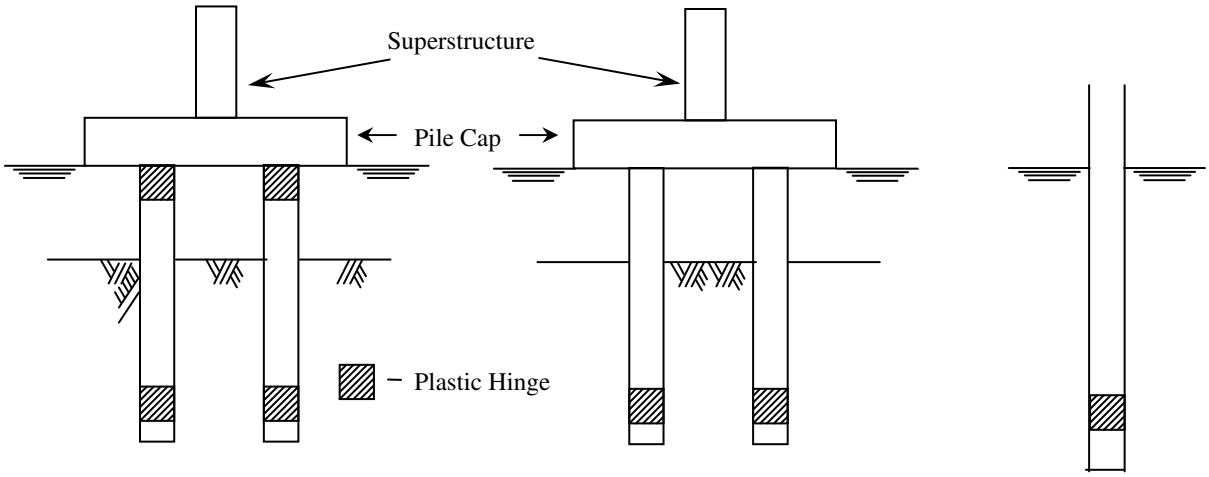

(a) Fixed Head Pile (b) Partially Fixed Head or Free Head Pile

Figure 2.5. Potential locations of plastic hinges in piles

Depending on the boundary condition of the pile head and the surrounding soil conditions, the curvature ductility demand in piles may differ significantly. For instance, deep foundations containing a boundary condition of a fixed pile to pile-cap connection at the pile head may be subjected to a curvature ductility demand under seismic loading. Therefore, it is of interest to investigate previous analytical work and case studies in order to attempt to quantify the curvature demand and/or curvature capacity needed for piles in different soil and boundary conditions. Several case studies are reported in the subsequent sections to aid in the process of quantifying the curvature demand and/or capacity. Section 2.4 further discusses the relevance of these values to the overall project.

2.3.2 Background of Curvature Ductility

Song et al. (2004) emphasized the necessity to gain a deeper understanding of the curvature demand utilizing an analytical model. In explaining this model, it was stated that deep foundations for buildings and bridges often rely on the use of concrete piles that are restrained from rotation at the pile head. With the lateral loads that the earthquakes induce, the fixity at the pile to pile-cap connection induces a large curvature demand in piles adjacent to the pile cap, causing potential for failure in the pile. When a large lateral load is applied to a pile foundation, a sequential yielding in the critical regions of piles will develop until forming a full plastic mechanism. A summary of the various limit states associated with this mechanism are provided below with illustrations in Figure 2.6:

- First yield limit state: characterized by a bending moment demand at the pile to pile-cap connection reaching the first yield moment of the pile section, where it is

assumed that the plastic hinge first forms at the pile head. The center of rotation in this case occurs at the ground level.

- Second yield limit state: a second plastic hinge forms at a depth greater than the depth of the first plastic hinge. Of important note is the continued lateral displacement after the formation of the second plastic hinge, which is facilitated by inelastic rotations in both plastic hinges.
- Ultimate limit state: this limit state is defined by the first flexural failure of a hinge and is dictated by the limiting curvature in either of the plastic hinges.

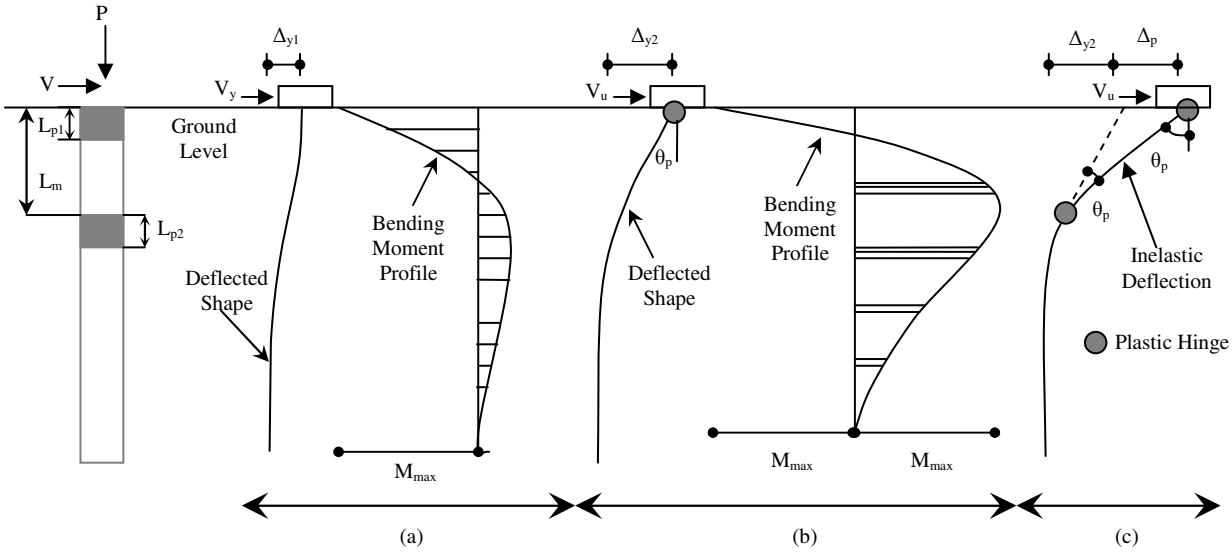

Figure 2.6. Deflected shape and bending moment distribution of a laterally loaded fixed-head pile (a) First yield limit state (b) Second yield limit state (c) Ultimate limit state (after Song et al., 2004)

The analysis model developed by Song et al. (2004), with focus on CIDH piles, defines the lateral response of fixed-head piles using the limit states defined above. This model also predicts the lateral stiffness, lateral strength and the curvature ductility demand in the pile and relates the displacement ductility factor of the pile to the local curvature ductility demand at the critical pile section for both cohesive and cohesionless soils. The curvature ductility

demand, which is different for the two plastic hinges, depends on the displacement ductility imposed on the pile. By limiting the curvature ductility demand within the plastic hinge region, the severity of the local damage can be controlled. The given analysis model can be summarized in the following manner:

- The lateral response of fixed-head piles is represented by a linear elastic response, followed by first yielding of the pile at the pile head and then by a full plastic mechanism with second plastic hinging at some depth below the pile head.
- The elastic response of the pile and its first yield limit state are determined using a classical solution of a flexural element supported by an elastic Winkler foundation. In this case, the soil is replaced by a series of springs, which provide a soil reaction that is proportional to the lateral deflection (p-y curves).
- The ultimate lateral strength, or the maximum lateral load that the pile can resist without failure, is determined using the flexural strength of the pile and an ultimate pressure distribution for the soil. The lateral strength of the pile can be determined by assuming that a sufficiently large deflection has occurred so that an ultimate soil pressure that extends to the depth of the maximum bending moment is fully developed. This depth depends on the flexural strength of the pile and the ultimate soil pressure of the soil and defines the location of the second plastic hinge, which in turn, influences the lateral strength and the ductility of the pile. The magnitude and distribution of the ultimate soil pressure acting on the pile depends on the failure mechanism of the soil, the shape of the pile cross-section, and the friction between the pile surface and the surrounding soil.

- A kinematic relation between the global displacement ductility factor and local curvature ductility demand is developed by assuming a concentrated plastic rotation at both plastic hinges. The kinematic relationship between displacement and curvature ductility demands is established through the dependency of the curvature ductility demand upon the ratio of the first yield lateral force to ultimate lateral force, the ratio of initial stiffness to post first yield stiffness, the depth to the second plastic hinge, and the plastic hinge length of the pile.

The extension of the above approach to piles in a pile supported footing will be relatively challenging because it is difficult to establish a relationship between the global displacement ductility factor and the local curvature ductilities of different piles. As detailed in Chapter 4, this problem may be alleviated by defining different displacement limits for the piles and incorporating these displacements in the definition of the global displacement ductility.

2.3.3 Analytical Work

2.3.3.1 Song, Chai, and Hale, 2004

In order to examine the usefulness of the model described in section 2.3.2, two reinforced concrete pile foundations with a fixed head embedded in two different soil types were examined by Song et al. These soils were soft clay and dense sand. The reinforced concrete piles were 22 inches (0.56 meters) in diameter and contained an embedment length of 64.3 feet (19.6 meters). The reinforcement of the pile was: (1) eight No. 22 longitudinal reinforcing bars, resulting in a longitudinal steel ratio of 0.012; and (2) No. 16 transverse

spiral reinforcement at a pitch of 3.5 inches, resulting in a confining steel ratio of 0.021 with a concrete cover of 3 inches.

The reinforced concrete fixed-head pile foundation was initially assessed in soft clay cohesive soil. In completing the analysis of the numerical model, the curvature demand results in 0.00132/inch for the CIDH pile.

The same reinforced concrete fixed-head pile foundation was next assessed in dense cohesionless sand at the first yield limit state of the pile in order to observe the correspondence between that limit state and the curvature ductility demand. In completing the numerical model, the curvature demand of 0.00145/inch was estimated. These values of curvature demand provide a target curvature for concrete piles under the conditions that Song et al. chose for their examples.

2.3.3.2 Banerjee, Stanton, and Hawkins, 1987

Single piles embedded in representative soil profiles were subjected to severe earthquake loading in order to analytically investigate the soil-pile interaction. The objective of the study was to compute the bending behavior of single piles embedded in soil profiles taken from three West Coast sites and associate the bending behavior of these piles under earthquake lateral loads. The cross-sectional properties of the piles that were analyzed are detailed in Table 2.1.

Table 2.1. Pile details for piles embedded into the three West Coast sites

Pile size (in.)	Cross-sectional area ($in.^2$)	Moment of inertia ($in.^4$)	Concentrated mass at the top (ton)
14	162	2105	60
18	268	5750	110
24	477	18,180	200
Note: γ = 150 pcf; E = 4750 ksi, ν = 0.15			

The analysis procedure utilized an updated and refined finite element model that was used in a previously performed study by Margason (1977). This procedure required modeling of the complete pile-soil system using elastic and equivalent linear visco-elastic finite elements. The analysis was performed in two steps: free-field analysis and interaction analysis, both in the frequency domain using the method of complex response. The free-field analysis determined compatible base rock motions and defined the boundary forces for the second step. The interaction analysis involved the complex harmonic equilibrium equations for the entire soil-pile system being solved iteratively at each frequency of excitation. This iteration process is necessary because non-linear behavior of the soil was included. The non-linear soil behavior was represented in an equivalent linear method by a secant modulus that was chosen to satisfy both the equilibrium and compatibility. As mentioned above, the piles were embedded in soil profiles taken from three West Coast sites: West Seattle, Tacoma, and San Francisco. Figures 2.7, 2.8, and 2.9 provide the soil properties at the three sites.

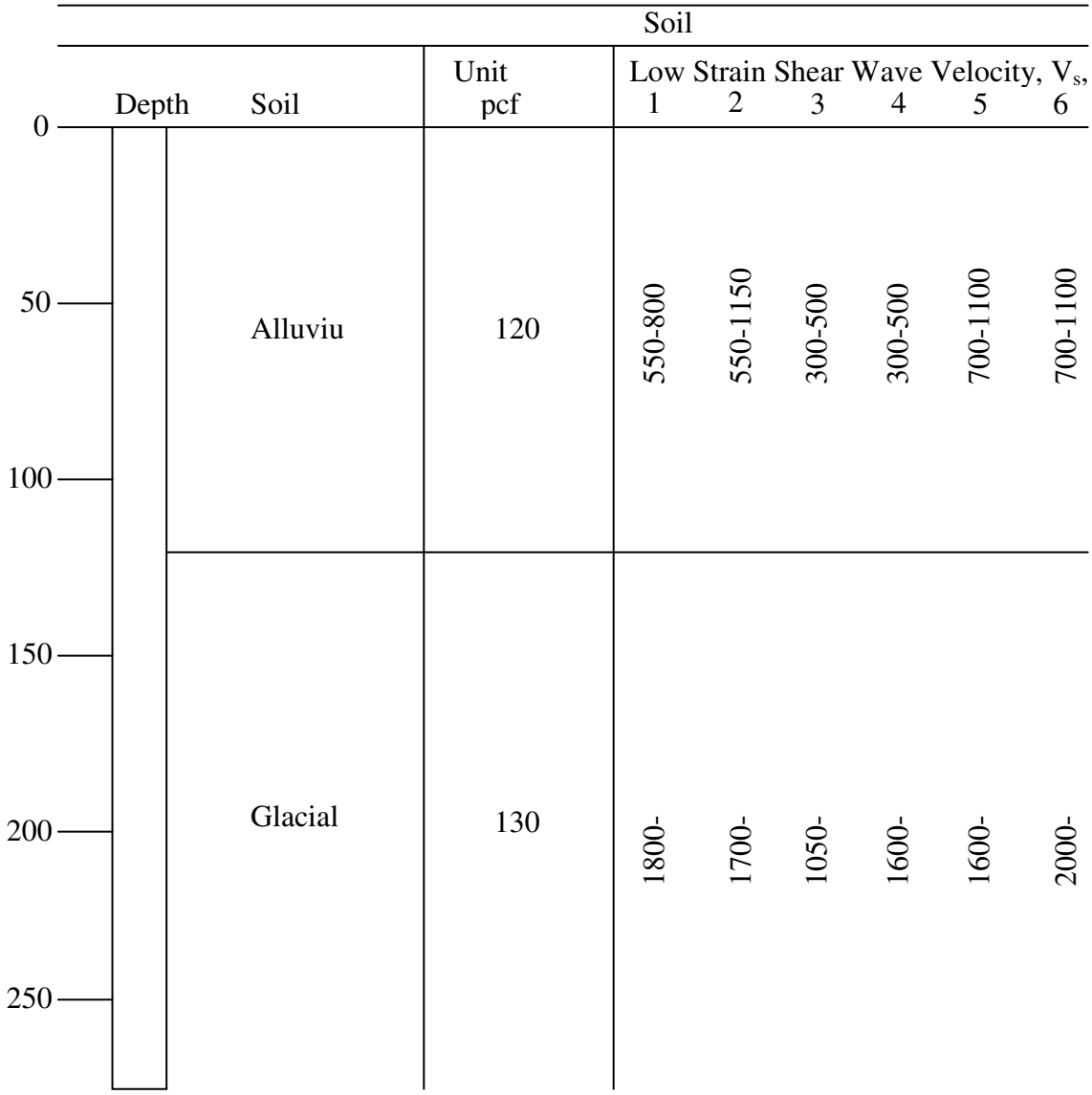

Figure 2.7. Soil properties at the West Seattle site

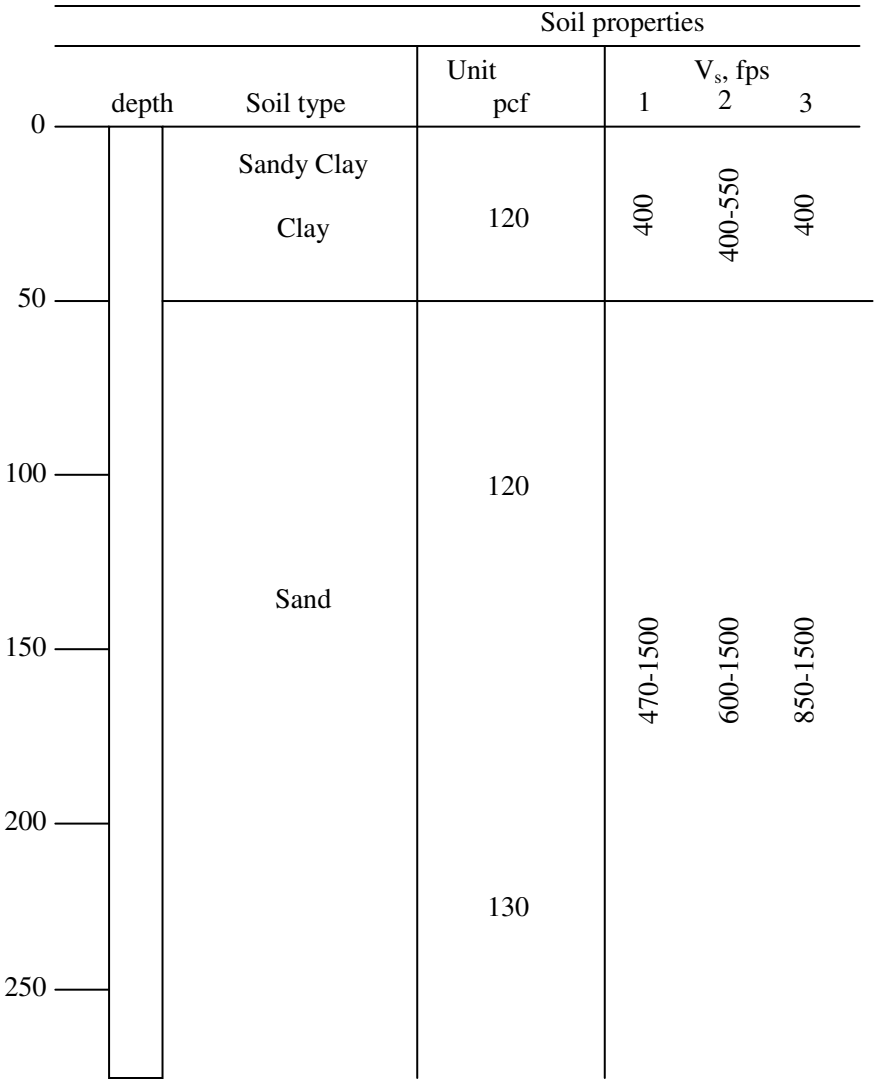

Figure 2.8. Soil properties at the Tacoma site

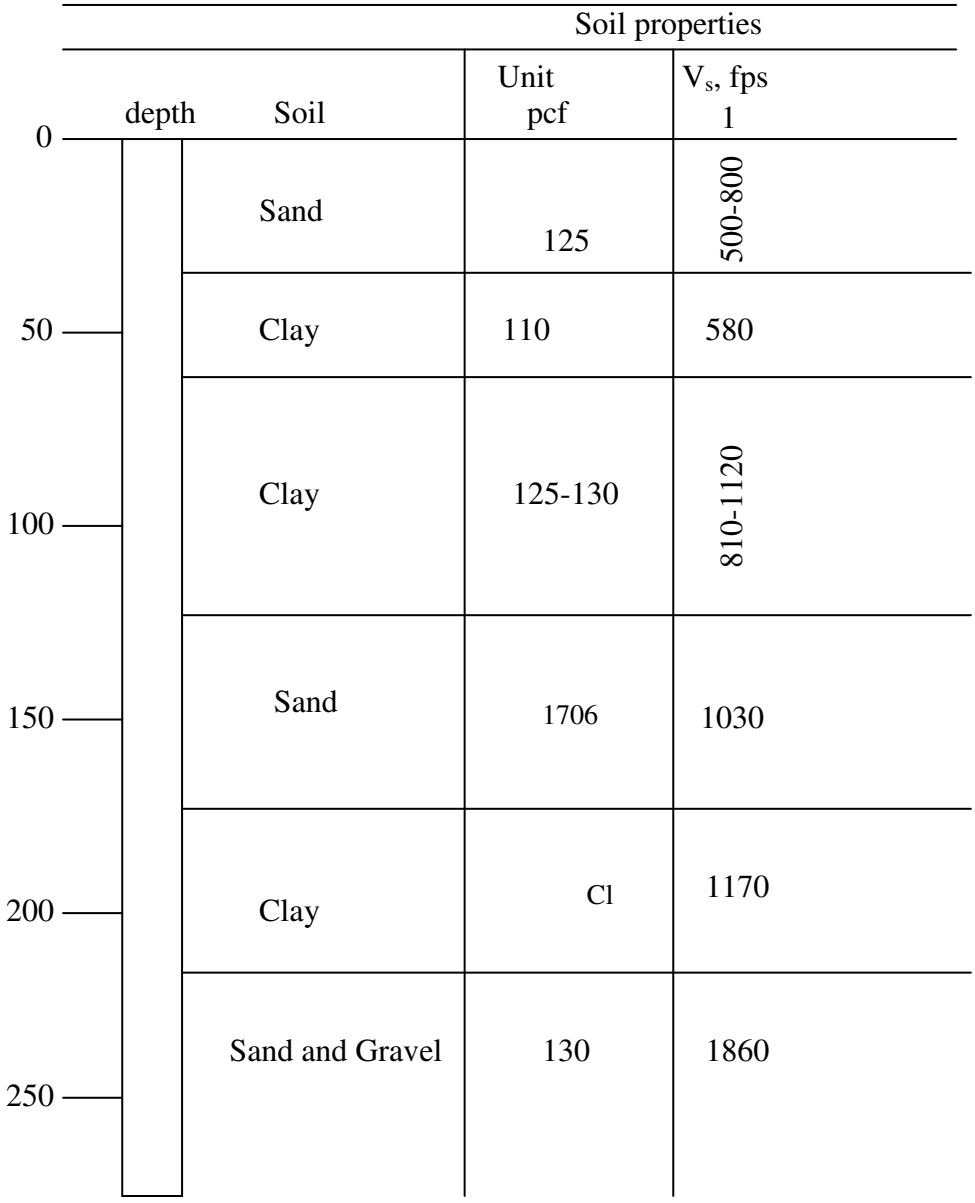

Figure 2.9. Soil properties at the San Francisco site

Through the two-step process, the following observations were made by the authors:

- the maximum induced curvature demands were significantly affected by the characteristics of the surrounding soils;
- the induced curvatures were larger in softer soil and especially severe at the interface between layers with significantly different modulus values;

- the induced curvatures were reduced as the pile size increased;
- for a severe earthquake in relatively poor soil conditions, i.e. the West Seattle site and the Tacoma site, the maximum induced pile curvatures ranged from 0.0001/inch to 0.00012/inch; and
- for the San Francisco site, the maximum induced pile curvature was 0.00022/inch.

2.3.4 Field Investigation

A number of investigations were conducted on piles after the occurrence of an earthquake to obtain information on the cause of pile failures and to estimate the curvature demand imposed on piles in real earthquakes. Based on this information, the following discussion aims to provide an upper bound values for the curvature demand that piles must be able to sustain in a major earthquake.

2.3.4.1 Koyamada, Miyamoto, and Tokimatsu, 2005

The Tokachi-Oki Earthquake, an earthquake with a magnitude of 8.0, occurred on September 26, 2003. It caused severe damage to the Konan junior high school in Hokkaido Japan, a three-story reinforced concrete frame building supported on high strength prestressed concrete pile foundations. In order to determine the main factors that caused the severe damage, a field investigation was performed, involving excavation of four perimeter piles. From this investigation, it was concluded that piles were damaged by compression failure with flexural cracks at the pile heads. These compression failures induced differential settlements of the superstructure, therefore leading to damage to the structure. Shear cracks were found in the walls of the school building and were caused by the collapse of the pile foundation. The pile foundations, composed of high-strength prestressed concrete piles, were

93.5 feet long with a diameter of 15.7 inches. Reinforcement details of the piles were not provided. The piles were embedded into a non-uniform layered soil, summarized in Table 2.5.

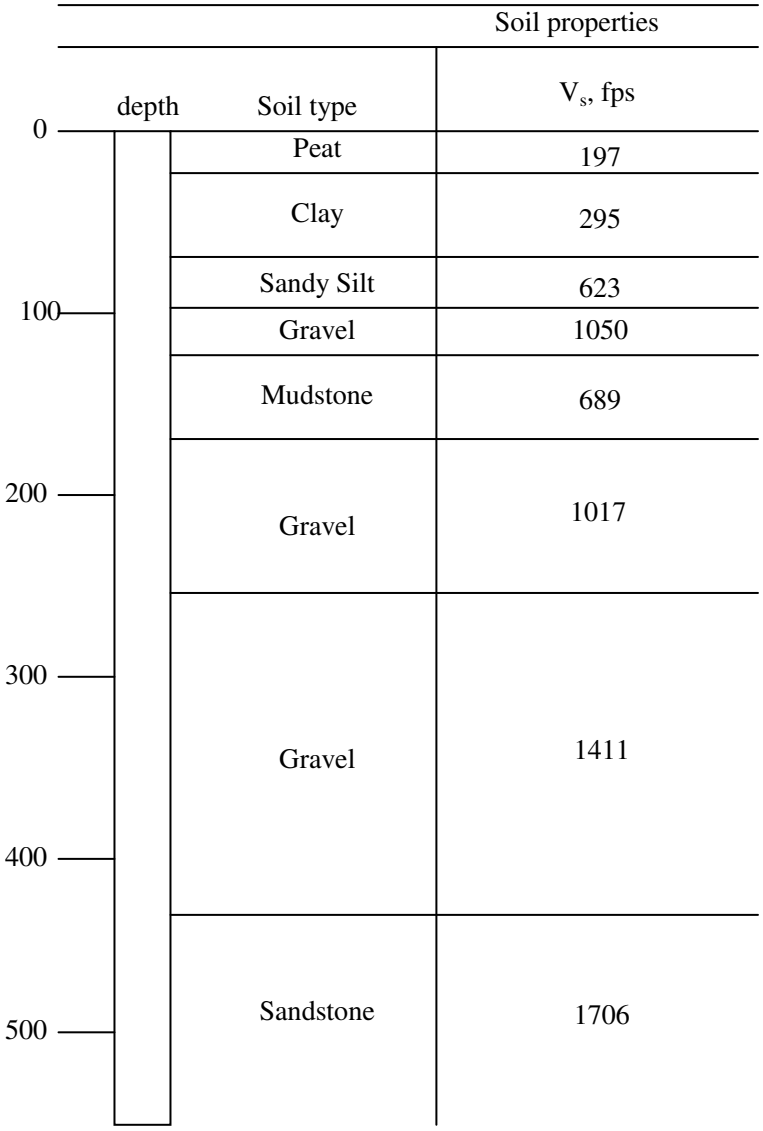

Table 2.5. Depths of soil layers at the Konan junior high school at Hokkaido, Japan

The factors causing the damage of the pile foundation were also verified by the researchers through analytical simulations. In this simulation model, a one-stick model with lumped mass idealized the superstructure whereas the pile foundation was modeled with

beam elements. The piles were connected to the free field soil through non-linear lateral and shear interaction springs. The non-linear behavior of piles was incorporated into the analysis by defining the relationships between the bending moment and the curvature, thus enabling evaluation of the degree of damage to piles. The kinematic bending moments and shear forces were computed by subjecting the analysis model to the recorded ground motion, without the superstructure. The inertial bending moments and shear forces of the superstructure were obtained by subtracting the kinematic bending moments and shear forces from the total bending moments and shear forces. It was found that the bending moment demand in the piles at the pile head, which included both the inertial and kinematic components, exceeded its ultimate moment capacity. This is consistent with the soil profile where peat exists over approximately 20 feet along the pile length. Furthermore, the maximum curvature demand at the pile head due to the imposed seismic load was determined to be about 0.00152/inch from the analysis and was found to be consistent with the damage obtained from the field investigation.

2.3.4.2 Lin, Tseng, Chiang, and Hung, 2005

Earthquakes such as the Niigata earthquake of 1964, the Kobe earthquake of 1995, and the Chi-Chi earthquake of 1999 caused lateral spreads, resulting in significant damage to the pile foundations of both bridges and buildings. Through excavation and field surveys, it was deduced that liquefaction may have caused the damage to the pile foundation, producing permanent ground displacement. A foundation model consisting of Winkler springs was utilized to model the non-linear soil response interaction, while the Bouc-Wen hysteretic model was used to stimulate the soil and pile material behavior.

Depending on the stiffness of the liquefied soil, the length of the pile exposed to the liquefied soil, the axial load imposed on the pile, and the bending stiffness of the pile, piles subject to lateral spreading due to soil liquefaction could potentially experience two distinct failure modes (Meyersohn, 1994):

1. lateral pile deflections induced by ground lateral spreading that may result in the pile reaching its bending capacity and hence develop a full moment capacity; and
2. the combined action of lack of sufficient lateral support due to the reduced stiffness of the liquefied soil and the lateral deflection imposed on the pile may result in pile buckling.

Since ground lateral spreads may be due to combined and simultaneous actions of permanent ground displacements and axial loads, separate analyses ought to be performed for studying the potential for bending and buckling failure of piles. In this article, the possible failure modes of the following three available pile foundations were studied in order to determine if the piles failed by bending or buckling.

Yachiyo Bridge, Japan

During the 1964 Niigata earthquake, the abutments and piers of the Yachiyo Bridge were damaged. The foundations of these abutments and piers used reinforced concrete piles, which were 32.8 feet in length and 11.8 inches in diameter. Reinforcement details of the piles were not provided. The pile foundations were embedded into a 36 foot deep layered soil composed of sandy silt, medium sand, and fine sand. Upon extraction, the piles were observed to be severely damaged at a depth of 26.2 feet from the top of the pile as well as containing horizontal cracks caused by significant flexural actions. The maximum curvature

that the reinforced concrete piles reached was reported to be 0.00021/inch, although authors did not discuss the procedure as to how this value was obtained.

Four-Story Building in Mikagehoma, Japan

The 1995 Kobe earthquake critically damaged the prestressed high-strength concrete pile foundations that supported a four-story building in Mikagehoma, Japan. The piles were 75.5 feet long and had a diameter of 13.8 inches. Reinforcement details of the piles were not provided. Field investigations revealed significantly wide pile cracks near the pile head, which caused apparent tilting of the entire building. The maximum curvature that the prestressed high-strength concrete piles reached was reported to be 0.00038/inch. Again, no information was provided as to how this value was determined.

Showa Bridge, Japan

The Showa Bridge was completely destroyed during the 1964 Niigata earthquake. The 12-span bridge was 75.5 feet in length. The piers of the Showa Bridge were composed of 0.07-inch thick driven steel pipe piles, which were 269 feet long and 24 inches in diameter. Reinforcement details of the piles were again not provided. The soil conditions surrounding the pile foundations were composed of liquefiable soil layer and a non-liquefied soil layer. The liquefiable soil layer slid horizontally 16.4 feet toward the center of the river, suggesting that the pile failures may have resulted from pile buckling. The maximum curvature that the steel pipe pile reached was estimated to be 0.000432/inch, although how this value was obtained was not discussed.

2.4 Target Curvature Demand

The literature summarized in the preceding sections indicated a target curvature ductility demand for piles in the range of 0.0002/inch to 0.00152/inch. Since the number of research articles providing this information is limited, the curvature capacities reported for various pile sections were also examined. In regards to the current project, these values are relevant because they provide a quantifiable range for curvature capacities for piles used in seismic regions and that if this range is unacceptable widespread damage to the pile foundation would have been observed during past earthquakes. Summarized in Table 2.6 are various curvature demands discussed in the above sections, while Table 2.7 lists reported curvature capacities for different piles used in seismic regions. By comparing the two tables, it is observed that the capacities in Table 2.7 range from 0.0002/inch to 0.00107/inch, and the maximum capacity of 0.00107/inch is about 40 percent lower than the maximum demand of 0.00152/inch that has reported to have caused pile damage. In the absence of a more refined data set, these upper values provide an indication for the maximum curvature that should be considered for the investigation presented in this report.

Table 2.6. Summary of curvature demands estimated for piles in the field during past earthquakes

Document	Reference	Pile Type	Pile Dimensions (in.)	Type of Loading	Curvature Demand (in^{-1})
Analytical model for ductility assessment of fixed-head concrete piles	Song, Chai, Hale-2004	reinforced concrete (CIDH)	D = 22	earthquake	0.00132
Analytical model for ductility assessment of fixed-head concrete piles	Song, Chai, Hale-2004	reinforced concrete (CIDH)	D = 22	earthquake	0.00145
Damage of piles caused by lateral spreading-back study of three cases	Lin, Tseng, Chiang, Hung-2005	reinforced concrete	D = 11.8 L^{*} = 393.6	1964 Niigata Earthquake	0.0002
Damage of piles caused by lateral spreading-back study of three cases	Lin, Tseng, Chiang, Hung-2005	prestressed high strength concrete pile	D = 13.8 L = 906	1995 Kobe Earthquake	0.000381
Damage of piles caused by lateral spreading-back study of three cases	Lin, Tseng, Chiang, Hung-2005	driven steel pile	D = 24 thickness = 0.07	1964 Niigata Earthquake	0.000432
Field inestigation and analysis study of damaged pile foundation during the 2003 Tokachi-Oki earthquake	Koyamada, Miyamoto, Tokimatsu-2005	prestressed high strength concrete pile	D = 15.7 L = 1122	2003 Tokachi-oki Earthquake	0.00152

L^{*} = length of pile

Table 2.7. Summary of curvature capacities reported for precast, prestressed concrete piles used in seismic regions

Document	Reference	Pile Type	Pile Dimensions (in.)	Type of Loading	Curvature Capacity (in^{-1})
Seismic design of prestressed concrete piling	Sheppard, 1980	square piles	16x16 L = 516	axially until 600 kips, then monotonically to failure	0.00023
Seismic design of prestressed concrete piling	Sheppard, 1981	square piles	18x18 L = 516	axially until 600 kips, then monotonically to failure	0.0002
Seismic design of prestressed concrete piling	Sheppard, 1980	square piles	12	axially until 200 kips by post-tensioning, then monotonically to failure	0.00028
Seismic design of prestressed concrete piling	Sheppard, 1980	square piles	12	prestressed to induce effect precompression of 700 kips, axially to 300 kips by post-tensioning and cyclically loaded	0.00031
Seismic design of prestressed concrete piling	Sheppard, 1980	square piles	12	prestressed to induce effect precompression of 700 kips, axially to 300 kips by post-tensioning and cyclically loaded	0.00107
Seismic performance of precast prestressed concrete piles	Banerjee, Stanton, Hawkins 1987	octogonal piles	14	cyclic lateral load tests	0.0008
Seismic performance of precast prestressed concrete piles	Banerjee, Stanton, Hawkins 1987	octogonal piles	14	cyclic	0.00081

Table 2.7. (continued)

Document	Reference	Pile Type	Pile Dimensions	Type of Loading	Curvature Capacity in^{-1}
Seismic performance of precast prestressed concrete piles	Banerjee, Stanton, Hawkins 1987	octogonal piles	14	cyclic	0.00092
Seismic performance of precast prestressed concrete piles	Banerjee, Stanton, Hawkins 1987	octogonal piles	14	cyclic	0.00065
Seismic performance of precast prestressed concrete piles	Banerjee, Stanton, Hawkins 1987	octogonal piles	14	cyclic	0.0003
Seismic performance of precast prestressed concrete piles	Banerjee, Stanton, Hawkins 1987	octogonal piles	14	cyclic	0.00045
Seismic performance of precast prestressed concrete piles	Banerjee, Stanton, Hawkins 1987	octogonal piles	14	cyclic	0.00033
Seismic performance of precast prestressed concrete piles	Banerjee, Stanton, Hawkins 1987	octogonal piles	14	cyclic	0.00093
Seismic performance of precast prestressed concrete piles	Banerjee, Stanton, Hawkins 1987	octogonal piles	14	cyclic	0.00031
Seismic performance of precast prestressed concrete piles	Banerjee, Stanton, Hawkins 1987	octogonal piles	14	cyclic	0.00041

2.5 Confinement Reinforcement

In order to enhance strength and toughness of the concrete core section of a prestressed precast concrete pile, transverse confining reinforcement is provided typically in the form of spirals. At the pile ends, the spirals are closely spaced in order to prevent bursting and splitting stresses that would be caused by the release of prestress and during driving. In the potential plastic hinge regions, closely spaced spirals are also needed to ensure adequate curvature capacity of the pile critical sections. In addition to increasing both the flexural strength and shear strengths, the spiral reinforcement also prevents premature buckling of the mild steel reinforcement. The following discussion provides a thorough explanation of the parameters necessary to determine the needed amount of the spiral reinforcement to ensure adequate ductility capacity of precast, prestressed sections as well as current confinement reinforcement requirements of several different design documents.

2.5.1 Parameters Affecting Confinement

The transverse confining reinforcement is typically quantified as a volumetric ratio of the core concrete section and symbolized by ρ_s. Using the variables shown in Figure 2.7, ρ_s can be defined as follows:

$$\rho_s = \frac{4A_{sp}}{D's} \qquad \text{(Eq. 2.1)}$$

where A_{sp} = the bar cross-sectional area of spiral reinforcement

D' = the diameter of the core concrete measured between the center of the spirals

s = longitudinal center-to-center spacing of transverse reinforcement

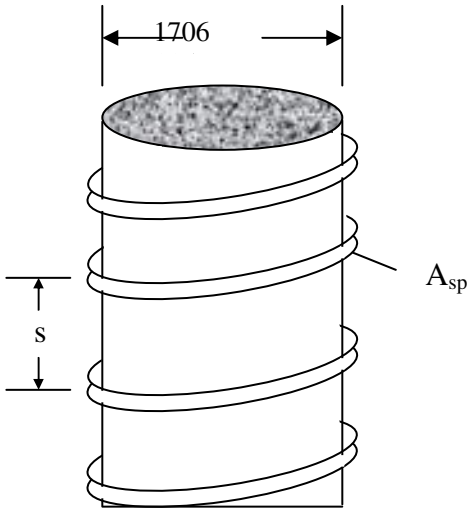

Figure 2.7. Core concrete confined by transverse reinforcement

Several different parameters influence the required amount of confinement reinforcement. These parameters can be identified by examining the variables defining the curvature ductility capacity or ultimate compression strain of the confined concrete. The curvature ductility of a core concrete section:

$$\mu_\phi = \frac{\phi_u}{\phi_y} \qquad \text{(Eq. 2.2)}$$

where μ_ϕ = curvature ductility;

ϕ_u = ultimate curvature; and

ϕ_y = yield curvature.

The ultimate curvature may be defined using the ultimate compression strain as

$$\phi_u = \frac{\varepsilon_{cu}}{c_u} \qquad \text{(Eq. 2.3)}$$

where ε_{cu} = the ultimate extreme fiber compression strain

c_u = the corresponding neutral-axis depth

According to Mander et al. (1988), the ultimate compression strain and the volumetric ratio of transverse reinforcement are related by

$$\varepsilon_{cu} = 0.004 + \frac{1.4\rho_s f_{yh} \varepsilon_{su}}{f_{cc}^{'}} \qquad \text{(Eq. 2.4)}$$

$$f_{cc}^{'} = f_c^{'}\left(2.254\sqrt{1+\frac{7.94 f_l^{'}}{f_c^{'}}}\right) - \frac{2 f_l^{'}}{f_c^{'}} - 1.254 \qquad \text{(Eq. 2.5)}$$

where ρ_s = the volumetric ratio of transverse reinforcement;

f_{yh} = the yield strength of the transverse reinforcement;

ε_{su} = the ultimate reinforcement strain capacity;

$f_{cc}^{'}$ = the compressive strength of the confined concrete;

$f_c^{'}$ = compressive strength of unconfined concrete; and

$f_l^{'}$ = effective lateral confining stress = $K_e \frac{2 f_{yh} A_{sp}}{D' s}$

K_e = confinement effectiveness coefficient

Given that ε_{cu} will also depend on the axial force, P, that the section will sustain at the ultimate limit state and the amount of longitudinal reinforcement ratio, ρ_l, it can be stated that the required value of ρ_s will be influenced by the following parameters: $f_c^{'}$, f_{yh}, ε_{su}, P, and ρ_l. Considering the other variables that are primarily used to express the key parameters in a non-dimensionalized form, the variables that ρ_s depends on are as follows:

- A_{ch} = cross sectional area of confined core of reinforced concrete section, measured out-to-out of the transverse reinforcement

- A_g = gross section area of the concrete section
- A_{st} = total area of mild longitudinal steel reinforcement
- d_b = longitudinal reinforcement bar diameter
- d_{sp} = transverse reinforcement bar diameter
- $f_c^{'}$ = compressive strength of unconfined concrete
- f_y = yield strength of longitudinal reinforcement
- f_{yh} = yield strength of transverse reinforcement
- f_{pc} = compressive stress in the concrete at the centroid of the cross section due to prestress (after losses)
- m = non-dimensional ratio equal to $f_y/0.85\ f_c^{'}$
- p_t = ratio of non-prestressed longitudinal column reinforcement, which is equal to A_{st}/A_g
- P = external axial force
- P_e = external axial force
- ρ_l = longitudinal steel reinforcement ratio

2.5.2 Transverse Reinforcement Requirements

The transverse reinforcement requirements specified in several codes and standards were considered in this study. These include the Uniform Building Code (UBC, 1997), International Building Code (IBC, 2000), the ASCE Minimum Design Loads for Buildings and other Structures (ASCE 7, 2005), the PCI Recommended Practice (PCI, 1993), the New Zealand Code of Practice for Concrete Structures (NZS, 2006), the Applied Technology

Council (ATC, 1996), and the American Concrete Institute (ACI, 2005). The subsequent sections discuss the requirements of transverse reinforcement from each of the aforementioned codes and how they apply to precast, prestressed piles.

2.5.2.1 Uniform Building Code (1997)

Prior to the introduction of the International Building Code, the Uniform Building Code was widely used in seismic regions. The 1997 edition of the Uniform Building Code (UBC, 1997) established the requirements for spiral reinforcement in prestressed concrete piles in Seismic Zones 3 and 4 as follows:

For piles 14 inches and smaller, $\rho_s \geq 0.021$

For piles 24 inches and larger, $\rho_s \leq 0.021$

2.5.2.2 International Building Code (2000), ASCE 7(2005), and PCI (1993)

The International Building Code (IBC, 2000) and the ASCE Minimum Design Loads for Buildings and other Structures (ASCE 7, 2005) adopt some of the requirements of the PCI Recommended Practice (PCI, 1993) and require the following minimum volumetric ratio of transverse reinforcement in the ductile region of precast, prestressed piles:

$$\rho_s = 0.25\left(\frac{f_c^{'}}{f_{yh}}\right)\left(\frac{A_g}{A_{ch}}-1\right)\left[0.5+\frac{1.4P}{f_c^{'}A_g}\right] \qquad \text{(Eq. 2.6)}$$

but not less than

$$\rho_s = 0.12\left(\frac{f_c^{'}}{f_{yh}}\right)\left[0.5+\frac{1.4P}{f_c^{'}A_g}\right] \qquad \text{(Eq. 2.7)}$$

or 0.007

and not to exceed

$$\rho_s = 0.021$$

The differences between the IBC and the PCI Recommended Practice involve the maximum ρ_s limit of 0.021 and the external axial load, *P*. The maximum value of 0.021 is only found in the IBC, while P is defined differently in the two codes as detailed below:

- The IBC defines P due to dead load, earthquake load, live load, roof load, snow load, and wind load, and is determined by either:

  $$P = 1.2D + 1.0E + f_1 L + f_2 S \qquad \text{(Eq. 2.8)}$$

  or

  $$P = 0.9D + (1.0E \; or \; 1.6W) \qquad \text{(Eq. 2.9)}$$

  where D = dead load;

  E = earthquake load;

  L = live load;

  S = snow load;

  f_1 = 1.0 or 0.5, depending on the type of live load; and

  f_2 = 0.7 or 0.2, depending on the roof configuration

- The PCI Recommended Practice defines the axial load as a combination of the external compressive load on the pile and the axial load on the pile due to the effective prestress. This combination is represented by the following equation:

  $$P = P_e + f_{pc} A_g \qquad \text{(Eq. 2.10)}$$

  where P_e = factored external axial load; and

  f_{pc} = effective prestress in concrete after all losses

Thus, in order to obtain the most practical value of P used in the volumetric ratio of the transverse reinforcement, the following combination of the IBC definition of P as well as the PCI Recommended Practice definition of P, should be utilized:

$$P = 1.2D + 1.0E + f_1 L + f_2 S + f_{pc} A_g \quad \text{(Eq. 2.11)}$$

or

$$P = 0.9D + (1.0E \; or \; 1.6W) + f_{pc} A_g \quad \text{(Eq. 2.12)}$$

2.5.2.3 New Zealand Code (2006)

There has been significant research done regarding the volumetric ratio of the transverse reinforcement in New Zealand (i.e., Joen and Park, 1990; Joen and Park, 1990; Priestley et al., 1981; and Park and Falconer, 1983), from which the PCI Recommended Practice for the minimum transverse reinforcement requirement was derived. The volumetric ratio of the transverse reinforcement used in earlier New Zealand tests on prestressed concrete piles to study the confinement issues was based on the following equations (Priestley et al., 1981):

$$\rho_s = 0.45\left(\frac{A_g}{A_{ch}} - 1\right)\left(\frac{f_c^{'}}{f_{yh}}\right)\left[0.375 + 1.25\frac{P_e}{f_c^{'} A_g}\right] \quad \text{(Eq. 2.13)}$$

but not less than

$$\rho_s = 0.15\left(\frac{f_c^{'}}{f_{yh}}\right)\left[0.375 + 1.25\frac{P_e}{f_c^{'} A_g}\right] \quad \text{(Eq. 2.14)}$$

From the research that was performed by Priestley et al. (1981), the recommended transverse reinforcement requirement for the 1982 New Zealand Design Code was

$$\rho_s = 0.45\left(\frac{A_g}{A_{ch}} - 1\right)\left(\frac{f_c^{'}}{f_{yh}}\right)\left[0.5 + 1.25\frac{P_e}{f_c^{'}A_g}\right] \qquad \text{(Eq. 2.15)}$$

but not less than

$$\rho_s = 0.12\left(\frac{f_c^{'}}{f_{yh}}\right)\left[0.5 + 1.25\frac{P_e}{f_c^{'}A_g}\right] \qquad \text{(Eq. 2.16)}$$

However, the New Zealand Code of Practice for Concrete Structures (NZS 3101, 1982) adopted the following format of the aforementioned equations:

$$\rho_s = 0.45\left(\frac{A_g}{A_{ch}} - 1\right)\left(\frac{f_c^{'}}{f_{yh}}\right)\left[0.375 + 1.25\frac{P_e}{\phi f_c^{'}A_g}\right] \qquad \text{(Eq. 2.17)}$$

but not less than

$$\rho_s = 0.15\left(\frac{f_c^{'}}{f_{yh}}\right)\left[0.375 + 1.25\frac{P_e}{\phi f_c^{'}A_g}\right] \qquad \text{(Eq. 2.18)}$$

where ϕ = the strength reduction factor for which values of 1.0 and 0.9 were recommended for research and design purposes, respectively. Joen and Park (1990) noted that the $P = P_e + f_{pc}A_g$ replaced the term P_e for prestressed concrete piles. In this reference, the displacement ductility factor, $\mu_\Delta = \frac{\Delta_u}{\Delta_y}$, was reported to be at least 8 when using the previously discussed spiral quantities in the potential plastic hinge regions. The 2006 New Zealand Code of Practice for Concrete Structures recommends the required volumetric ratio of spirals based on further experimental testing and analysis (Watson et al., 1994). The resulting design equation in the current New Zealand Standard 3101 is the greater of either

$$\rho_s = \frac{(1.3 - p_t m)}{2.4}\left(\frac{A_g}{A_{ch}}\right)\left(\frac{f_c^{'}}{f_{yh}}\right)\left(\frac{P}{\phi f_c^{'}A_g}\right) - 0.0084 \qquad \text{(Eq. 2.19)}$$

or

$$\rho_s = \frac{A_{st}}{110 d_{sp}} \frac{f_y}{f_{yh}} \frac{1}{d_b} \qquad \text{(Eq. 2.20)}$$

Equation 2.20 is related to the lateral restraint of the longitudinal bars against premature buckling, thus is not applicable to prestressed piles in which the strands are not expected to experience any compressive strains.

2.5.2.4 ATC-32 (1996)

In the United States, in order to ensure adequate ductile performance of bridge piers, the following requirement is recommended by ATC-32 (ATC, 1996).

$$\rho_s = 0.16\left(\frac{f_c^{'}}{f_{yh}}\right)\left[0.5 + 1.25\frac{P_e}{f_c^{'} A_g}\right] + 0.13\left(\rho_l - 0.01\right) \qquad \text{(Eq. 2.21)}$$

According to Priestley et al., (1992), for prestressed concrete piles, the above equation can be modified by replacing P_e with P, and thus:

$$\rho_s = 0.16\left(\frac{f_c^{'}}{f_{yh}}\right)\left[0.5 + 1.25\frac{P}{f_c^{'} A_g}\right] + 0.13\left(\rho_l - 0.01\right) \qquad \text{(Eq. 2.22)}$$

where $P = P_e + f_{pc}A_g$. This document further states that the adequacy of the spiral reinforcement ought to be checked by comparing the displacement demand of the pile with its capacity. In this process, an appropriate equation for the ultimate compression strain should be used.

2.5.2.5 ACI Code (2005)

The ACI 318-05 requires the minimum amount of the transverse reinforcement in circular concrete sections in the following form.

$$\rho_s = 0.45\left(\frac{f_c^{'}}{f_{yh}}\right)\left(\frac{A_g}{A_{ch}} - 1\right) \qquad \text{(Eq. 2.23)}$$

but not less than

$$\rho_s = 0.12\left(\frac{f_c^{'}}{f_{yh}}\right) \qquad \text{(Eq. 2.24)}$$

Since the introduction of the 1999 version of the ACI code, the prestressed concrete piles in high seismic regions are required to satisfy the above equations for the volumetric ratio of spirals in the plastic hinge regions. It is noted that Eq. 2.23 was derived considering only the effects of axial load and may not be applicable when the pile is subjected to flexural and axial load effects.

2.5.2.6 Summary

Figures 2.8 and 2.9 provide graphical comparison of the different design equations for the volumetric ratio of the transverse reinforcement, in which some of the requirements are omitted because they are nearly identical to those plotted in these figures. Figure 2.8 portrays spiral requirements for a 14-inch octagonal pile with $f_c^{'}$ = 8000 psi, f_{yh} = 60 ksi, and a 2 inch concrete cover, whereas Figure 2.9 shows spiral requirements for a 24-inch octagonal pile with $f_c^{'}$ = 8000 psi, f_{yh} = 60 ksi, and a 2 inch concrete cover. From these two figures, the following observations are made:

- The required ρ_s for prestressed piles differ significantly between design codes. At both low and high axial loads, this difference is more than a factor of three.
- Except for the ACI 318-05, the required ρ_s increases with an increase in the external compressive axial load ratio.

- The NZS 3101-2006 requires the highest amount of confinement for high external axial loads, whereas ACI 318-02 requires the highest amount of confinement for low external axial loads.
- The ACI requirement for both piles is significantly high at small axial loads and translates to #3 spiral reinforcement at a spacing of less than 0.75 inches. Such a requirement is difficult to meet in practice as it causes significant construction challenges. The main objective of the current study is to eliminate such difficulties, yet provide rational and satisfactory amounts of transverse reinforcement in prestressed precast concrete piles.

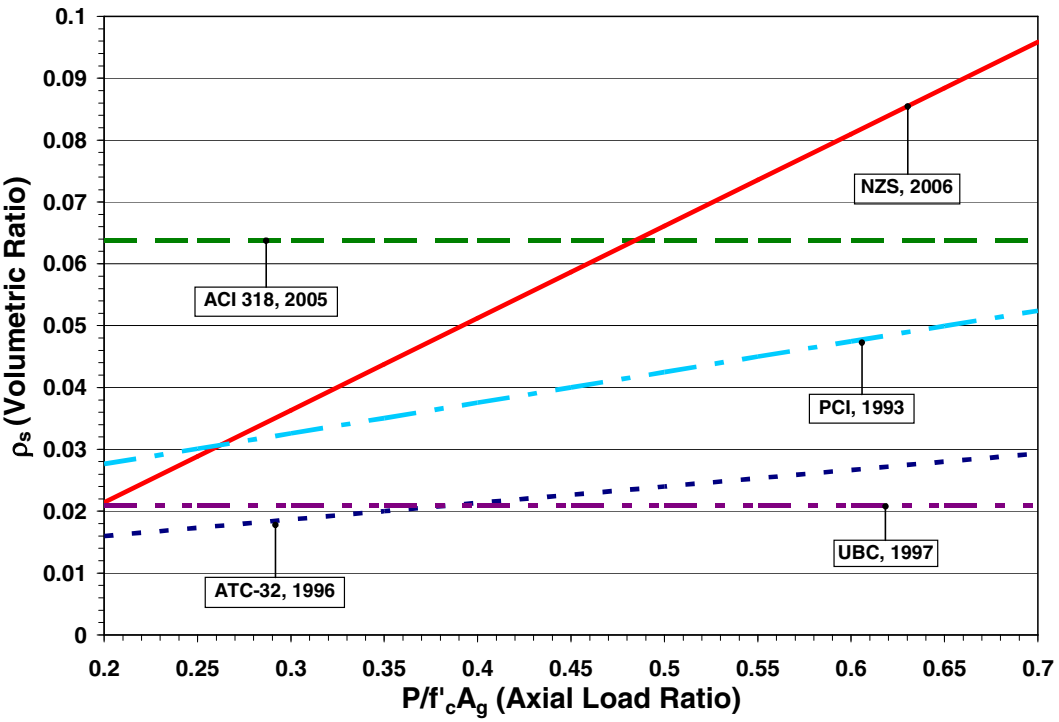

Figure 2.8. Spiral volumetric ratios for a 14-inch octagonal prestressed pile

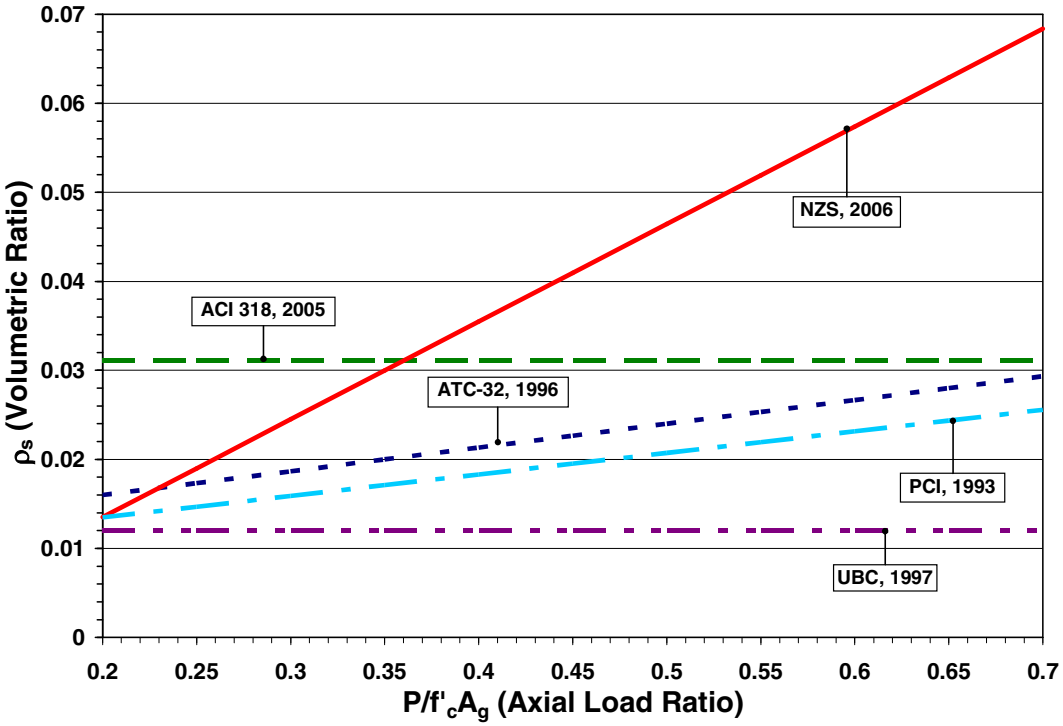

Figure 2.9. Spiral volumetric ratios for a 24-inch octagonal prestressed pile

CHAPTER 3. DEVELOPMENT OF A RATIONALE APPROACH TO DESIGNING TRANSVERSE REINFORCEMENT FOR CONFINEMENT PURPOSES

3.1 Objective

The preceding chapter included an overview of several equations that may be utilized for the design in transverse reinforcement for prestressed concrete piles in areas of high seismic risk. The discussion concluded with a concern of the lack of conformity between the different design equations and construction challenges associated with some of the recommended requirements. Furthermore, several of these equations did not offer a rationale approach to designing piles with the necessary amount of confinement. In most cases, the target curvature ductility for the confined prestressed sections is not specified. Therefore, the objective of this project is to develop a design equation that determines the minimum transverse reinforcement in order to achieve a target ductility over a given range of axial loads in prestressed concrete piles used in high seismic regions.

3.2 Development of a New Equation

3.2.1 Existing Equations of Interest

To commence the development of a new rationale equation for designing confinement reinforcement in prestressed piles, four of the existing equations were carefully

examined as the starting point. These equations are as follows and the reasons for selecting these equations are discussed below.

1. ACI-318 (2005)

$$\rho_s = 0.45\left(\frac{f_c^{'}}{f_{yh}}\right)\left(\frac{A_g}{A_{ch}}-1\right) \geq 0.12\left(\frac{f_c^{'}}{f_{yh}}\right) \qquad \text{(Eq. 3.1)}$$

2. New Zealand Standard (2006)

$$\rho_s = \frac{(1.3 - p_t m)}{2.4}\left(\frac{A_g}{A_{ch}}\right)\left(\frac{f_c^{'}}{f_{yh}}\right)\left(\frac{P}{\phi f_c^{'} A_g}\right) - 0.0084 \qquad \text{(Eq. 3.2)}$$

3. ATC-32 (1996)

$$\rho_s = 0.16\left(\frac{f_c^{'}}{f_{yh}}\right)\left[0.5 + \frac{1.25 P_e}{f_c^{'} A_g}\right] + 0.13\left(\rho_l - 0.01\right) \qquad \text{(Eq. 3.3)}$$

4. PCI Recommended Practice (1993)

$$\rho_s = 0.25\left(\frac{f_c^{'}}{f_{yh}}\right)\left(\frac{A_g}{A_{ch}}-1\right)\left[0.5 + \frac{1.4P}{f_c^{'} A_g}\right] \qquad \text{(Eq. 3.4)}$$

3.2.1.1 ACI-318 (2005) Equation

The equation for spiral reinforcement found in the ACI 318-2005 has been part of the code since 1963. Several tests and experiences show that a section designed by this equation will contain more than an adequate ductility and toughness (ACI, 2005). The amount of spiral reinforcement that the ACI equation provides was developed to ensure the load-carrying capacity of concentrically loaded columns such that their capacity after spalling of cover will equal or slightly exceed the strength based on the unconfined concrete strength and gross sectional area. It is not until the concrete cover spalls off that the effect of the

spiral reinforcement in increasing the load-carrying strength of the core concrete will be recognized (ACI, 2005). Since the focus is on concentrically loaded columns, the transverse reinforcement requirement for concrete sections subjected to flexure and axial loads is not expected to vary as a function of the external axial load and this was witnessed in Figures 2.8 and 2.9.

The significance of the ACI recommendation is the minimum bound portion of the equation. In the development of the new equation, which is hereafter referred to as the ISU equation, this minimum bound should be ensured as this is a requirement for all concrete sections. When meeting this requirement, the applied axial load on the pile will be taken as zero.

According to the ACI 318-2005, the allowable spacing of the transverse steel is not to exceed the smallest of the following:

1. d/4;
2. eight times the diameter of the smallest longitudinal bars;
3. 24 times the diameter of the hoop bars; and
4. 12 inches.

3.2.1.2 New Zealand Standard (2006)

Equation 3.2, based on the work of Watson et al. (1994), is of particular interest as it is the only equation that considers the curvature ductility demand as a variable in the quantification of the amount of transverse reinforcement. The non-simplified version of this equation that includes the curvature ductility demand is presented in Eq. 3.5, whereas the simplified equation, given in Eq. 3.2 and provided below for convenience, assumes a

curvature ductility of 20. The objective in studying this equation is to determine how the curvature ductility could potentially be incorporated into the confinement equation.

$$\rho_s = \frac{(\phi_u / \phi_y - 33 p_t m + 22)}{111}\left(\frac{A_g}{A_{ch}}\right)\left(\frac{f_c^{'}}{f_{yh}}\right)\left(\frac{P}{\phi f_c^{'} A_g}\right) - 0.0084 \qquad \text{(Eq. 3.5)}$$

$$\rho_s = \frac{(1.3 - p_t m)}{2.4}\left(\frac{A_g}{A_{ch}}\right)\left(\frac{f_c^{'}}{f_{yh}}\right)\left(\frac{P}{\phi f_c^{'} A_g}\right) - 0.0084 \qquad \text{(Eq. 3.2)}$$

The permitted center-to-center vertical spacing of transverse reinforcement must be less than one-quarter of either the smallest lateral dimension or the diameter of the column or pier. This limitation is set to ensure adequate confinement of the core concrete. The maximum vertical spacing of the transverse steel is kept relatively small because the concrete is confined mainly by arching between the spiral or hoops. Hence, if the vertical spacing is too large, a significant depth of unconfined concrete will penetrate into the concrete core between the spirals or hoops. This essentially reduces the effectiveness of the confined concrete core section.

3.2.1.3 Applied Technology Council-32 (1996)

The ATC-32 equation ranks as the most influential equation due to the transverse reinforcement requirement with respect to the previously discussed code equations. Figure 3.1 and Figure 3.2 portray the four design equations of interest. Figures 3.1 and 3.2, respectively, provide spiral requirements for a 14-inch square prestressed pile and a 16-inch octagonal prestressed pile with $f_c^{'}$ = 8000 psi, f_{yh} = 60 ksi, and a 2 inches of cover. In these figures, the ATC-32 equation provides the minimum amount of transverse reinforcement in comparison to the other equations of interest. Furthermore, this equation is widely used in

seismic design of bridge columns in the United States and targets a curvature ductility of 13 with the anticipation of having 50 percent more reserve capacity beyond the target value (ATC, 1996).

The tolerable center-to-center spacing of the transverse steel is limited by the smallest of the following:

1. one bar diameter;
2. 1-1/3 times the maximum size of the coarse aggregate; or
3. one inch.

3.2.1.4 PCI Recommended Practice (1993)

The equation that is provided in the PCI Recommended Practice code requires relatively high amounts of transverse reinforcement when compared to the ATC-32 equation. This requirement is specifically necessary in highly ductile regions, and not over the entire length of the pile. The PCI recommended equation is of importance as this provides the current industry practice for designing transverse reinforcement for precast, prestressed piles in high seismic regions. The PCI equation is included in Figures 3.1 and 3.2 to give its relation to the other equations of interest.

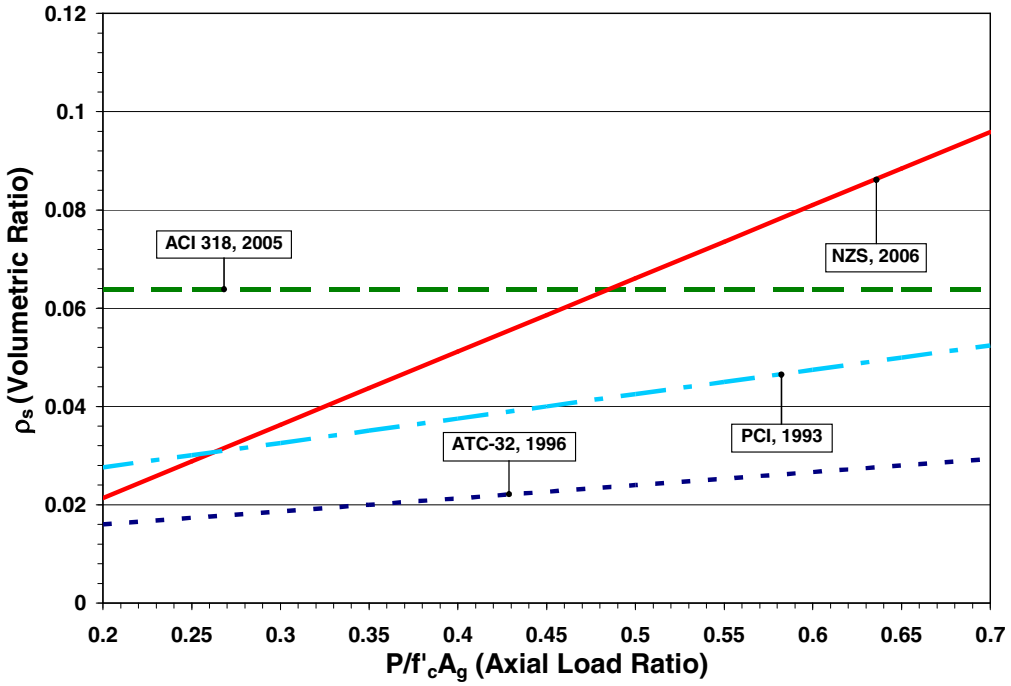

Figure 3.1. Spiral volumetric ratio of the equations of interest for a 14-inch square pile

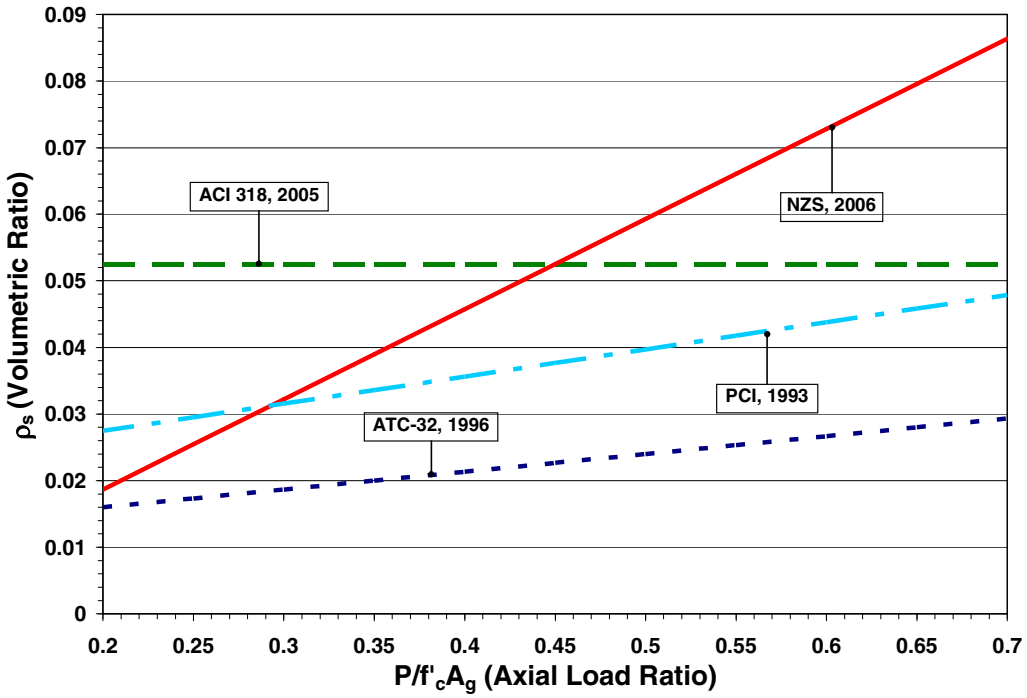

Figure 3.2. Spiral volumetric ratio of the equations of interest for a 16-inch octagonal pile

3.2.2 Process of Development

The process of development of a new equation began with the ATC-32 confinement equation as the basis, which is reproduced below for convenience.

$$\rho_s = 0.16\left(\frac{f_c^{'}}{f_{yh}}\right)\left[0.5 + 1.25\frac{P_e}{f_c^{'}A_g}\right] + 0.13\left(\rho_l - 0.01\right) \qquad \text{(Eq. 3.6)}$$

Several modifications to the above equation were investigated in order to better adapt this equation to prestressed concrete piles. These modifications and the initially recommended equation are presented in the subsequent sections.

3.2.2.1 Modifications to the Base Equation

In examining the ATC-32 equation and assuming $\rho_l = \rho_\rho$, where ρ_ρ is the ratio of prestressed reinforcement, it became apparent the $0.13\left(\rho_l - 0.01\right)$ term will introduce a negative value since ρ_l values in concrete piles are typically less than 0.01. Hence, it was decided that the $\left(\rho_l - 0.01\right)$ term should not be included in the confinement equation required for prestressed piles.

As mentioned in Section 3.2.1, the ACI equation was of interest because of the minimum bound of the equation, provided here for convenience.

$$\rho_s \geq 0.12\left(\frac{f_c^{'}}{f_{yh}}\right) \qquad \text{(Eq. 3.7)}$$

An objective in the development of the ISU equation was to embed the minimum bound of the ACI equation, so that when the applied axial load, *P*, is equal to zero, the resulting requirement for the transverse reinforcement would be the minimum amount of transverse

reinforcement required by ACI 318-05. To achieve this objective, the constant 0.5 in the ATC-32 equation was altered such the new constant times the factor 0.16 would yield 0.12. Hence,

$$0.16 * x = 0.12$$
$$\text{or } x = 0.75$$

Therefore, in addition to dropping the $(\rho_l - 0.01)$ term, the second modification needed in the ATC-32 equation was to replace the constant 0.5 with 0.75.

The axial load, P, was the next parameter that was studied in further detail. The ATC-32 equation considers the axial load to be the applied axial load. In the case of prestressed concrete sections, an additional compressive load is introduced through pre-tensioning of the piles. Priestley et al., (1992), suggests that for prestressed concrete piles, the axial load term within the ATC-32 equation should be altered to $P = P_e + f_{pc}A_g$, where P_e and f_{pc} and A_g are the externally applied axial load, the prestressing force and the cross-sectional area of the pile section, respectively. Investigation of the parameter P, further discussed in a later section in this chapter (i.e., Section 3.4.1), revealed that the axial load parameter in the confinement equation should not include the $f_{pc}A_g$ term, unlike Eqs. 2.11 and 2.12.

The final modification to the ATC-32 equation began with an examination of the parameter A_g. A modification to this parameter was necessary because the transverse reinforcement is to confine the core area and not the gross area. Consequently, the final modification to the ATC-32 equation was to replace the parameter A_g with A_{ch}, to rationalize the confinement equation.

3.2.2.2 Preliminary Equation

Taking the above modifications into account, Eq. 3.8 was established as a preliminary equation to determine the minimum transverse reinforcement required for prestressed concrete piles subjected to a range of axial loads in high seismic regions.

$$\rho_s = 0.16\left(\frac{f_c^{'}}{f_{yh}}\right)\left[0.75 + 1.25\frac{P}{f_c^{'}A_{ch}}\right] \qquad \text{(Eq. 3.8)}$$

The requirement from the above equation is plotted against the previously discussed equations of interest in Figures 3.3 and 3.4. These figures provide spiral reinforcement requirements for a 16-inch and a 24-inch octagonal pile, with $f_c^{'}$ = 8000 psi, f_{yh} = 60 ksi, and 2 inches of cover concrete.

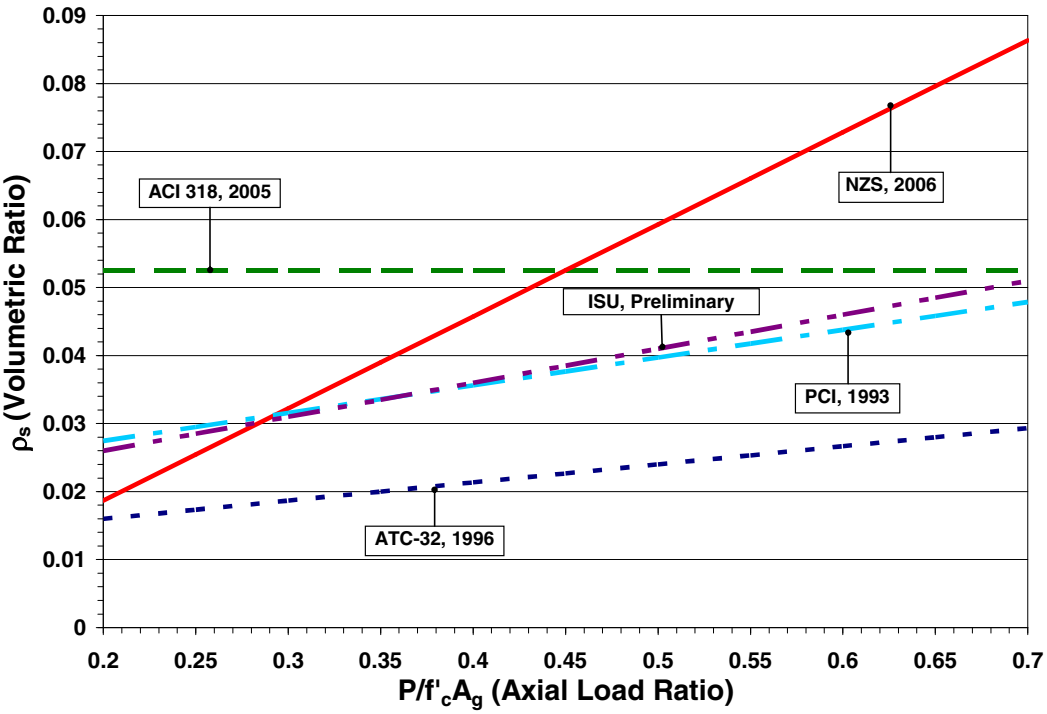

Figure 3.3. Comparison of spiral volumetric reinforcement requirement for a 16-inch octagonal pile with the preliminary equation

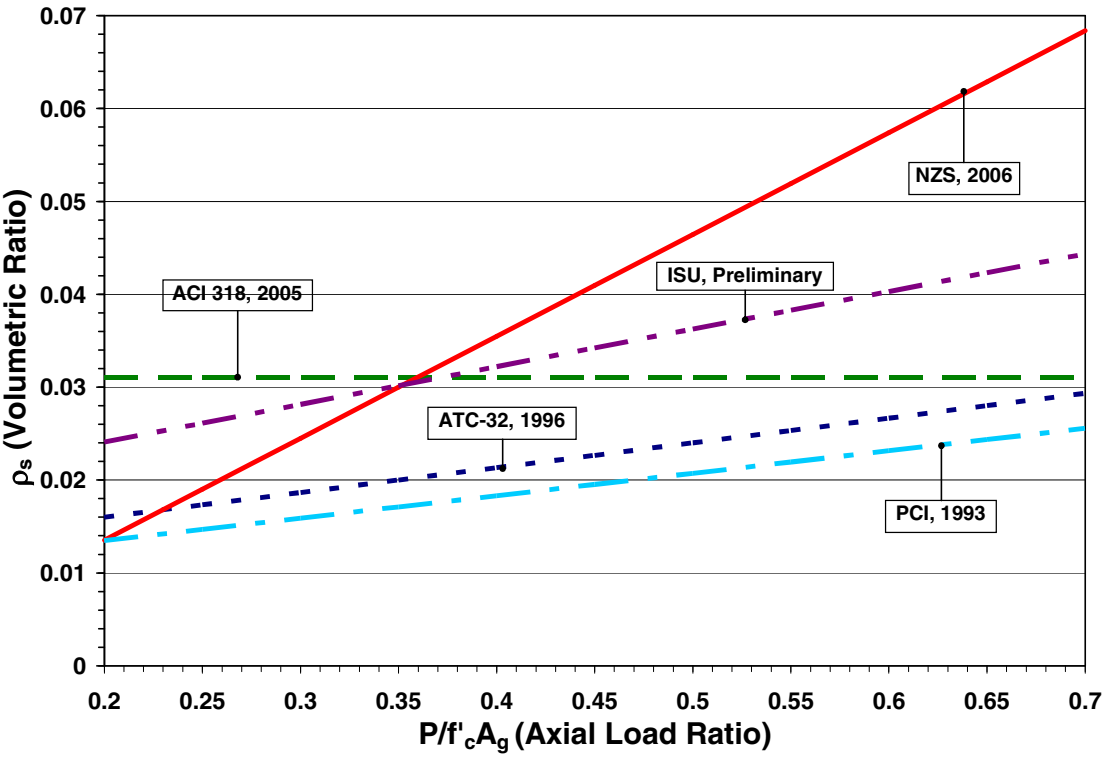

Figure 3.4. Comparison of spiral volumetric reinforcement requirement for a 24-inch octagonal pile with the preliminary equation

From Figures 3.3 and 3.4, it is observed that the preliminary equation and the PCI equation require similar amounts of confinement reinforcement for the 16-inch octagonal pile. However, these requirements differ by a factor of 1.5 for the 24-inch octagonal pile. For both examples, the ATC-32 requirements are as much as 43 percent lower than the requirements according to Eq. 3.8 for the 16-inch octagonal section and 34 percent lower than the requirements for the 24-inch octagonal section.

3.3 Moment-Curvature Analyses

To determine the curvature ductility capacity of a section, it is necessary to perform a moment-curvature analysis. There are several programs available to perform such an

analysis; however, only a few of them are suitable for analyzing prestressed concrete sections. Two such programs were selected for performing moment-curvature analyses in this project: ANDRIANNA (Dowell, 2002) and OpenSees (Mazzoni et al., 2004). These programs are discussed in the subsequent sections, followed by discussion on idealization of the moment-curvature response of prestressed pile sections.

3.3.1 ANDRIANNA

ANDRIANNA is intended to be used as a tool for efficiently analyzing reinforced and prestressed concrete sections under monotonic loading (Dowell, 2002). As a user-friendly program, the input process for ANDRIANNA is fairly straightforward. ANDRIANNA has the capabilities to analyze reinforced concrete as well as prestressed concrete sections. The program is composed of two FORTRAN modules: the GEOmetry pre-processor and the MONOtonic analysis tool. The GEO module allows a detailed section to be defined, while the MONO module performs the monotonic moment-curvature analysis of the section defined in the GEO module.

The GEO module allows a user to define a detailed section with a minimal amount of input. It contains the capabilities to define section holes, confined concrete regions as well as holes within the confined regions. Longitudinal reinforcement can be classified as a straight pattern or a circular pattern, and prestressing strands can be prescribed individually, with an appropriate initial stress for each strand.

The MONO module takes the section described in the GEO module and performs a moment-curvature analysis. In this process, any external axial load is taken into account, as well as definitions of the key properties of materials that make up the section. The material

behavior can be viewed graphically to ensure accuracy of the input data. The stress-strain curves of both the unconfined and confined concrete follow the model recommended by Mander et al. (1988), while the stress-strain curve of the prestressing strand is based on the Menegotto-Pinto model (1973). The effect of confinement may be defined as:

1. volumetric ratios of the transverse confinement reinforcement in the two principal directions; or
2. confining stress and ultimate compressive strain capacity in the two principal directions.

A shortcoming to the program is that the maximum number of fibers that can be used to discretize the section is 30. Therefore this limitation led to the investigation of the program OpenSees for conducting the moment-curvature analyses of prestressed pile sections.

3.3.2 OpenSees

OpenSees, an acronym for Open System for Earthquake Engineering Simulation, is a software framework that allows users to simulate the seismic response of both structural and geotechnical systems (Mazzoni et al., 2004). OpenSees aims to improve the modeling and computational simulation through community input, and is thus continually developing. The capabilities of this software include modeling and analyzing the non-linear response of systems. In OpenSees, moment-curvature analyses are performed as an incremental analysis on a zero length section, defined by two nodes, both located at (0.0, 0.0). The zero-length section is defined using a fiber-based approach, which is outlined below, together with the analysis approach for a prestressed pile section.

- Identify a set of key points that will define the section of the pile
- Create the nodes for the model
- Create the models for materials represented in the section and assign each region of the section with the corresponding material model (i.e., confined concrete, unconfined concrete, prestress strands, etc.)
- Define the element type to be utilized
- Define the external axial load and set the analysis parameters

OpenSees allows sections to be defined by either circles or polygons, or a combination of the two. The octagonal pile sections were thus defined in a fashion similar to that shown in Figure 3.5, while the square sections were defined as illustrated in Figure 3.6. Because OpenSees was eventually used for performing the moment-curvature analyses in this report because of its superior capabilities, the following sections in this chapter include a thorough discussion of the material models used for characterizing the confined and unconfined concrete, and the prestress strands.

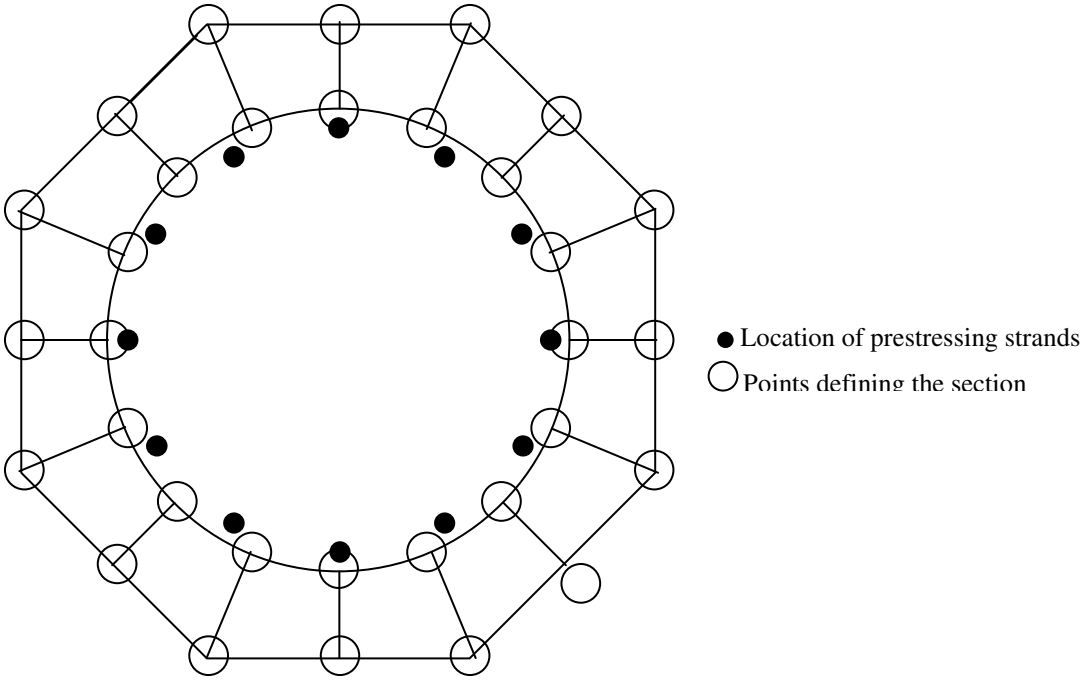

Figure 3.5. Definition of an octagonal pile section in OpenSees

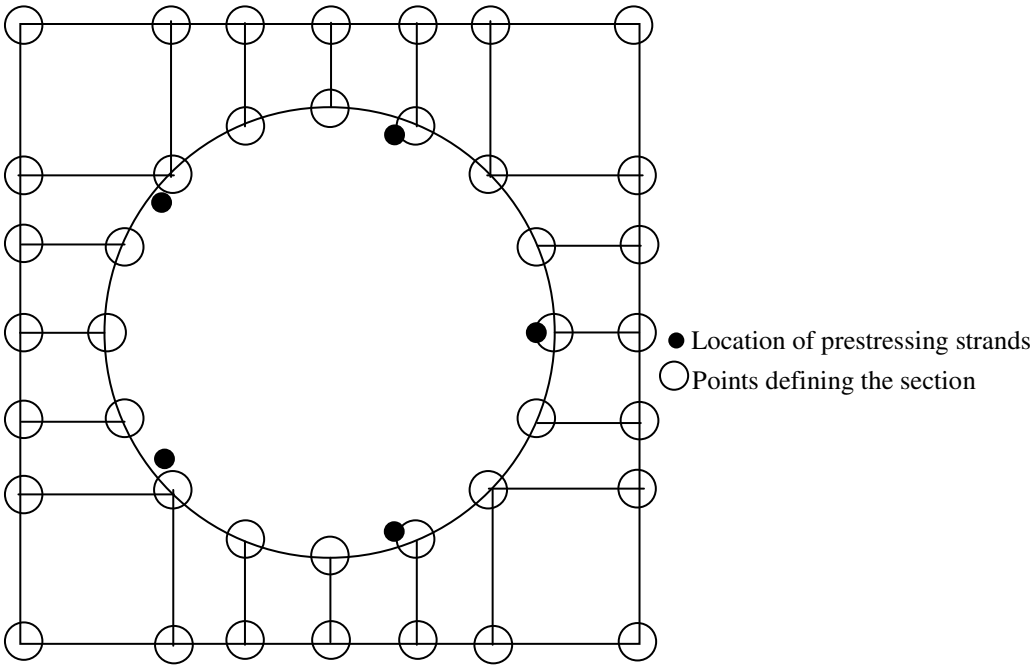

Figure 3.6. Definition of a square pile section in OpenSees

3.3.2.1 Confined and Unconfined Concrete Material Model

The concrete material model that was utilized for the moment-curvature analyses in OpenSees was Concrete06 uniaxial material model. Implemented by Waugh (2007), this material model follows the recommendations of Chang and Mander (1994) with simplification for unloading and reloading hysteretic rules. The model takes eight input parameters to define the monotonic envelope, shown in Figure 3.7. The input is provided in the following form:

uniaxialMaterial Concrete06 $matTag $$f_c$ $$\varepsilon_c$ $$E_c$ $$f_t$ $$\varepsilon_t$ $$x_p$ $$x_n$ $r

where $matTag = unique material tag

$$f_c$ = peak compression stress

$$\varepsilon_c$ = strain at peak compression stress

$$E_c$ = initial elastic modulus of the concrete

$$f_t$ = peak tensile stress

$$\varepsilon_t$ = strain at peak tensile stress

$$x_p$ = non-dimensional strain that determines where the straight line portion begins in tension

$$x_n$ = non-dimensional strain that determines where the straight line portion beings in compression

$r = parameter that controls the descending branch

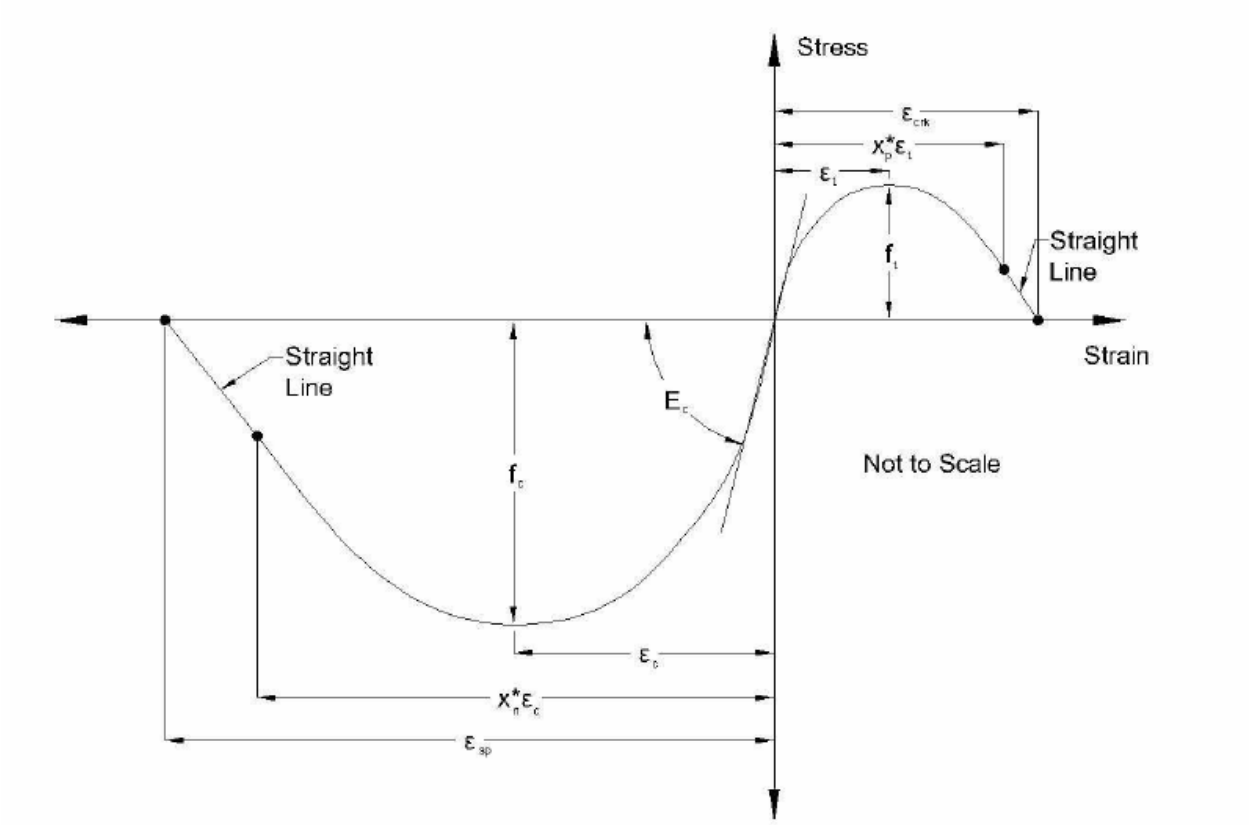

Figure 3.7. Monotonic envelope of Chang and Mander (1994) as shown by Waugh (2007)

Unconfined Concrete

For unconfined concrete with just a peak strength from a cylinder test, the recommended values for the above parameters in US customary units are as follows:

f_{c0} = unconfined cylinder strength (psi)

ε_{c0} = unconfined concrete strain at peak compressive strength

$$\varepsilon_{c0} = \frac{f_c^{'\frac{1}{4}}}{4000} \qquad \text{(Eq. 3.9a)}$$

$$E_c = 185000 * \left(f_c^{'}\right)^{\frac{3}{8}} \quad \text{(psi)} \qquad \text{(Eq. 3.9b)}$$

$$f_t = 7.5 * \sqrt{f_c^{'}} \qquad \text{(psi)} \qquad \text{(Eq. 3.9c)}$$

$$\varepsilon_t = \frac{2 * f_t}{E_c} \qquad \text{(Eq. 3.9d)}$$

$x_p = 2$ (recommended by Waugh)

$x_n = 30$ (recommended by Waugh)

$$r = \frac{f_c^{'}}{750} - 1.9 \qquad \text{(Eq. 3.9e)}$$

Confined Concrete

Confinement increases the strength and the ductility of concrete. To account for these effects, the peak strength and the strain at the peak strength must be increased, while the value of r must be decreased. The confined concrete strength can be calculated based on the following equation:

$$f_{cc}^{'} = f_{c0}^{'} * (1 + k_1 * x') \qquad \text{(Eq. 3.10)}$$

where $f_{cc}^{'}$ = peak concrete strength of confined concrete

$f_{c0}^{'}$ = unconfined peak concrete strength

$$k_1 = A * \left(0.1 + \frac{0.9}{1 + B * x'} \right) \qquad \text{(Eq. 3.11a)}$$

$$x' = \frac{f_{11} + f_{12}}{2 f'_{c0}} \qquad \text{(Eq. 3.11b)}$$

where, f_{11} and f_{12} = maximum lateral confinement pressures in the two orthogonal directions

$$A = 6.886 - (0.6069 + 17.275r) e^{-4.989r} \qquad \text{(Eq. 3.11c)}$$

$$B = \frac{4.5}{\frac{5}{A}\left(0.9849 - 0.6306e^{-3.8939\,r}\right) - 0.01} \qquad \text{(Eq. 3.11d)}$$

$$\varepsilon_{cc} = \varepsilon_{c0}\left(1 + 5k_1 * x'\right) \qquad \text{(Eq. 3.11e)}$$

$$E_c = 185000 * \left(f_c^{'}\right)^{\frac{3}{8}} \qquad \text{(Eq. 3.11f)}$$

$x_n = 30$ (recommended by Waugh)

The ultimate strain capacity and the corresponding strength of the concrete are defined in Concrete06 using the recommendation of Mander et al. (1988). Accordingly,

$$\varepsilon_{cu} = 2 * \varepsilon_{c0} + \frac{1.4 * \rho_x * f_{yh} * \varepsilon_{su}}{f_{cc}^{'}} \qquad \text{(Eq. 3.12)}$$

$$E_{\sec} = \frac{f_{cc}^{'}}{\varepsilon_{cc}} \qquad \text{(Eq. 3.13)}$$

$$r' = \frac{E_c}{E_c - E_{\sec}} \qquad \text{(Eq. 3.14)}$$

$$f_{cu} = \frac{f_{cc}^{'} * \left(\frac{\varepsilon_{cu}}{\varepsilon_{cc}}\right) * r'}{r' - 1 + \left(\frac{\varepsilon_{cu}}{\varepsilon_{cc}}\right)^{r'}} \qquad \text{(Eq. 3.15)}$$

The simplest way to determine f_{cu} is to calculate the ultimate strain and stress from Eq. 3.12 and Eq. 3.15, and then iterate on r using Eq. 3.16. This iteration requires the use of an equation solver or the command "goal seek" in EXCEL. It is possible to solve for r in a closed form; however, the resulting equation is very complicated and harder to use than

solving iteratively for *r* (Waugh, 2007). The values of *r* for this study ranged from 1.3 to 2.15.

$$f_{cu} = f_{cc}^{'}\left(\frac{n*\left(\frac{\varepsilon_{cu}}{\varepsilon_{cc}}\right)}{1+\left(n-\frac{r}{r-1}\right)\left(\frac{\varepsilon_{cu}}{\varepsilon_{cc}}\right)+\frac{\left(\frac{\varepsilon_{cu}}{\varepsilon_{cc}}\right)^{r}}{r-1}}\right) \qquad \text{(Eq. 3.16)}$$

$$n = \frac{E_c * \varepsilon_{cc}}{f_{cc}^{'}} \qquad \text{(Eq. 3.17)}$$

3.3.2.2 Material Model for Prestressing Strands

The prestressing strands in pile sections were modeled using two uniaxial material objects, which represent the uniaxial stress-strain relationships. The specific commands that were utilized for the moment-curvature analyses of the pile sections were the elastic-perfectly-plastic uniaxial material object and elastic-perfectly-plastic gap uniaxial material object. The input of the elastic perfectly-plastic uniaxial material model is in the following form:

uniaxialMaterial ElasticPP $matTag $E $epsyP <$epsyN $eps0>

where $matTag = unique material object integer tag

$E = tangent

$epsyP = strain or deformation at which material reaches plastic state in tension

$epsyN = strain at which material reaches plastic state in compression (optional, default: tension value)

$eps0 = initial strain (optional, default: zero)

Figure 3.8 provides a graphical view of the input parameters for the elastic perfectly-plastic uniaxial material object.

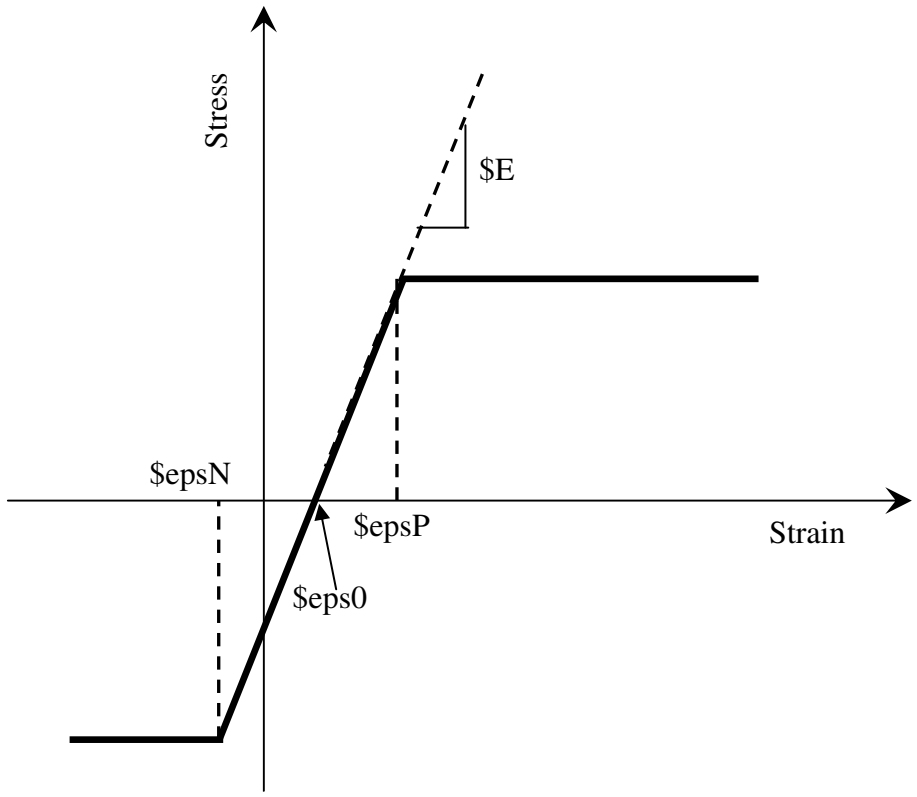

Figure 3.8. Input parameters required for an elastic-perfectly-plastic uniaxial material object in OpenSees (Mazzoni et al., 2004)

The input of the elastic perfectly-plastic gap uniaxial material model is in the following form:

uniaxialMaterial ElasticPPGap $matTag $E $Fy $gap

where $matTag = unique material object integer tag

$E = tangent stiffness

$Fy = stress or force at which material reaches plastic state

$gap = initial gap (strain or deformation)

It should be noted that in order to create a compression-only gap element, NEGATIVE values need to be specified for $Fy and $gap. Figure 3.9 provides a graphical view of the expected material behavior and the input parameters needed for a tension gap, while Figure 3.10 provides the same information for a compression gap. Appendix C contains a sample input used for a moment-curvature analysis that was performed in OpenSees.

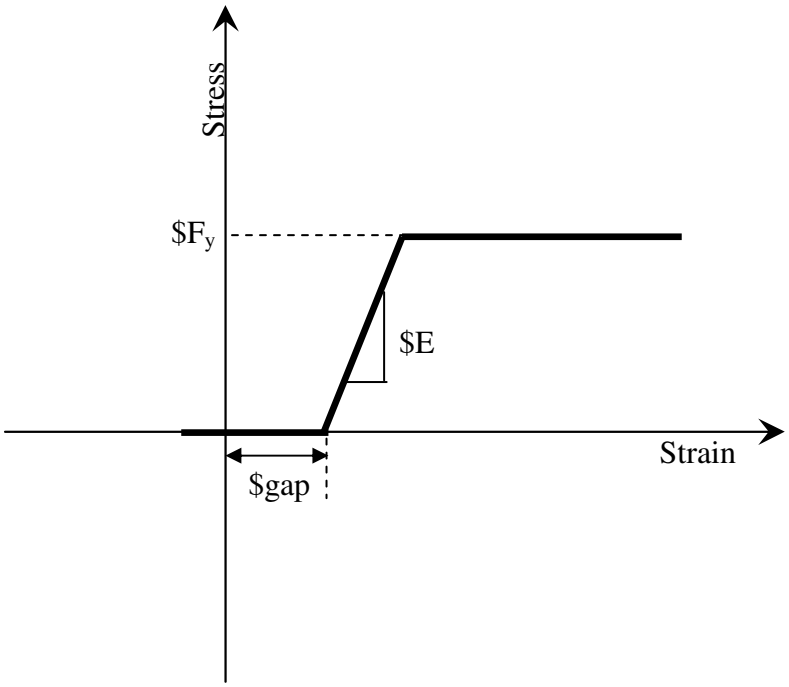

Figure 3.9. Input parameters required for an elastic-perfectly-plastic tension gap uniaxial material object (Mazzoni et al., 2004)

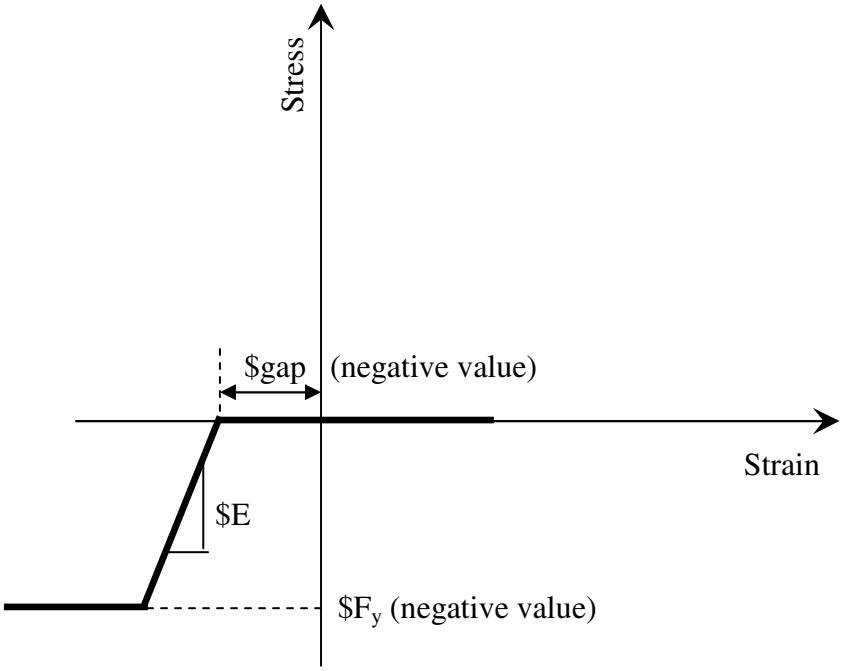

Figure 3.10. Input parameters needed for an elastic-perfectly-plastic compression gap uniaxial material object (Mazzoni et al., 2004)

Analysis was conducted to verify the results of the two programs. A 16-inch octagonal section, with $f_c^{'}$ = 6000 psi, f_{pc} = 700 psi, and an axial load ratio of 0.2 was analyzed using ANDRIANNA and OpenSees. The moment-curvature responses of both analyses are plotted in Figure 3.11.

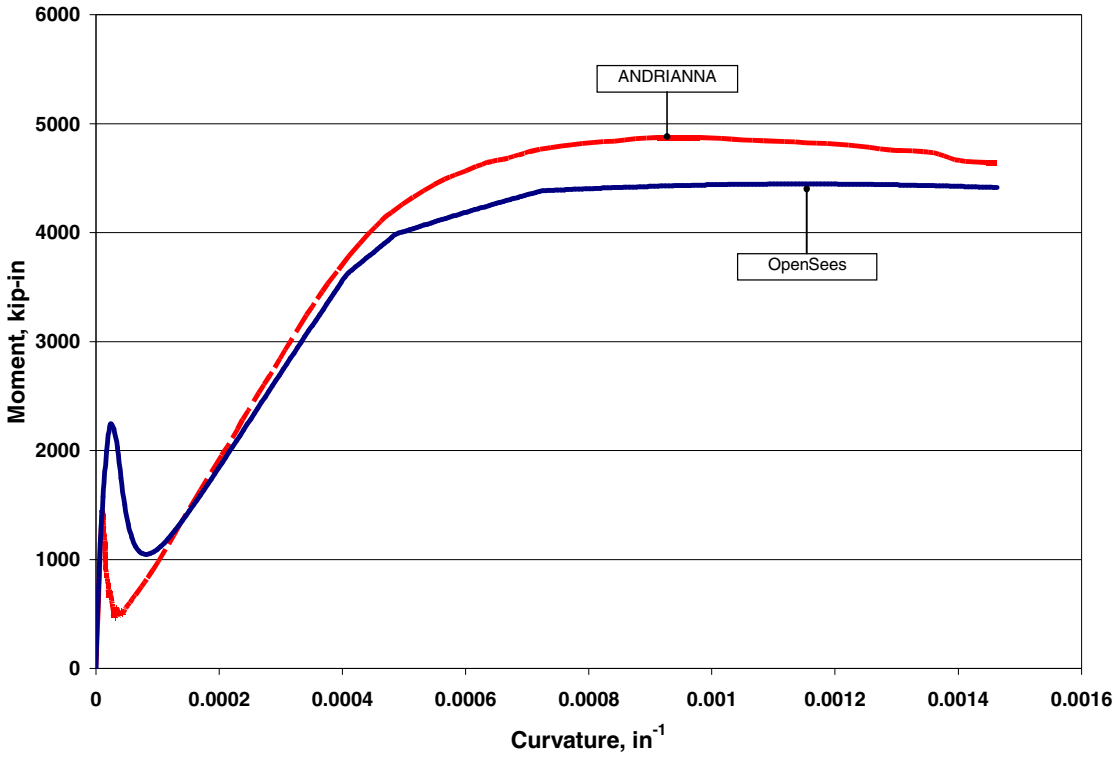

Figure 3.11. Moment-curvature response comparing ANDRIANNA and OpenSees

With fairly similar behavior confirming the accuracy of both programs, OpenSees was chosen for conducting the analyses in this project for the following reasons:

- it offers more control related to the fiber size;
- it contains more support avenues, as it is a program that is constantly being developed; and
- it offers a variety of material models that are advantageous for verifying the behavior of given materials.

3.3.3 Moment-Curvature Idealization

A moment-curvature response may be better idealized using a bi-linear approximation (Priestley et al., 1996), although an elastic perfectly-plastic approximation has been

suggested in some documents (i.e., Caltrans, 2004). This idealization is necessary to determine the yield and ultimate curvatures so that the curvature ductility capacity of a concrete section can be defined. In order to idealize a moment-curvature response, some key moments and the corresponding curvatures must be identified. These moments include the first yield moment, the ultimate moment, and the nominal moment of the cross section of a member. Defining these moments and corresponding curvatures consistently is of paramount importance so that the effects of various parameters on curvature ductility capacity can be adequately studied.

These key moments and curvatures can be easily identified in reinforced concrete sections, in which the first yield condition is typically defined by the first yielding of the mild steel reinforcement. However, there are several challenges involved in defining the idealized moment-curvature response of prestressed sections, especially piles that are detailed with only prestressing steel and large cover concrete. Due to the limited information on idealization of prestressed concrete piles in literature, several different options for idealizing moment-curvature responses of prestressed concrete piles were explored. The following subsections present details of the finalized idealization along with the challenges that were associated with this process.

3.3.3.1 First Yield Moment

A bi-linear idealization should have an elastic portion, followed by a plastic portion. For prestressed concrete sections, the first yield moment cannot be related to the yielding of the longitudinal reinforcement for two reasons:

1. the yielding of prestressing steels is not well defined (Naaman, 2004);

2. the non-linearity in a prestressed section is typically initiated by the non-linear response of concrete as demonstrated in Figure 3.12.

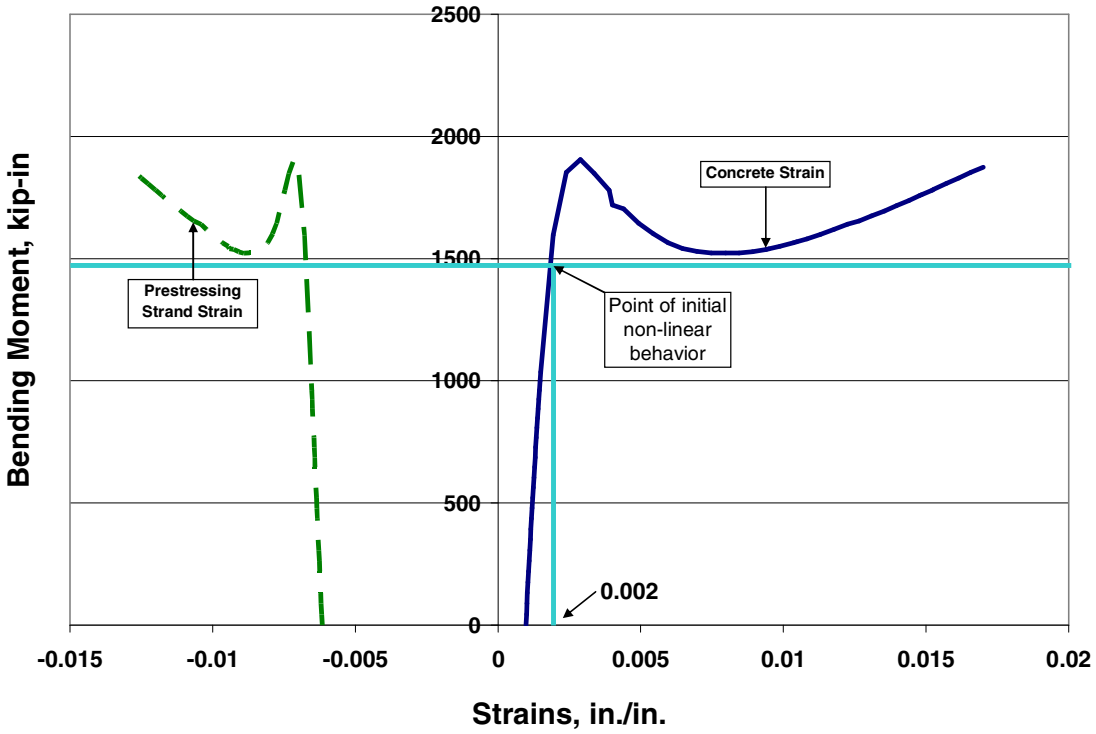

Figure 3.12. Concrete and prestress steel strains versus moment for a 16-inch prestressed concrete octagonal pile section

Therefore, the first yield moment for prestressed concrete piles is defined using a concrete strain of 0.002 in/in, which is the strain associated with the initial non-linear behavior of concrete, as illustrated in Figure 3.12. The first yield curvature, $\phi_y^{'}$, is thus equal to the curvature corresponding to a concrete strain value of 0.002 in./in. or the first yield moment.

3.3.3.2 Ultimate Moment

Using the information found in the literature, the ultimate moment was characterized by one of the following three conditions, whichever occurs first:

1. the ultimate moment is equal to 80 percent of the peak moment resistance of the section;
2. the moment corresponding to the first occurrence of a strain of 0.04 in./in. in a prestressing strand;
3. the moment associated with a strain in the extreme compression fiber of the core concrete equal to the ultimate concrete strain of ε_{cu}, defined by Eq. 2.4.

In all of the analyses performed as part of this study, the ultimate moment was controlled by the third condition.

3.3.3.3 Nominal Moment

For normal reinforced concrete sections, the nominal moment capacity is defined as the moment associated with the strain in the extreme concrete compressive fiber equal to a value of 0.004 in./in. or the strain in the longitudinal reinforcement equal to a value of 0.015 in/in, whichever occurs first (Priestley et al., 1996). Using this information, the yield curvature is found by extrapolating the elastic portion of the idealized curve (i.e., by a line extending from the origin to the point defining the first yield) to the nominal moment capacity, which can be expressed as follows:

$$\phi_y = \frac{M_n}{M'_y}\phi'_y \qquad \text{(Eq. 3.18)}$$

where ϕ_y = yield curvature

M_n = nominal moment capacity

M'_y = first yield moment

ϕ'_y = first yield curvature

Figure 3.13 portrays a moment-curvature relationship for a normal concrete section and identifies the first yield moment, first yield curvature, nominal moment capacity, and yield curvature as defined by Eq. 3.18.

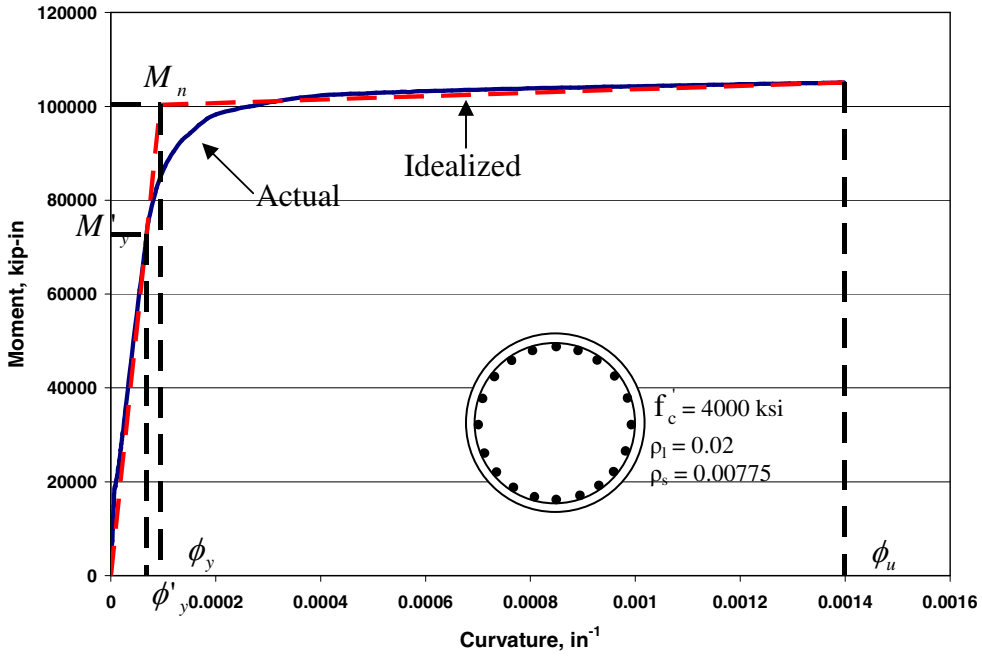

Figure 3.13. Moment-curvature response for a normal concrete section and idealized response

The moment-curvature responses of prestressed concrete pile sections have somewhat unique characteristics. An example of this response is shown in Figures 3.14a, 3.14b, and 3.14c, in which it is seen that a large dip in the moment value follows the first peak due to spalling of the cover concrete that initiates as the extreme cover concrete reaches a strain of approximately 0.003 in./in. The prestressed concrete piles represented in Figures 3.14a, 3.14b, and 3.14c have the following characteristics: axial load ratio of 0.2, f_c' of 6000 psi, and f_{pc} of 1100 psi. Furthermore, it is noted that the pile sections typically have no mild steel reinforcement and thus using a steel strain of 0.015 is meaningless. With this in mind, defining the nominal moment capacity using a concrete strain of 0.004 in./in. or a strain value

in extreme prestressing stand was investigated. However, neither of these definitions provided satisfactory idealized responses for the moment-curvature response of prestressed pile sections. Consequently, an alternative definition was established for the idealized moment-curvature of these pile sections.

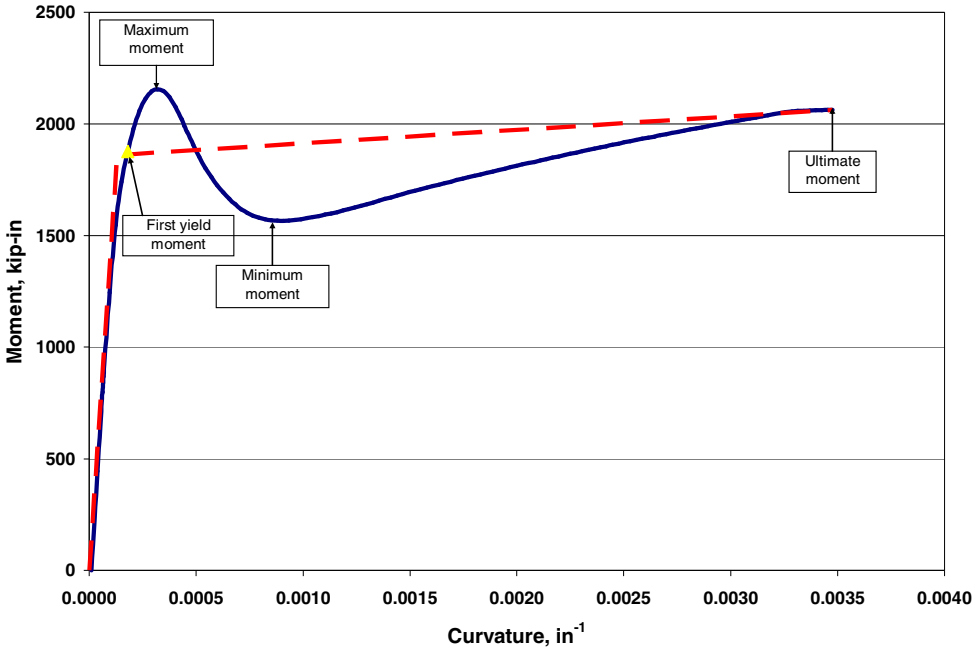

Figure 3.14a. Moment-curvature response of a 16-inch octagonal shaped prestressed concrete pile section

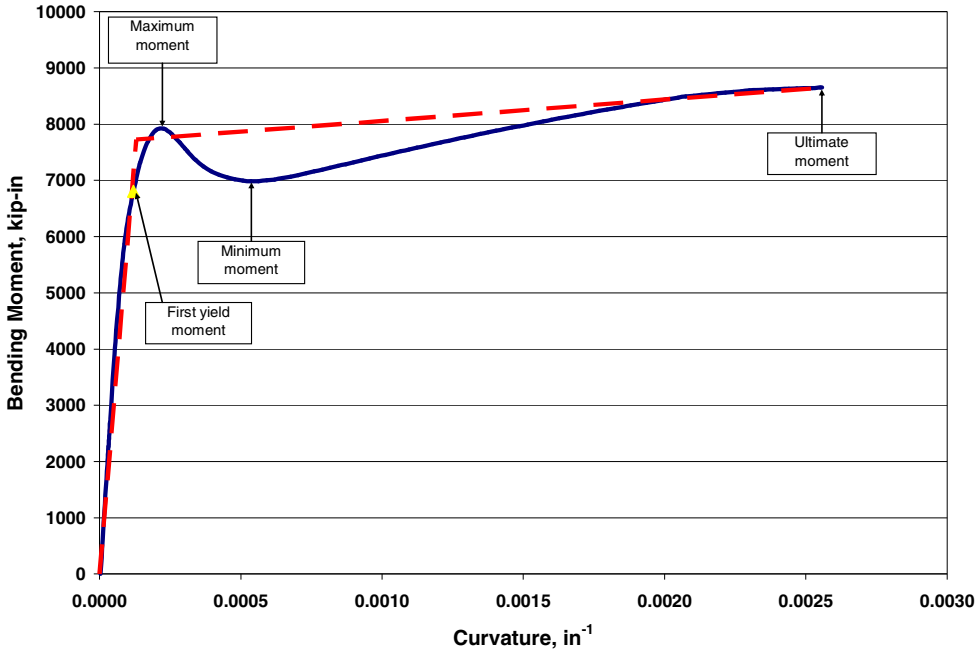

Figure 3.14b. Moment-curvature response of a 24-inch octagonal shaped prestressed concrete pile section

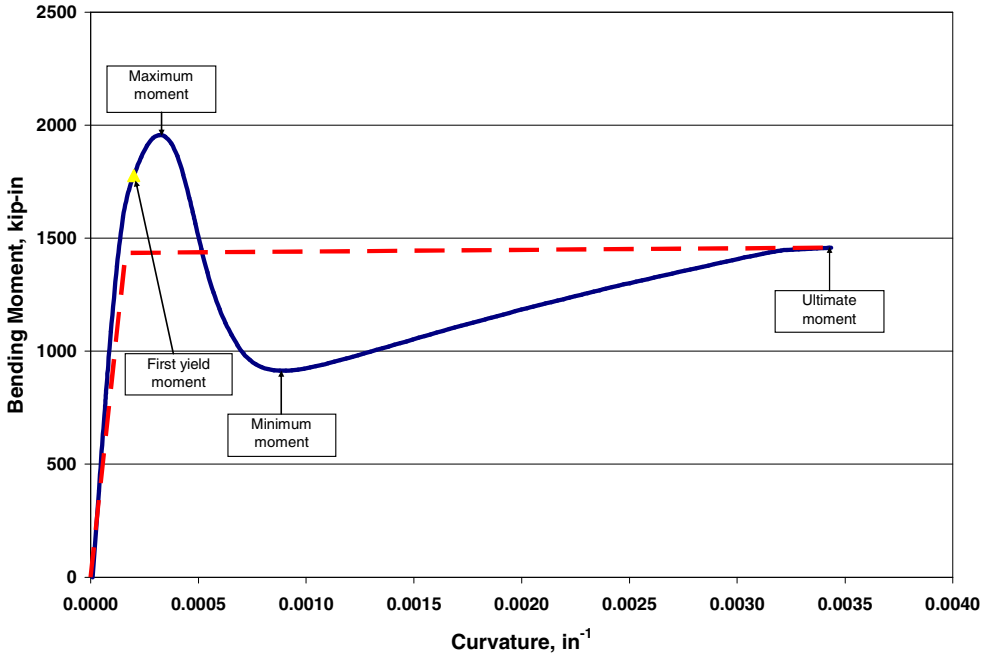

Figure 3.14a. Moment-curvature response of a 14-inch square shaped prestressed concrete pile section

With the presence of the dip in the moment-curvature relationship (see Figure 3.14), the second line in the bi-linear idealization of a prestressed pile section needed to be defined in a manner that would provide an approximate balance of the areas between the actual and the idealized moment-curvature curves, beyond the first yield point. Of the different options considered, the average of the maximum moment and the minimum moment that occurred between the first yield moment and the ultimate moment was found to be reasonably consistent and simple to define the nominal moment capacity of prestressed concrete pile sections. Note that the minimum moment would typically occur when the cover concrete is completely crushed, whereas the maximum moment may correlate with the ultimate moment capacity of the section. In the remainder of this report, this nominal moment definition is consistently used for prestressed pile sections along with Eq. 3.18 to find the yield curvature. In Figures 3.14a, 3.14b, and 3.14c the idealized response (as per the definition presented above) is included, which shows a satisfactory correlation between the actual and idealized responses.

3.3.4 Analysis Variables

In the evaluation of the adequacy of the confinement reinforcement requirements for prestressed pile sections, varying the following variables was considered important.

- $f_c^{'}$
- f_{pc}
- Section dimensions and shapes
- Axial load ratio, defined by $\dfrac{P_e}{f_c^{'} A_g}$ (Eq. 3.19)

The $f_c^{'}$ values that were investigated were 6000 psi, 8000 psi, and 10000 psi, while the f_{pc} were varied in the range from 700 psi to $0.2 f_c^{'}$. The different pile sections that were considered for this project were the 16-inch octagonal pile section, 24-inch octagonal pile section, and 14-inch square pile section. Figure 3.15, 3.16, and 3.17 summarize the different analysis cases chosen for evaluation of the preliminary transverse reinforcement requirements presented in Eq. 3.8. The sections to follow discuss in detail the variations used for the axial load ratios.

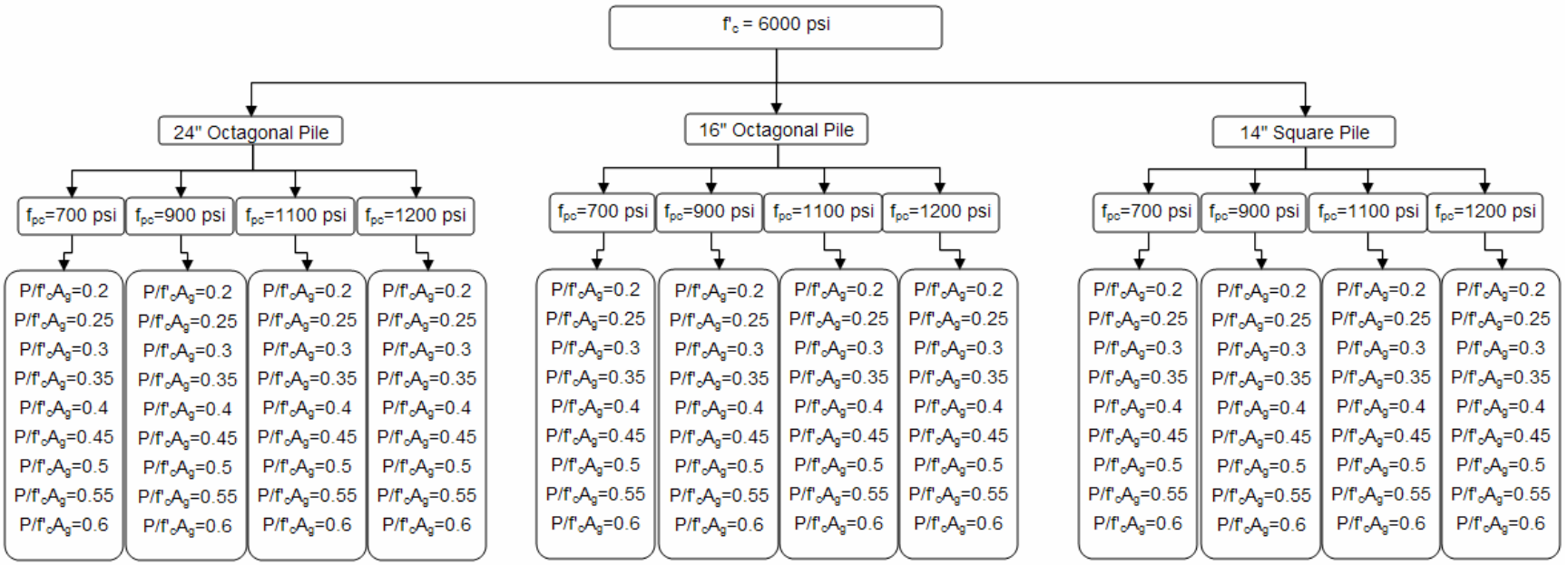

Figure 3.15. Details of different pile sections selected for evaluation of the preliminary confinement equation with $f_c^{'}$ equal to 6000 psi and f_{pc} values of 700 psi, 900 psi, 1100 psi, and 1200 psi

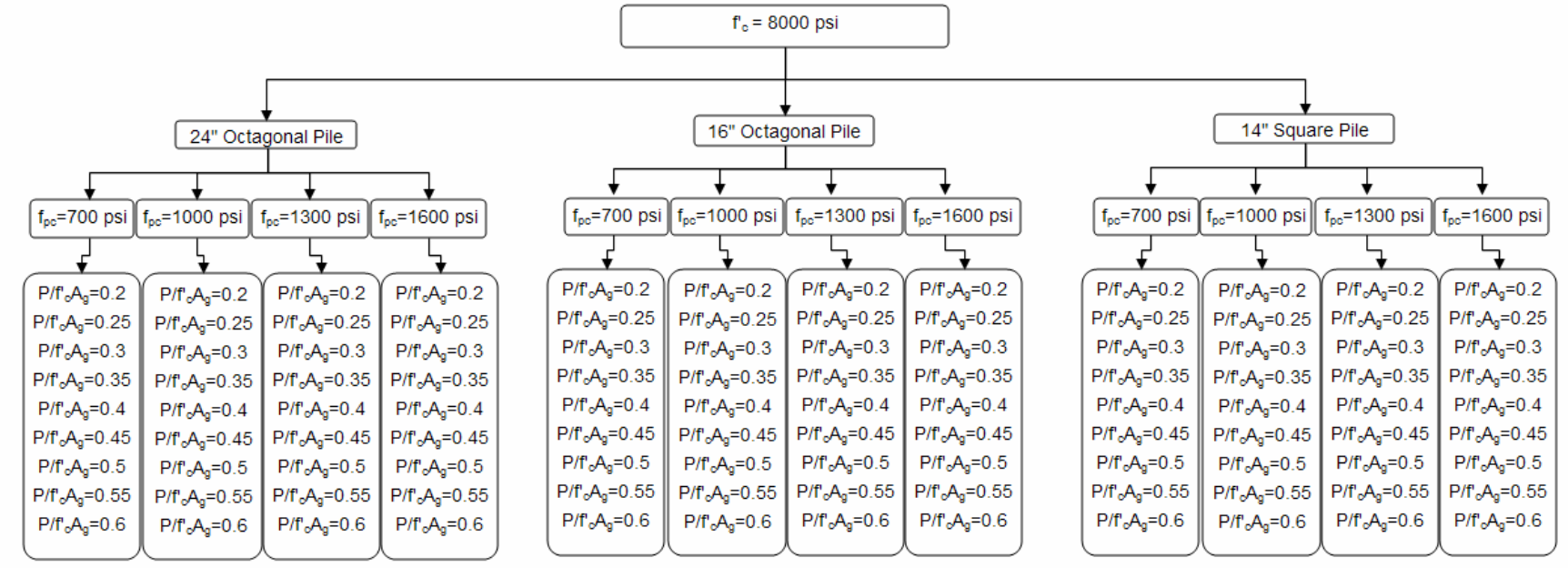

Figure 3.16. Details of different pile sections selected for evaluation of the preliminary confinement equation with $f_c^{'}$ equal to 8000 psi and f_{pc} values of 700 psi, 1000 psi, 1300 psi, and 1600 psi

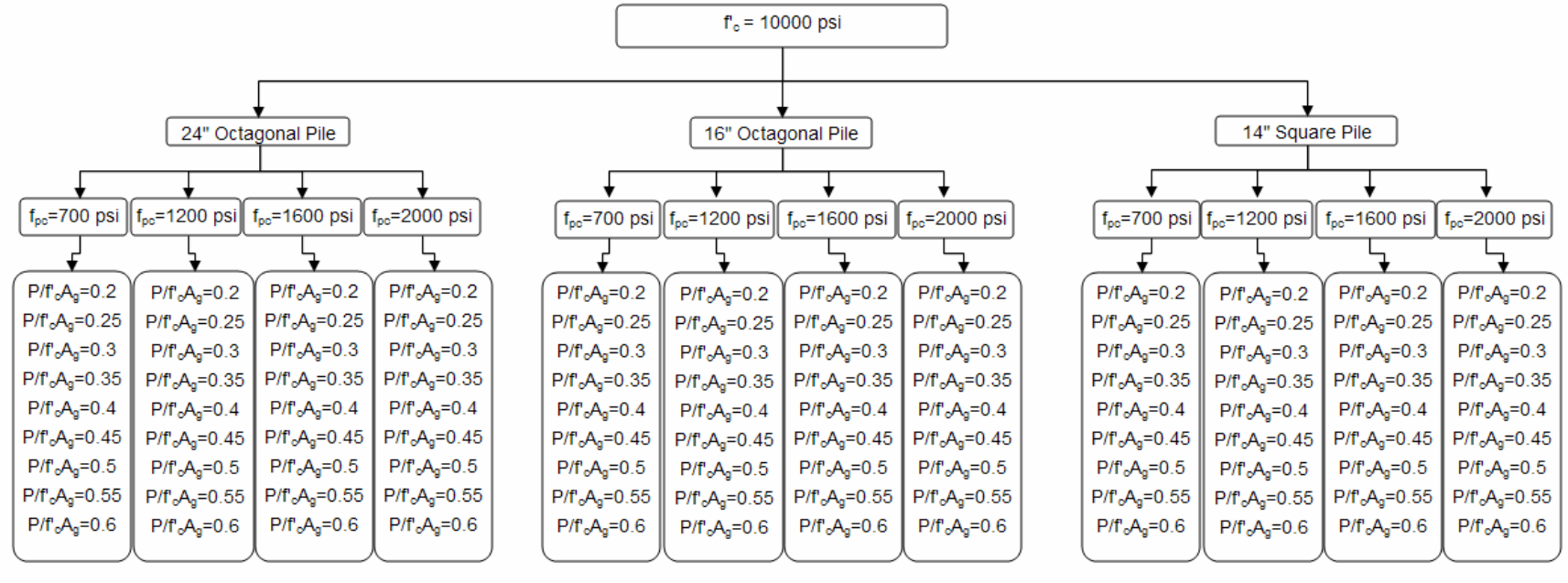

Figure 3.17. Details of different pile sections selected for evaluation of the preliminary confinement equation with $f_c^{'}$ equal to 10,000 psi and f_{pc} values of 700 psi, 1200 psi, 1600 psi, and 2000 psi

3.3.4.1 Limits n External Axial Load Ratios

According to the PCI Design Handbook (2004), the allowable external axial load, *N*, which a pile may be subjected to is described in the following form:

$$N = \left(0.33 f_c^{'} - 0.27 f_{pc}\right) A_g \qquad \text{(Eq. 3.20)}$$

Through rearrangements of the variables in the above equation, the limitations on the axial load ratio were examined as follows:

$$\frac{N}{f_c^{'} A_g} = \left(0.33 - 0.27 \frac{f_{pc}}{f_c^{'}}\right) \qquad \text{(Eq. 3.21)}$$

The PCI Design Handbook specifies limits on the compressive stress in the concrete at the centroid of the cross section due to the prestressing after losses, f_{pc}, to a range between 700 psi and $0.2 f_c^{'}$. Assuming $f_c^{'}$ = 10,000 psi to estimate the maximum possible axial load ratio, and inserting 700 psi for f_{pc} into Eq. 3.21 gives:

$$\frac{N}{f_c^{'} A_g} = \left(0.33 - 0.27 \frac{(700)}{10000}\right)$$

$$= \left(0.33 - 0.27(0.07)\right)$$

$$= 0.28$$

Assuming $f_c^{'}$ = 10,000 psi to estimate the maximum possible axial load ratio, and inserting 0.2 times 10,000 psi for f_{pc} into Eq. 3.21 gives

$$\frac{N}{f_c^{'} A_g} = \left(0.33 - 0.27 \frac{(0.2(10000))}{10000}\right)$$

$$= \left(0.33 - 0.27(0.2)\right)$$

= 0.31

Accordingly, the resulting limit on the external axial load ratio for prestressed piles is 0.28 to 0.31. Therefore, it appears that prestressed piles summarized in Figures 3.15, 3.16, and 3.17 should not be subjected to an axial load ratio greater than about 0.3. However, this limitation on the axial load ratio was considered irrelevant for two reasons:

1. a rationale for enforcing Eq. 3.20 could not be found; and
2. precast piles shown in Figures 3.15, 3.16, and 3.17 with axial load ratios larger than 0.28 to 0.31 are used in current practice.

3.3.4.2 New Limits on Axial Load Ratios

In this report, a new limit for the external axial load ratios is suggested for prestressed piles using two key curvature values: the curvature when crushing initiates in unconfined concrete and spalling begins, ϕ_{sp}, and the curvature corresponding to the cracking moment, ϕ_{cr}. The moment at which the crushing of the unconfined concrete begins was defined using a concrete strain of 0.004 in./in.

The cracking moment for a prestressed concrete section is defined using the equation in the PCI Design Handbook (2004) as

$$M_{cr} = S_{bc}\left[\frac{P}{A} + \frac{Pe}{S_b} + f_r\right] - M_{nc}\left(\frac{S_{bc}}{S_b} - 1\right) \qquad \text{(Eq. 3.22)}$$

where S_{bc} = section modulus with respect to the tension fiber of the prestressed composite section;

P = a combination of the externally applied design load and the prestress force after losses;

A = cross-sectional area;

e = eccentricity of design load or prestressing force parallel to the axis measured from the centroid of the section;

S_b = section modulus with respect to the bottom fiber of the precast section

f_r = modulus of rupture of concrete; and

M_{nc} = moment due to beam self weight plus dead loads applied before composite action.

Several of the terms in the Eq. 3.22 can be eliminated when finding the cracking moment of prestressed concrete pile sections. With the assumptions of concentrically applied axial load with the centroid of the pile section and a uniformly distributed strand pattern, the eccentricity term may be eliminated in Eq 3.22. Furthermore, the moment associated with self weight is also not required except for the fact that the self weight of the pile may increase the axial load, which can be included in P. Therefore, the cracking moment equation can be reduced to

$$M_{cr} = S_{bc}\left[\frac{P}{A} + f_r\right] \qquad \text{(Eq. 3.23)}$$

Upon determination of curvatures at the cracking moment and at the moment corresponding to the first crushing of the cover concrete, which corresponds to a concrete strain of 0.004 in/in, the dependency of the moment-curvature response of pile sections on the order in which these two events occurred was investigated. It became apparent that if the curvature associated with the cracking of concrete is less than the curvature associated with the spalling of concrete, the moment-curvature response was found to be dependable with a small dip associated with spalling of the cover concrete and a difference of less than about 20

percent between the idealized moment and the actual resistance at any given curvature, as illustrated in Figure 3.18. However, if ϕ_{cr} is greater than ϕ_{sp}, as in Figure 3.19, the moment drop due to spalling was significant and the difference between the idealized moment and the actual resistance, at any given curvature, was as high as 80 percent. This behavior, influenced by large axial loads on the piles, was considered unacceptable for piles in seismic regions. Therefore, it was concluded that the axial load in prestressed piles should be limited such that ϕ_{cr} will not exceed ϕ_{sp}.

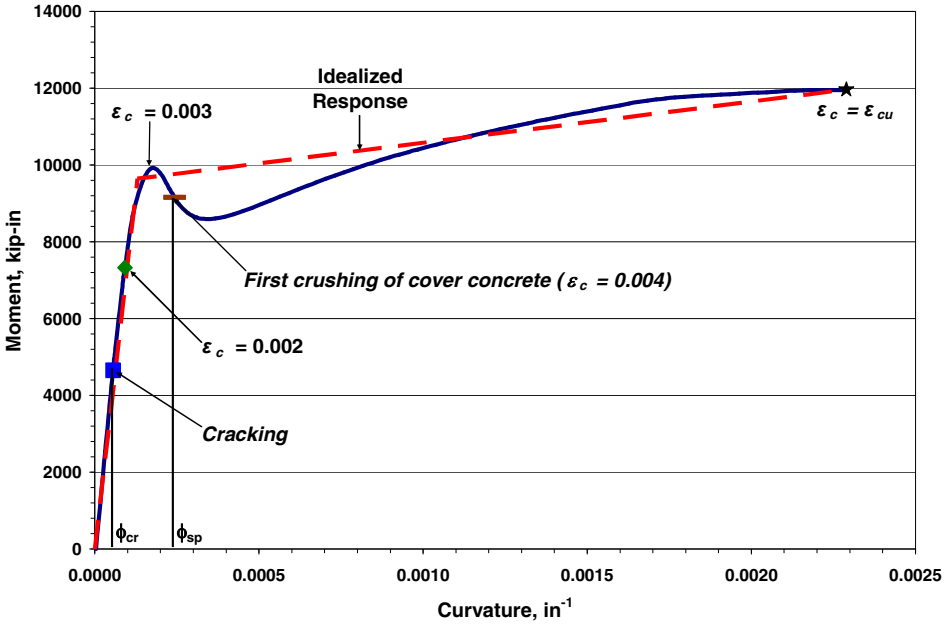

Figure 3.18. Moment-curvature response showing the case of $\phi_{cr} < \phi_{sp}$ for a 24-inch octagonal prestressed pile section with axial load ratio of 0.3, f_c' of 8000 psi, and f_{pc} of 1300 psi

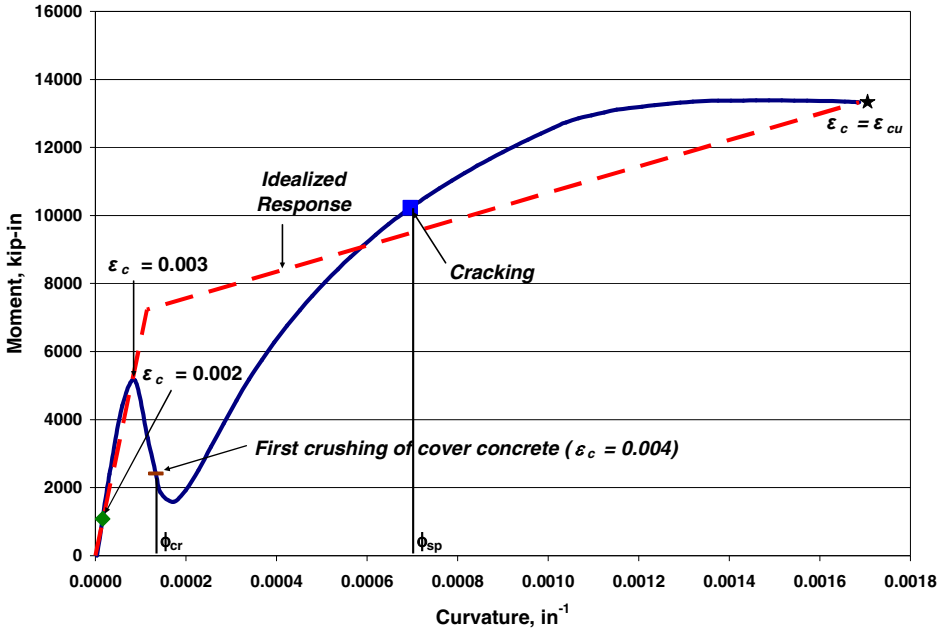

Figure 3.19. Moment-curvature response showing the case of ϕ_{cr} << ϕ_{sp} for a 24-inch octagonal prestressed pile section with axial load ratio of 0.6, $f_c^{'}$ of 10000 psi, and f_{pc} of 1600 psi

3.4 Improvements to the Preliminary Equation

The suitability of the preliminary equation, provided below for convenience, for quantifying the minimum confinement reinforcement was examined by performing moment-curvature analyses on 16-inch and 24-inch octagonal piles, as well as 14-inch square pile sections and estimating their curvature ductility capacities as per Eq. 3.24:

$$\rho_s = 0.16\left(\frac{f_c^{'}}{f_{yh}}\right)\left[0.75+1.25\frac{P}{f_c^{'}A_{ch}}\right] \qquad \text{(Eq. 3.24)}$$

$$\mu_\phi = \frac{\phi_u}{\phi_y} \qquad \text{(Eq. 3.25)}$$

The values of ϕ_y and ϕ_u were obtained using the moment-curvature idealization presented in Section 3.3.4.2. It was observed that the curvature ductility typically increased as the applied axial load ratio increased, resulting in a spread of the curvature ductility capacity in the range of 19 to 28 for the octagonal prestressed pile sections. The analysis of the square section resulted in a curvature ductility range of 12 to 47. It was thus concluded that the dependency of the preliminary confinement equation on the axial load ratio was too large. With this in mind, the constant terms of the equation, specifically the 0.16 and the 0.75 were investigated in order to lessen the dependency of the equation on the axial load ratio. Through a small set of section analyses, it was determined that the two constants needed to be replaced by 0.06 and 2.8, respectively. With this change, the confinement equation can be expressed as

$$\rho_s = 0.06 \frac{f_c^{'}}{f_{yh}} \left(2.8 + \frac{1.25P}{f_c^{'} A_{ch}} \right) \qquad \text{(Eq. 3.26)}$$

In Eq. 3.26, if the axial load on the pile is zero, the minimum amount of transverse reinforcement results in

$$\rho_s = 0.168 \frac{f_c^{'}}{f_{yh}} \qquad \text{(Eq. 3.27)}$$

Eq. 3.27 requires 40 percent greater than what the ACI code requires as its minimum reinforcement. Although this increase in the minimum requirement of transverse reinforcement is necessary to lessen the dependency of the confinement equation on the axial load, it is noted that the resulting minimum confinement reinforcement is generally less than that currently used in practice. Furthermore, it is important to realize that the 40 percent increase in the minimum reinforcement corresponds to a 63 percent reduction on the equation's dependency on the axial load ratio. Such a modification is expected to help

quantify the confinement reinforcement with adequate consideration to both the flexural action and the external axial load. As discussed in Section 3.2.2.1, the minimum reinforcement requirement corresponding to zero axial load is reduced to smaller values when the design calls for moderate or low ductility in the prestressed pile sections.

Figures 3.20 and 3.21 show the spiral requirements, respectively, for a 14-inch and a 24-inch octagonal pile with $f_c^{'}$ = 8000 psi, f_{yh} = 60 ksi, and 2 inches of cover concrete. From these figures, it is observed that the modified equation nearly consistently requires less confinement reinforcement than that stipulated by the preliminary equation. The exception to this occurs for piles with larger sections subjected to small axial load ratios. Also observed in these figures is that the modified equation shows less increase in the confinement reinforcement as the axial load increases. Recall that in comparison to the ATC-32 requirements, the preliminary ISU equation differed as much as 43 percent lower than the ATC-32 requirements for a 14-inch octagonal section and 34 percent for a 24-inch octagonal section. The difference between the preliminary ISU equation and the ATC-32 equation is approximately 34 percent for the 24-inch octagonal section, regardless of the axial load ratio. With the modified ISU equation, the difference increases slightly to 37 percent for lower axial load ratios, but is significantly reduced to 12 percent for higher axial load ratios. These differences should not be of a concern as they provide reinforcement for different mean ductility values as detailed in Section 3.4.1.

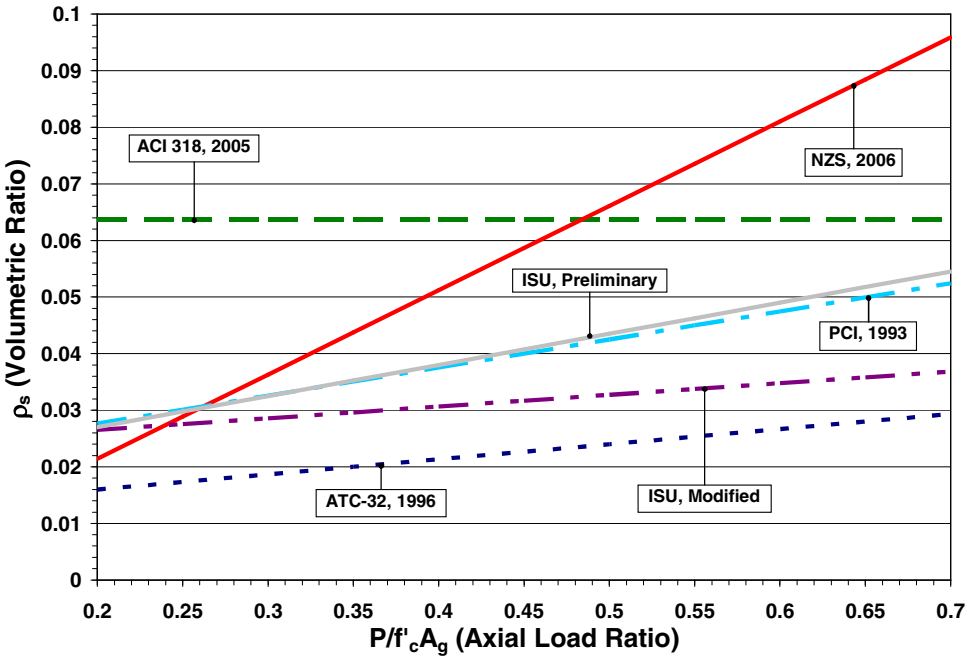

Figure 3.20. Spiral volumetric ratio comparison for a 14-inch octagonal pile with the modified ISU equation

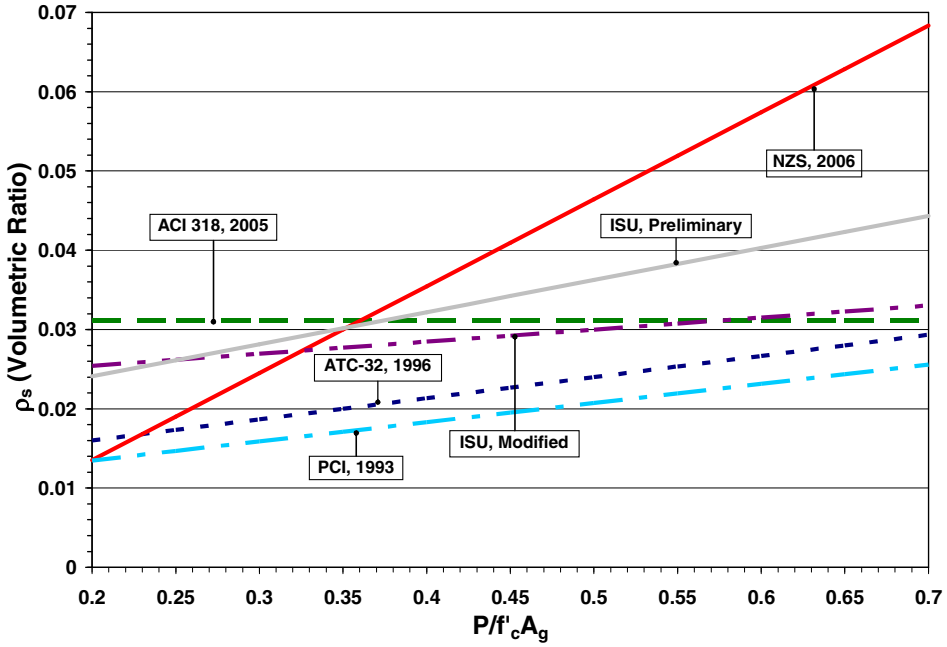

Figure 3.21. Spiral volumetric ratio comparison for a 24-inch octagonal pile with the modified ISU equation

3.4.1 Results of the Octagonal Sections Analyzed by the Modified Equation

The curvature ductility capacity of prestressed pile sections designed according to Eq. 3.26 was examined for the cases summarized in Figure 3.22, following the criteria established for the first yield moment, the ultimate moment, and the nominal moment. The extended axial load ratio limitation was utilized throughout the analysis process. A total of 150 moment-curvature analyses were completed on octagonal pile sections. The average ductility obtained from the analyses was 19.2 with a standard deviation of 1.3. The results of these analyses are presented in tabular form in Table 3.1 as well as in graphical form in Figure 3.22.

Table 3.1. A summary of the curvature ductility capacities obtained from OpenSees for the octagonal sections using the modified confinement equation (i.e., Eq. 3.26)

Axial Load Ratio							
	0.2	**0.25**	**0.3**	**0.35**	**0.4**	**0.45**	**0.5**
16-inch octagonal pile with f'$_c$ = 6000 psi							
fpc-700	19.1	19.6	20.3	20.7	20.8	21.5	22.8
fpc-900	19.5	20.0	20.6	20.4	20.2	20.1	**x**
fpc-1100	19.5	20.0	19.9	19.5	19.4	19.4	**x**
fpc-1200	19.4	19.9	19.4	19.0	18.6	19.4	**x**
16-inch octagonal pile with f'$_c$ = 8000 psi							
fpc-700	19.3	19.7	20.5	20.7	21.1	22.0	**x**
fpc-1000	19.6	20.2	20.7	20.7	21.3	22.1	**x**
fpc-1300	19.8	21.7	20.0	19.7	19.6	20.3	**x**
fpc-1600	19.6	19.3	18.9	18.6	18.8	19.3	**x**
16-inch octagonal pile with f'$_c$ = 10000 psi							
fpc-700	19.4	19.8	20.4	20.4	20.8	22.4	**x**
fpc-1200	19.6	20.2	20.2	20.6	21.1	22.3	**x**
fpc-1600	19.9	19.9	19.5	19.4	19.8	21.0	**x**
fpc-2000	19.8	19.1	18.7	18.5	19.0	**x**	**x**
24-inch octagonal pile with f'$_c$ = 6000 psi							
fpc-700	19.3	19.3	19.2	19.1	18.9	18.5	18.4
fpc-900	18.8	18.8	18.6	18.4	17.9	17.7	17.5
fpc-1100	18.4	18.3	18.3	17.9	17.7	17.1	16.9
fpc-1200	18.3	18.3	18.0	17.7	17.2	16.9	16.7
24-inch octagonal pile with f'$_c$ = 8000 psi							
fpc-700	19.6	19.7	19.7	19.5	19.2	18.9	17.2
fpc-1000	19.5	19.3	19.1	18.8	18.4	18.1	18.2
fpc-1300	19.0	18.8	18.7	18.0	17.5	17.3	**x**
fpc-1600	18.6	18.3	17.9	17.3	16.9	16.7	**x**
24-inch octagonal pile with f'$_c$ = 10000 psi							
fpc-700	19.9	19.8	20.1	19.7	19.2	19.3	**x**
fpc-1200	19.6	19.5	19.1	18.5	18.1	17.9	**x**
fpc-1600	19.2	18.8	18.0	17.7	17.3	17.1	**x**
fpc-2000	18.5	18.0	17.3	16.7	16.4	16.1	**x**

x Not considered due to $\phi_{cr} > \phi_{sp}$

**Average μ_ϕ = 19.2; Standard Deviation = ±1.3

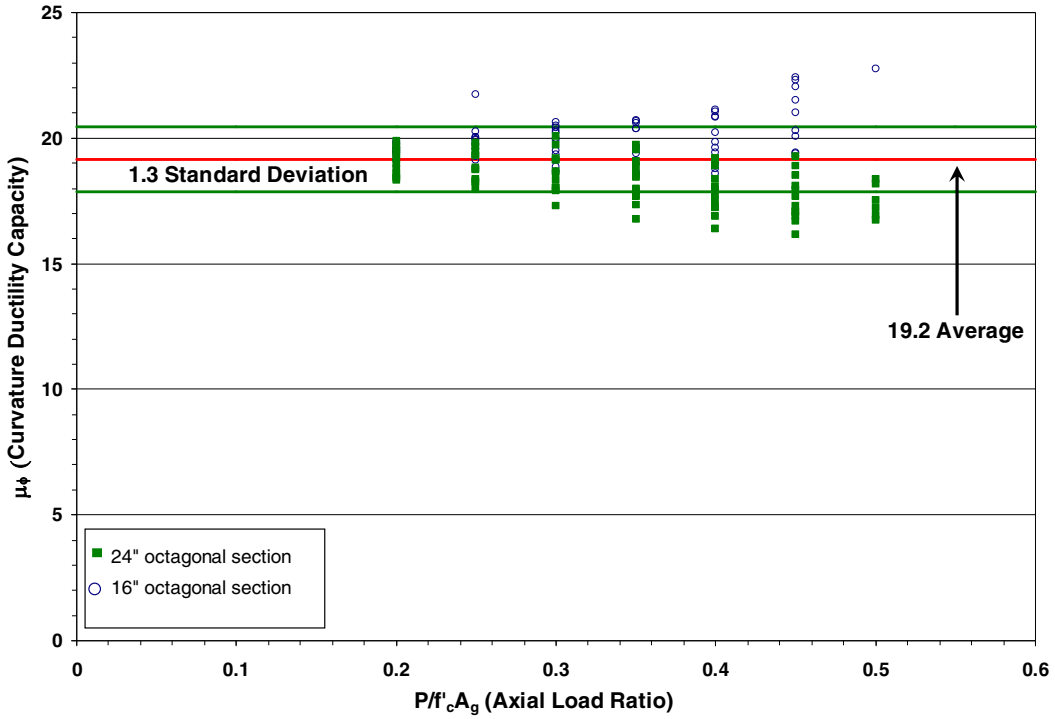

Figure 3.22. Curvature ductility capacity of 16-inch and 24-inch prestressed pile sections with confinement reinforcement as per Equation 3.26

As seen in these summaries, the curvature ductility capacities of the pile analyzed was in the range of 16.1 to 22.8, with an average value of 19.2 and standard deviations of ±1.3. It is also observed that the 16-inch pile sections show ductility capacities from 18.5 to 22.8 while the 24-inch pile section has capacities in the range from 16.1 to 20.1. The main reason for the dependency of the curvature ductility capacity on the selected pile dimension was attributed to the difference in the A_g/A_{ch} value between pile sections. For example, the 24-inch octagonal pile section has an A_g/A_{ch} ratio of 1.51, whereas the 16-inch octagonal section has an A_g/A_{ch} ratio of 1.87. The reduction in A_g/A_{ch} value effectively reduced the confinement reinforcement, resulting in a reduction in the curvature ductility capacity. Upon realization of this issue, a final modification was made to the confinement equation as detailed in the following section.

In Table 3.1, it is also observed that the initial prestressing has some influence on the curvature ductility capacity of prestressed pile sections, particularly at large axial load ratios. However, it was found that these variations are largely due to influence of f_{pc} (the compressive stress in the concrete at the centroid of the cross section due to the prestressing after losses) on the yield curvature (ϕ_y) rather than on the ultimate curvature (ϕ_u). An attempt to include f_{pc} in the confinement equation led to unnecessary conservative amounts of confinement reinforcement for piles with lower axial load ratios. Therefore, it was decided not to include f_{pc} in the confinement equation.

3.5 Recommended Confinement Equation

It is identified in the previous section that the confinement equation should account for the difference in A_g/A_{ch} value. This is because the confinement reinforcement is needed for the core concrete while the axial load ratios are typically defined using the gross area of the pile section. Using the 16-inch octagonal pile section from previously discussed sections as the basis, because of its average ductility of approximately 20, it is suggested that Eq. 3.26 be modified as follows:

$$\rho_s = 0.06\left(\frac{f_c^{'}}{f_{yh}}\right)\left(2.8+\left(\frac{1.25P}{f_c^{'}A_{ch}}\right)\left(\frac{1.87A_{ch}}{A_g}\right)\right) \qquad \text{(Eq. 3.28)}$$

where 1.87 (or $\frac{1}{0.53}$) is the A_g/A_{ch} ratio for the 16-inch octagonal pile section. Therefore, the above equation can be simplified to

$$\rho_s = 0.06\left(\frac{f_c^{'}}{f_{yh}}\right)\left(2.8+\frac{1.25P}{0.53f_c^{'}A_g}\right) \qquad \text{(Eq. 3.29)}$$

With this modification, the confinement equation will require the same amount of spiral reinforcement for all pile sections subjected to the same axial load ratio. Providing the same amount of transverse reinforcement will lead to the same value for $f_l^{'}$, which in turn ensures the same $f_{cc}^{'}$, and ε_{cu} for different pile sections. However, the ultimate curvature is commonly defined as follows:

$$\phi_u = \frac{\varepsilon_{cu}}{c_u} \qquad \text{(Eq. 3.30)}$$

Since the distance from the neutral axis to the extreme compression fiber of each section is different, the resulting ultimate curvature for different pile sections will not be the same. As the pile section dimension also influences the yield curvature, the resulting ductility capacity for the different pile sections are expected to be comparable.

The finalized confinement equation proposed for the design of prestressed piles is plotted in Figures 3.23 and 3.24 against the previously discussed equations of interest. Figure 3.23 plots the spiral requirements for a 14-inch octagonal pile with $f_c^{'}$ = 8000 psi, f_{yh} = 60 ksi, and 2 inches of cover concrete, while Figure 3.24 plots the spiral requirements for a 24-inch octagonal pile with $f_c^{'}$ = 8000 psi, f_{yh} = 60 ksi, and 2 inches of cover concrete.

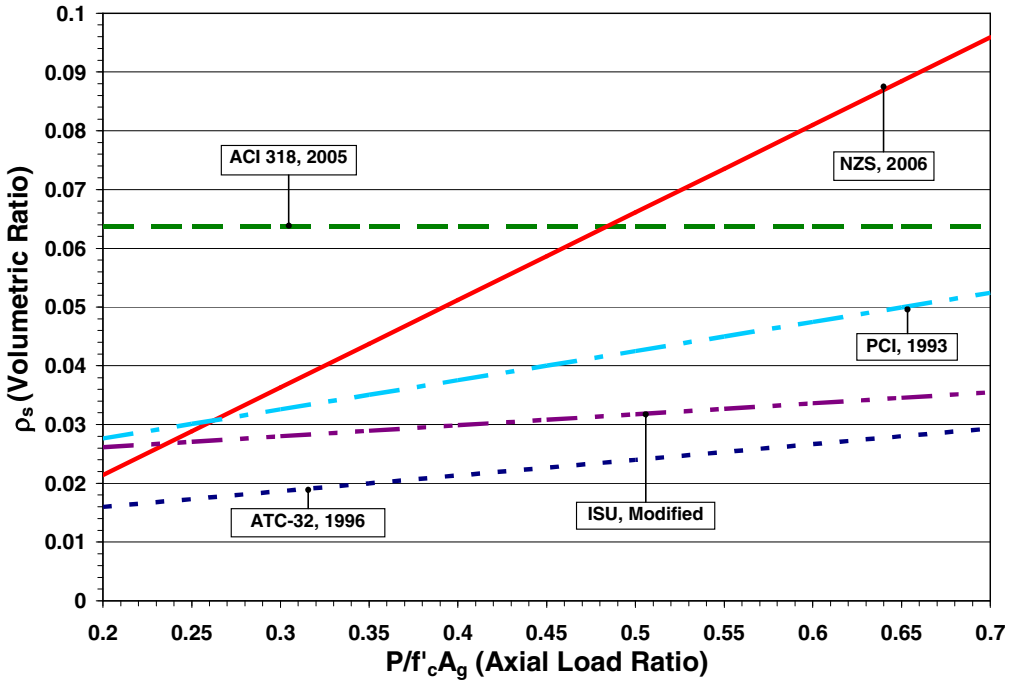

Figure 3.23. Spiral volumetric ratio comparison for a 14-inch octagonal pile with the finalized ISU equation

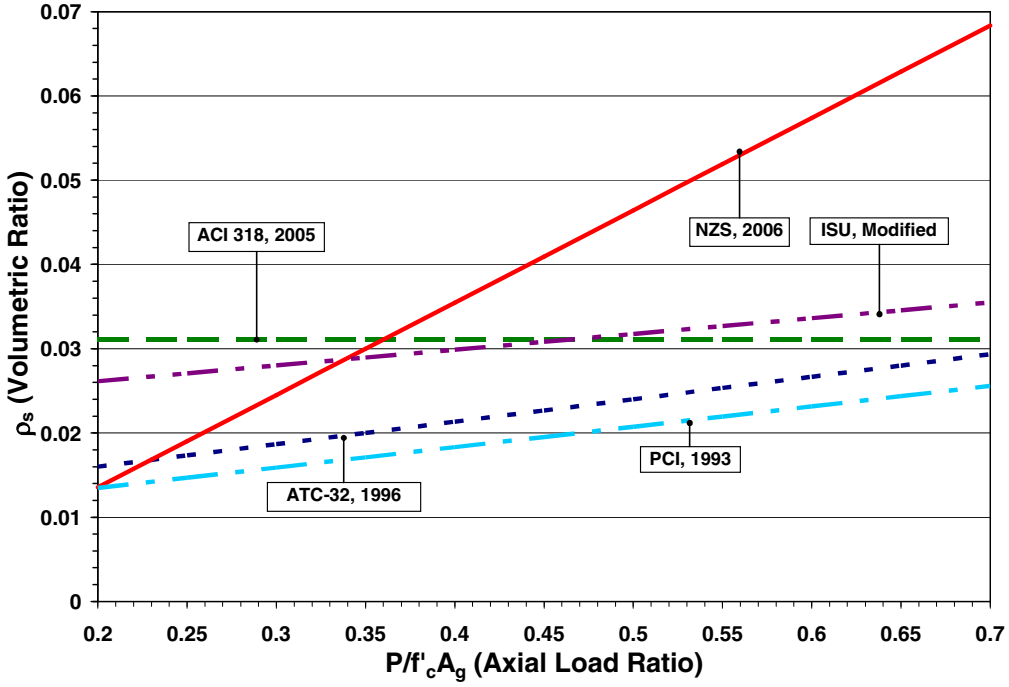

Figure 3.24. Spiral volumetric ratio comparison for a 24-inch octagonal pile with the finalized ISU equation

3.6 Verification for Octagonal Pile Sections

The validity of the confinement equation finalized in Eq. 3.28 was investigated using the various analysis options suggested for octagonal sections in Figures 3.15, 3.16, and 3.17 and the moment-curvature idealization established in Section 3.3.3. The extended axial load ratio limitation as described in Section 3.3.4 was utilized throughout the analysis process. A total of 152 moment-curvature analyses were completed, which resulted in an average ductility of 19.4 and standard deviations of ±1.1. The results of these analyses are presented in tabular form in Table 3.2, as well as in graphical form in Figure 3.25.

Table 3.2. A summary of the curvature ductility capacities obtained from OpenSees for the octagonal sections using the finalized confinement equation (i.e., Eq. 3.28)

Axial Load Ratio							
	0.2	**0.25**	**0.3**	**0.35**	**0.4**	**0.45**	**0.5**
16-inch octagonal pile with f'$_c$ = 6000 psi							
fpc-700	19.1	19.6	20.3	20.7	20.8	21.5	22.8
fpc-900	19.5	20.0	20.6	20.4	20.2	20.1	**x**
fpc-1100	19.5	20.0	19.9	19.5	19.4	19.4	**x**
fpc-1200	19.4	19.9	19.4	19.0	18.6	19.4	**x**
16-inch octagonal pile with f'$_c$ = 8000 psi							
fpc-700	19.3	19.7	20.5	20.7	21.1	22.0	**x**
fpc-1000	19.6	20.2	20.7	20.7	21.3	22.1	**x**
fpc-1300	19.8	20.5	20.0	19.7	19.6	20.3	**x**
fpc-1600	19.6	19.3	18.9	18.6	18.8	19.3	**x**
16-inch octagonal pile with f'$_c$ = 10000 psi							
fpc-700	19.4	19.8	20.4	20.4	20.8	22.4	**x**
fpc-1200	19.6	20.2	20.2	20.6	21.1	22.3	**x**
fpc-1600	19.9	19.9	19.5	19.4	19.8	21.0	**x**
fpc-2000	19.8	19.1	18.7	18.5	19.0	**x**	**x**
24-inch octagonal pile with f'$_c$ = 6000 psi							
fpc-700	19.7	19.8	19.7	19.6	19.5	19.1	19.0
fpc-900	19.1	19.2	19.2	19.0	18.6	18.2	18.1
fpc-1100	18.8	18.8	18.7	17.8	17.9	17.6	17.5
fpc-1200	18.7	18.7	18.5	18.2	17.7	17.4	17.2
24-inch octagonal pile with f'$_c$ = 8000 psi							
fpc-700	20.2	20.2	20.3	20.1	19.8	19.5	19.6
fpc-1000	19.8	19.8	19.6	19.4	18.9	18.7	18.7
fpc-1300	19.3	19.2	18.9	18.5	18.1	17.8	17.7
fpc-1600	18.9	18.7	18.4	17.8	17.4	17.2	**x**
24-inch octagonal pile with f'$_c$ = 10000 psi							
fpc-700	20.3	20.3	20.6	20.3	19.8	19.6	19.7
fpc-1200	20.0	19.9	19.6	19.0	18.6	18.5	**x**
fpc-1600	19.5	19.2	18.8	18.2	17.8	17.6	**x**
fpc-2000	18.8	18.4	17.8	17.2	16.9	16.6	**x**
average	19.5	19.6	19.5	19.3	19.2	19.5	18.9

x Not considered due to $\phi_{cr} > \phi_{sp}$

**Average μ_ϕ = 19.4; Standard Deviation = ±1.1

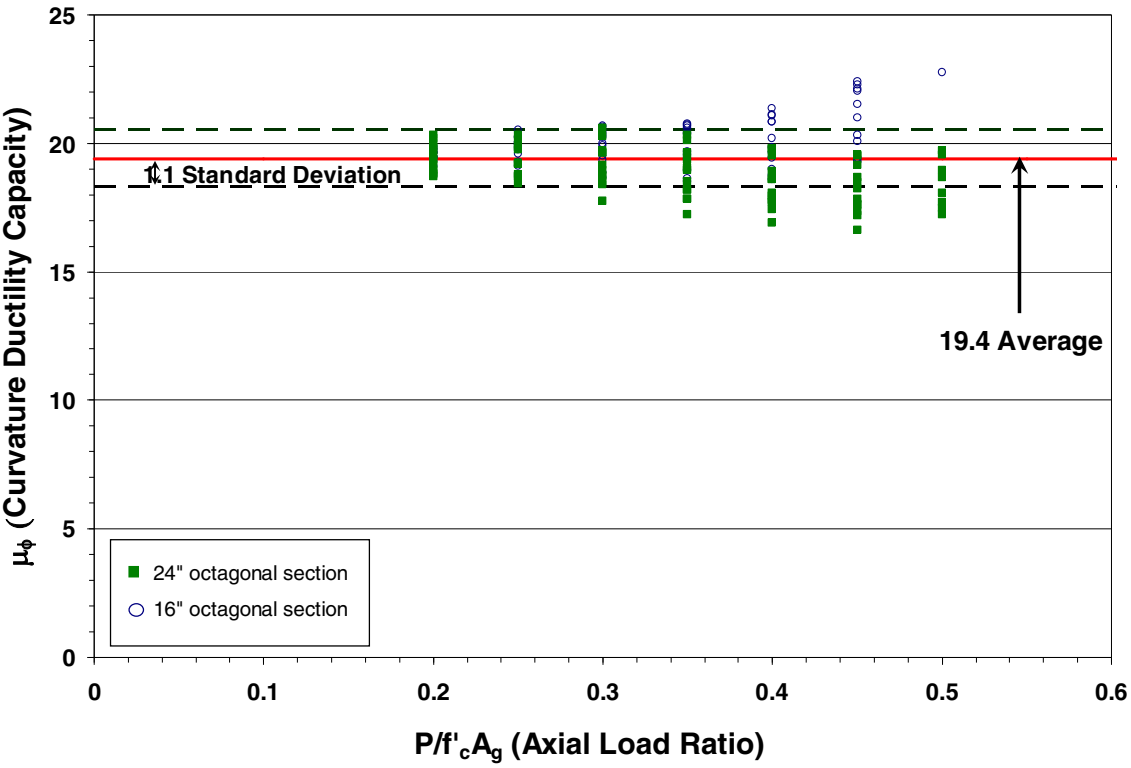

Figure 3.25. Curvature ductility capacity of 16-inch and 24-inch prestressed pile sections with confinement reinforcement as per Eq. 3.28

As seen in these summaries, the curvature ductility capacities of the pile analyzed is in the range of 16.6 to 22.8. It was also observed that the 16-inch pile shows ductility capacities from 18.5 to 22.8 while the 24-inch pile has capacities from 16.6 to 20.6. Although accounting for the difference in the A_g/A_{ch} ratio, Eq. 3.28 does not seem to improve the differences in the ductility capacity range for these two pile types. The impact on the curvature ductility capacity for the square pile sections are detailed in Section 3.7.

3.6.1 Influence of Concrete Strength on Curvature Ductility Capacity

Upon investigating the influence of the concrete strength on the curvature ductility capacity portrayed in Table 3.2, it became apparent that the concrete strength had little to no effect on the curvature ductility capacity. Figures 3.26 and 3.27 plot the curvature ductility

capacities calculated for the 16-inch and 24-inch octagonal sections, respectively, against the compressive strength of the unconfined concrete. Notice that regardless of the axial load ratio, the curvature ductility capacities remain fairly constant. This result is not surprising considering the effects of the unconfined compressive strength of the concrete were accounted for in the ISU confinement equation. Figures 3.28 and 3.29 plot the curvature ductility capacities calculated for the 16-inch and 24-inch octagonal sections, respectively, against the compressive stress in the concrete at the centroid of the cross section due to prestress (after losses). From these figures, it is observed that there is no apparent trend caused by the change in f_{pc}.

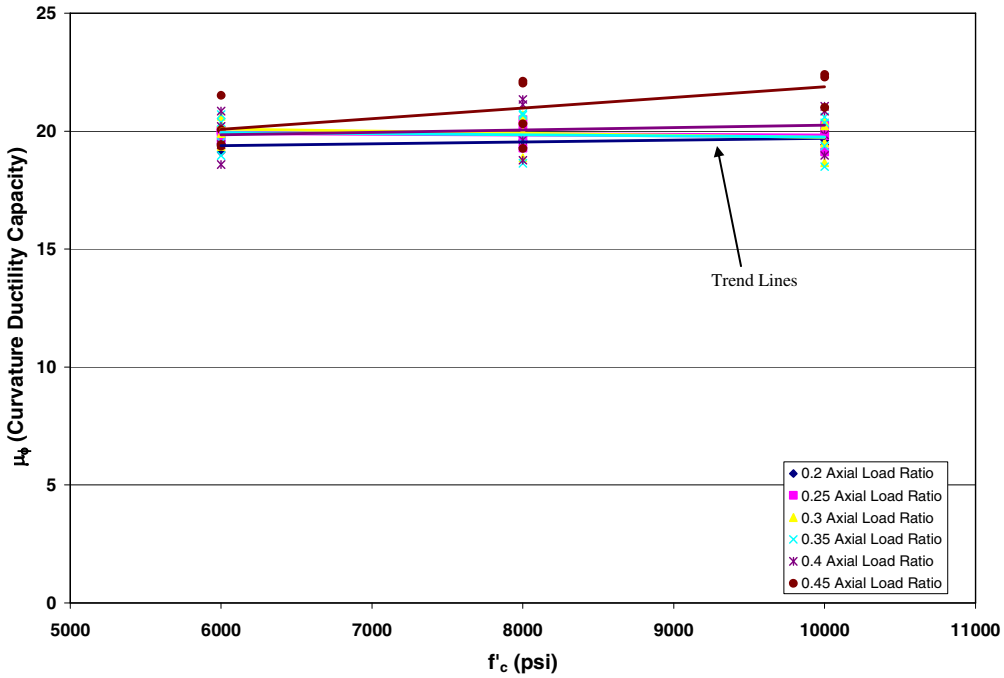

Figure 3.26. Influence of the concrete strength on the curvature ductility capacity for a 16-inch octagonal section

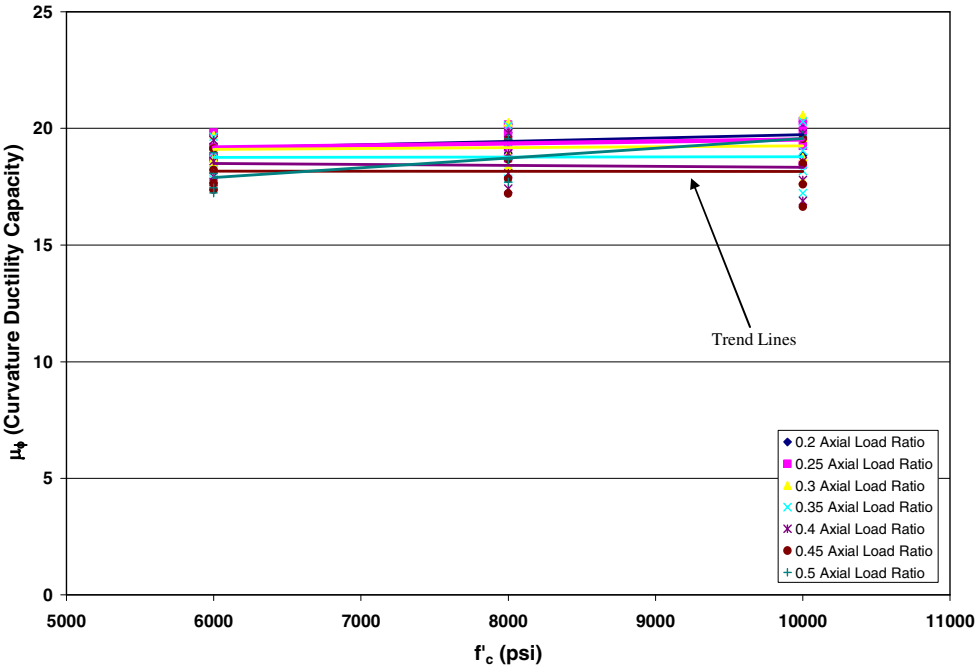

Figure 3.27. Influence of the concrete strength on the curvature ductility capacity for a 24-inch octagonal section

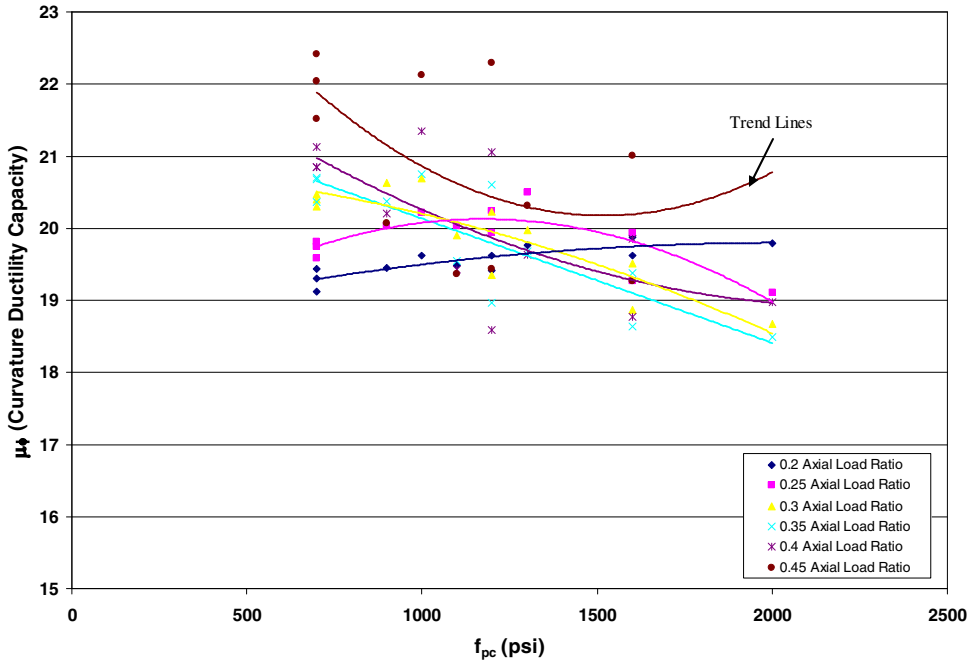

Figure 3.28. Influence of f_{pc} on the curvature ductility capacity for a 16-inch octagonal section

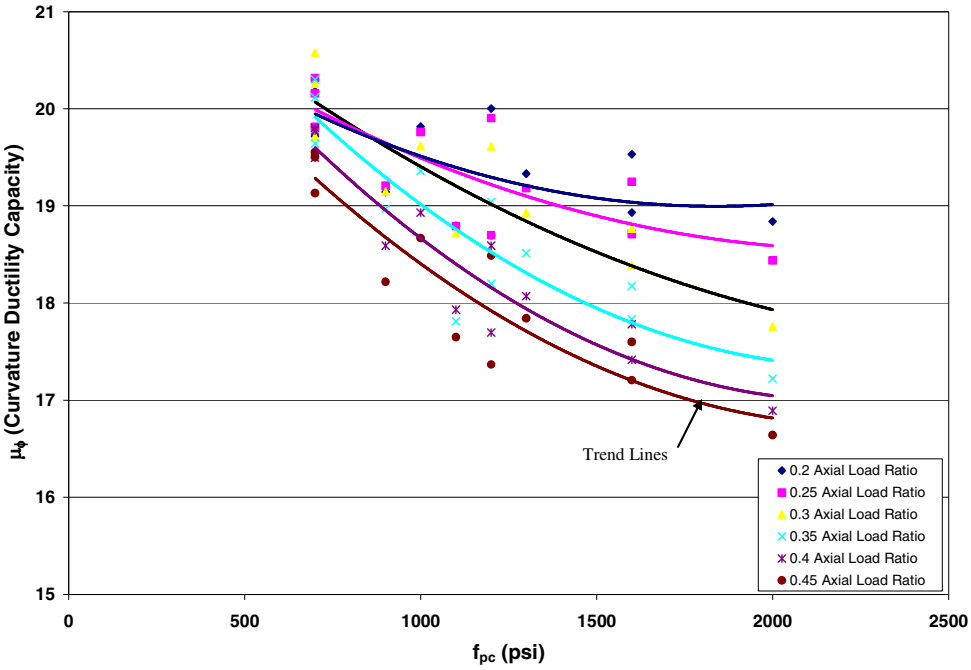

Figure 3.29. Influence of f_{pc} on the curvature ductility capacity for a 24-inch octagonal section

3.7 Verification for Square Pile Sections

The solid square is a widely used section in the precast, prestressed industry. Chapter 2 provides details of various square sections being utilized in current practice. With the preliminary confinement equation, the 14-inch square section, produced a wide range of curvature ductility capacities in the range between 12 and 47 (Section 3.4). With the modified equation, the ductility range for the 14-inch square section was found to be large, reaching values as high as 28. With the finalized confinement equation, the curvature ductility capacities of this pile section improved to a range from 19.5 and 27.6. However, several other concerns regarding the square prestressed pile sections emerged. From the moment-curvature response of different pile sections with $f_c^{'}$, f_{pc}, and axial load ratios as main variables, it was observed that the strength drop due to the spalling of cover concrete

became significant that the functionability of the pile became a question of uncertainty. Being a commonly used pile type for bridges and buildings, the uncertainty of the square section is of utmost importance. With these concerns, the recommendations regarding the square section are presented in Chapter 5.

Further modifications to the confinement equation were investigated using $f_c^{'}$, f_{pc}, and axial load ratios as variables, but an additional reduction in the range of curvature ductility values for square prestressed pile sections was unable to be achieved. This lack inability to reduce the range of the curvature ductility values results from the large area of concrete being spalled. The gross area of the square section of interest is 196 in^2 and the corresponding core is 78.54 in^2. This reduction in area upon the spalling of the unconfined concrete decreases the section by approximately 60 percent. With this reduction in area, the moment-curvature response results in a large drop. Figure 3.26 provides an example of the moment-curvature relationship for an analyzed 14-inch square section with an axial load ratio of only 0.2.

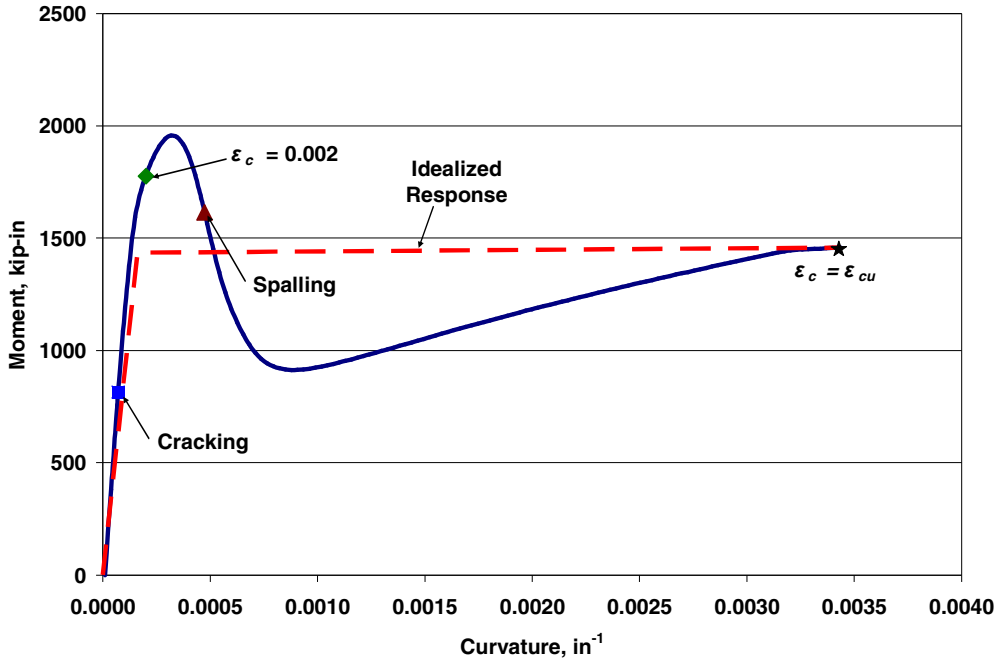

Figure 3.30. Moment-curvature relationship for a 14-inch square section with $f_c^{'}$ of 6000 psi, f_{pc} of 1200 psi, and a 0.2 axial load ratio

With the information in the preceding paragraphs, the following limitation was placed on the analysis of square sections: when the drop in the moment-curvature relationship exceeded 40 percent of the maximum moment, the analyses of a given square section were completed.

Figure 3.31 provides the curvature ductility capacity results of the analysis performed on the 14-inch square section while confining the section with the ISU equation. Table 3.6 provides a tabular form of the results, both taking the above limitation into account. The average of the curvature ductility for the 14-inch square section was 22.7 with standard deviations of ±2.5.

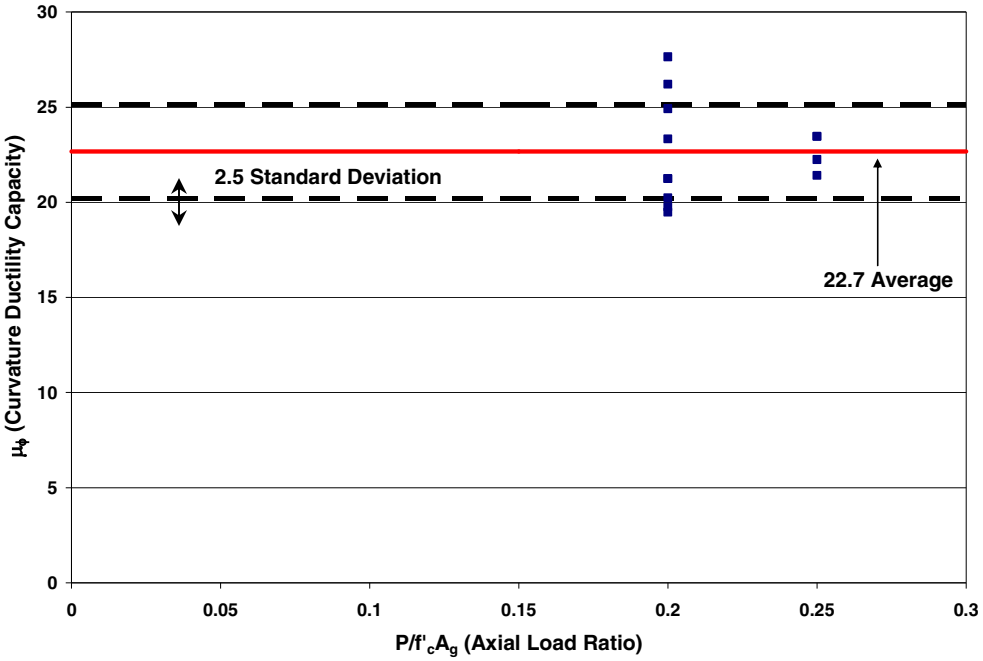

Figure 3.31. Curvature ductility capacity of 14-inch prestressed pile section with confinement reinforcement as per Eq. 3.42

Table 3.3. A summary of curvature ductility capacities obtained from OpenSees for the square section using the finalized confinement equation (i.e., Eq. 3.42)

	0.2	0.25	0.3	0.35	0.4	0.45	0.5	0.55	0.6
14-inch square pile with f'$_c$ = 6000 psi									
fpc-700	19.49	21.42	x	x	x	x	x	x	x
fpc-900	20.24	22.24	x	x	x	x	x	x	x
fpc-1100	21.25	23.47	x	x	x	x	x	x	x
fpc-1200	21.25	23.47	x	x	x	x	x	x	x
14-inch square pile with f'$_c$ = 8000 psi									
fpc-700	23.33	x	x	x	x	x	x	x	x
fpc-1000	24.92	x	x	x	x	x	x	x	x
fpc-1300	26.21	x	x	x	x	x	x	x	x
fpc-1600	27.64	x	x	x	x	x	x	x	x
14-inch square pile with f'$_c$ = 10000 psi									
fpc-700	19.77	x	x	x	x	x	x	x	x
fpc-1200	x	x	x	x	x	x	x	x	x
fpc-1600	x	x	x	x	x	x	x	x	x
fpc-2000	x	x	x	x	x	x	x	x	x

x Not analyzed due to established limitiations;
Average μ_ϕ = 22.7 ; Standard Deviation = ±2.5

3.8 Integration of μ_ϕ in the Confinement Equation

The final parameter that was to be included in the ISU equation was the curvature ductility demand. From the observations made from the influence of the concrete strength and the axial load on the curvature ductility capacities, it became evident that including the curvature ductility demand term in the form of $\mu_\phi / constant$ within the ISU equation would be sufficient and simple. In order to determine the placement of this ratio, the confinement reinforcement was plotted versus the curvature ductility capacity and the relationship was observed. In general, the relationship between the confinement reinforcement and the curvature ductility capacity was linear. A sample of this plot is provided in Figure 3.32,

which plots the confinement reinforcement of a 16-inch octagonal section versus its corresponding curvature ductility capacity. Thus, the ratio was included outside the parenthesis containing the axial load ratio.

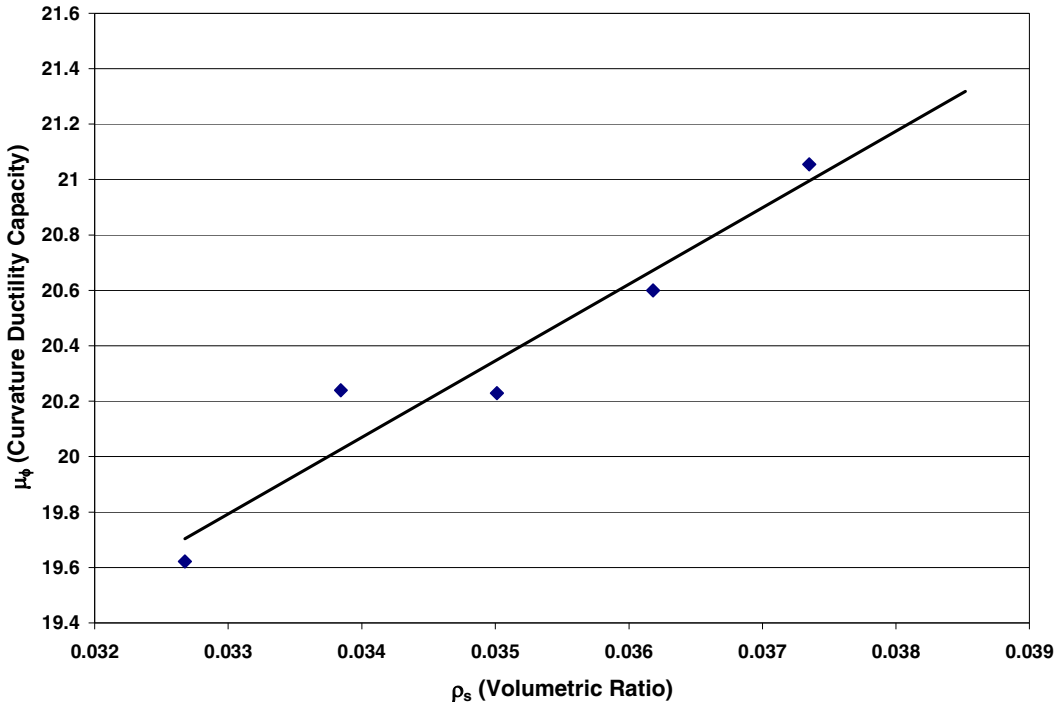

Figure 3.32. Relationship between the confinement reinforcement of a 16-inch octagonal section and the corresponding curvature ductility over axial load ratios ranging from 0.2 to 0.4

The constant within the ratio was determined using the average value of the curvature ductility and the calculated standard deviation. Because of the concerns regarding the square section, only values form the octagonal sections were utilized in determining the constant. The average of the curvature ductility capacities of the octagonal sections was 19.4 with standard deviations of ±1.1. The constant within the ratio was calculated by subtracting the standard deviation from the average and rounding it to the nearest whole number. The

resulting value was 18. Hence, the curvature ductility demand term was included in the equation in the following manner:

$$\rho_s = 0.06\left(\frac{f_c^{'}}{f_{yh}}\right)\left(\frac{\mu_\phi}{18}\right)\left(2.8+\left(\frac{1.25P}{f_c^{'}A_{ch}}\right)\left(\frac{1.87A_{ch}}{A_g}\right)\right) \qquad \text{(Eq. 3.31a)}$$

or

$$\rho_s = 0.06\left(\frac{f_c^{'}}{f_{yh}}\right)\left(\frac{\mu_\phi}{18}\right)\left(2.8+\left(\frac{1.25P}{0.53f_c^{'}A_g}\right)\right) \qquad \text{(Eq. 3.31b)}$$

It is expected that the ISU equation, as written above, will ensure a curvature ductility capacity of the value selected for μ_ϕ. To prove this fact, Eq. 3.31 was analyzed for curvature ductility demand values of 6 and 12. Figure 3.27 plots the results from this investigation when examined with a curvature ductility demand of 12 and Figure 3.28 graphs the results of the equation when examined with a curvature ductility demand of 6. Notice in each figure that the curvature ductility demands of 6 and 12 are always attained.

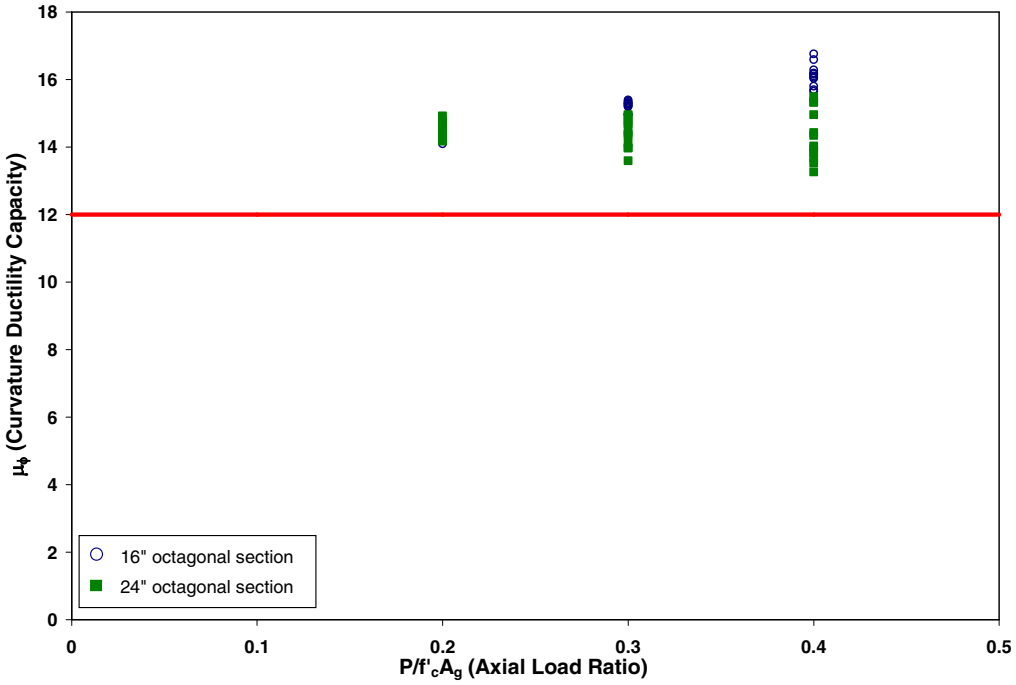

Figure 3.33. Analysis results of prestressed pile sections that used the ISU equation with a curvature ductility demand of 12

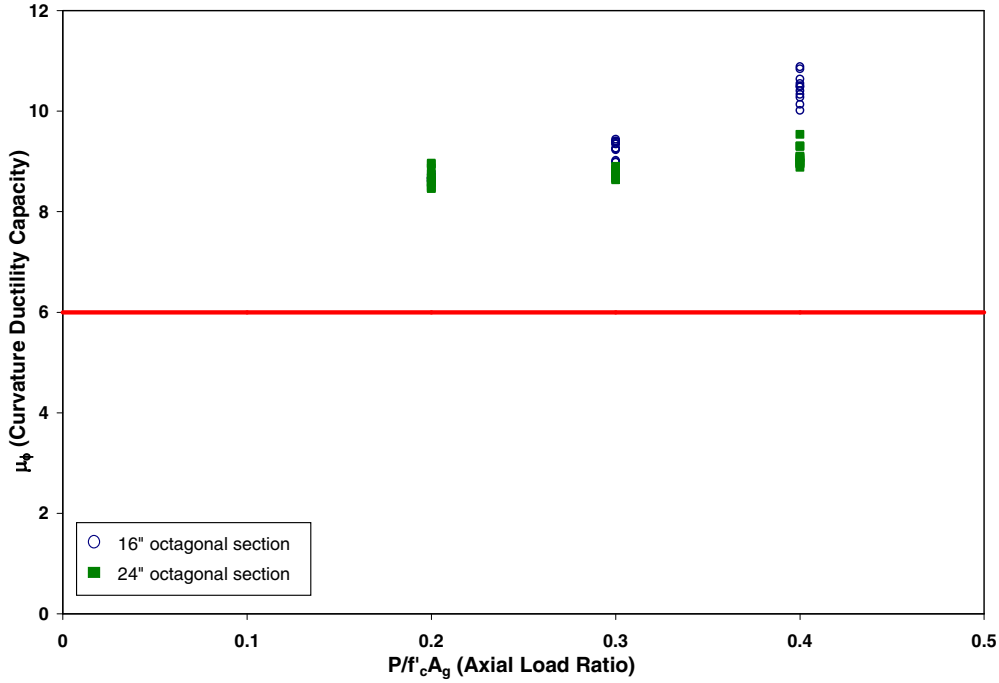

Figure 3.34. Analysis results of prestressed pile sections that used the ISU equation with a curvature ductility demand of 6

CHAPTER 4. ANALYSIS OF PILES UNDER LATERAL LOADS TO ESTABLISH DISPLACEMENT LIMITS

4.1 Introduction

Chapter 3 provided results from over 200 moment-curvature analyses performed on octagonal and square pile sections that were confined with the reinforcement recommended by the newly developed equation (Eq. 3.28). The compressive strength of unconfined concrete, the compressive stress in the concrete gross section due to prestress (after losses), and the axial load ratio were the primary variables in these analyses. The seismic design approach, discussed in Section 1.4 of this report, indicates that the current codes call for piles in pile-supported footings to be designed with the intent that the piles will not experience significant inelastic actions unless piles are extended above ground to directly support the superstructure. With this in mind, the curvature capacities that were established in Chapter 3 through the moment-curvature analyses were used to perform a set of lateral load analyses to determine the combined influence of the confinement and soil type on the lateral displacement limits of the pile, thereby accounting for influence of soil types on precast, prestressed pile behavior.

4.2 Objective

The lateral load analyses aimed to establish permissible limits of lateral displacements for precast, prestressed piles in different soil conditions by utilizing the curvature capacities reported in Chapter 3. The “permissible limit” eventually defines the

displacement that a specific pile, in a given soil, can undergo prior to experiencing failure in accordance with the confinement requirement of Eq. 3.42. Through these analyses, it is intended to provide designers with a design process that ensures design of confinement reinforcement in piles consistent with the assumptions made for the design of columns and superstructure in accordance with the capacity design principles.

4.3 Overall Design Process

In the current design practice, there is a disconnect in that the expected performance of pile supported footings is not integrated into the design of structure above the ground level, which is expected to undergo inelastic response under design-level earthquakes. Despite the assumption that piles should remain elastic during an earthquake response, piles in a pile-supported footing can experience some inelastic actions. Consequently, the structure above ground will not experience the expected level of inelastic response, thus affecting the energy dissipation ability of the structure. Therefore, it is important to integrate the expected pile foundation displacement in the overall design of the superstructure. With this in mind, an overall seismic design process that integrates the expected foundation displacement is presented in Figure 4.1, which involves the following steps:

1. Define pile properties: length, cross-sectional dimensions, reinforcement details, moment of inertia, section area, modulus of elasticity, moment-curvature relationship that includes the effect of confinement reinforcement, and the external loading.
2. Define soil profile and appropriate properties, taking into account the variability of the average undrained shear strength, the strain at 50 percent of the ultimate shear stress of the soil, and the initial modulus of subgrade reaction.

3. Define the pile head conditions.

4. Define the target displacement and the permissible displacement, where the target displacement refers to the desired displacement by the designer and the permissible displacement refers to the lateral displacement limit that the pile can sustain without failure. This limit should be established accounting for the confinement reinforcement, pile head boundary condition, and the soil surrounding the pile.

5a. If the target and permissible displacements are the same, provide the critical pile region with confinement as per Eq. 3.28.

5b. If the target and permissible displacements are different, provide the critical pile region with confinement as per Eq. 3.31b.

6. Define the ductility of the structural system, including the effect of the target displacement of the pile supported footing.

6. Complete the design of the structure above ground level, ensuring that the foundation displacement will never exceed the target displacement.

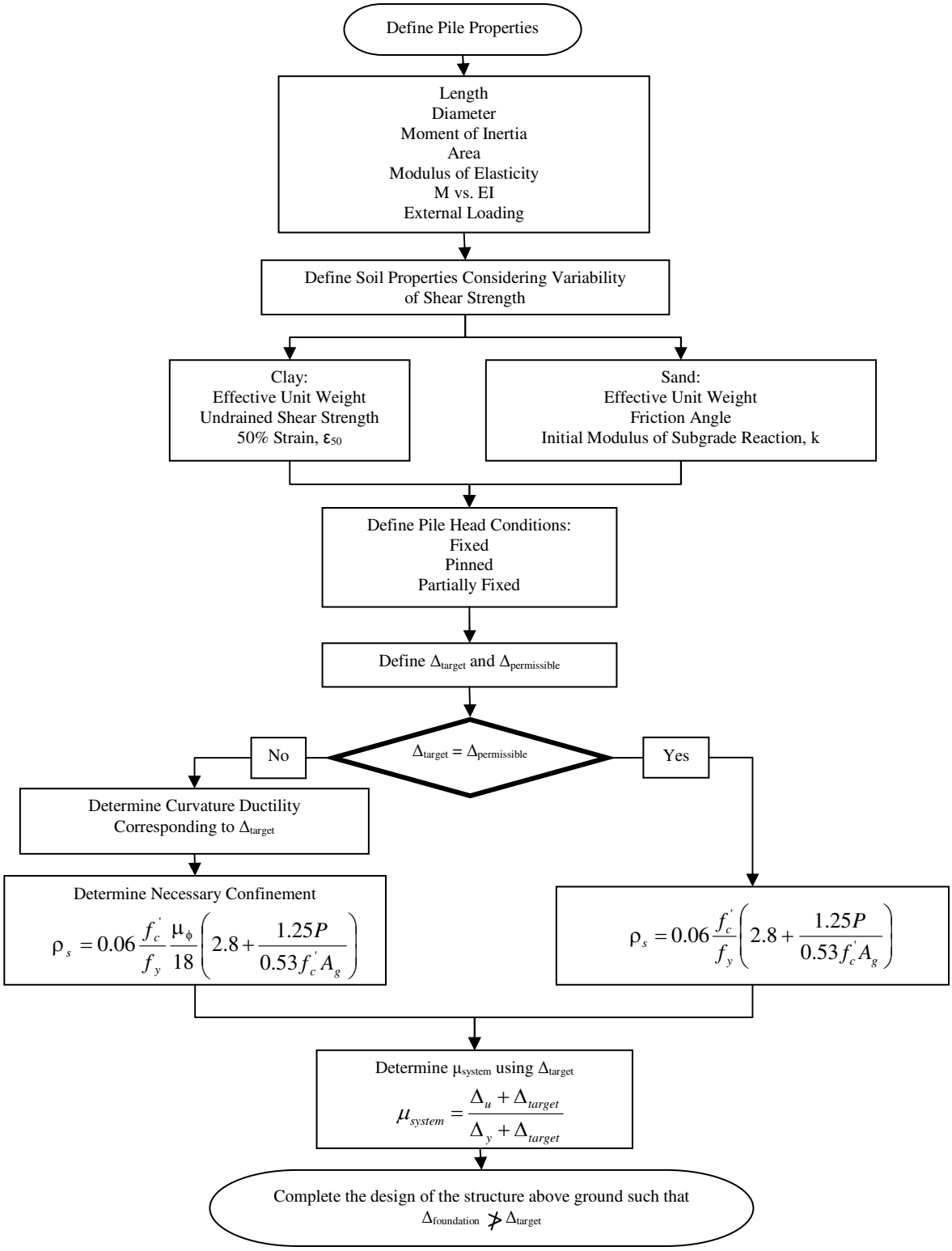

Figure 4.1. Proposed design process integrating the expected pile foundation displacement in the overall seismic design of the structure

4.4 Soil-Pile Interaction Analyses

The lateral load behavior of a pile foundation and its lateral displacement capacity are dictated by its structural properties, pile head fixity, and the stiffness and strength of the soil surrounding the upper portion of the pile and of the soil in the vicinity of the pile cap (if the foundation includes a pile cap). These variables determine the distribution of the soil reaction along the pile length, influencing its resistance to lateral loads and the corresponding lateral deflection for a given lateral force. To study the lateral load behavior of piles in different soil conditions and establish their permissible displacements, LPILE Plus Version 5.0 (Ensoft, Inc. 2004) was utilized. The following section gives a general description of the LPILE program. Subsequent sections provide a brief description of the theory used in LPILE, general capabilities of LPILE, and conclude with the results from the LPILE analysis pertaining to the current study.

4.5 LPILE

LPILE is a commercial program that includes the capability to analyze a pile subjected to lateral loading by treating it as a beam on an elastic foundation. The soil behavior in LPILE is modeled with nonlinear springs with prescribed load-deflection curves, known as p-y curves, which are internally generated by the computer program based on soil type and key properties or could be entered by the user. The p-y curves of various soil types in LPILE follow published recommendations available in the literature and are discussed in detail later in this section. The nonlinear behavior of a pile can be accommodated in LPILE by defining the moment-curvature response of the pile sections at appropriate places. For a given problem with appropriate boundary conditions, LPILE can analyze the response of a

pile under monotonic loading and produce deflection, shear, bending moment, and soil response along the pile length.

4.5.1 Solution Process

Figure 4.1 schematically shows a model for a laterally loaded pile including the p-y curves that represent the nonlinear behavior of the soil.

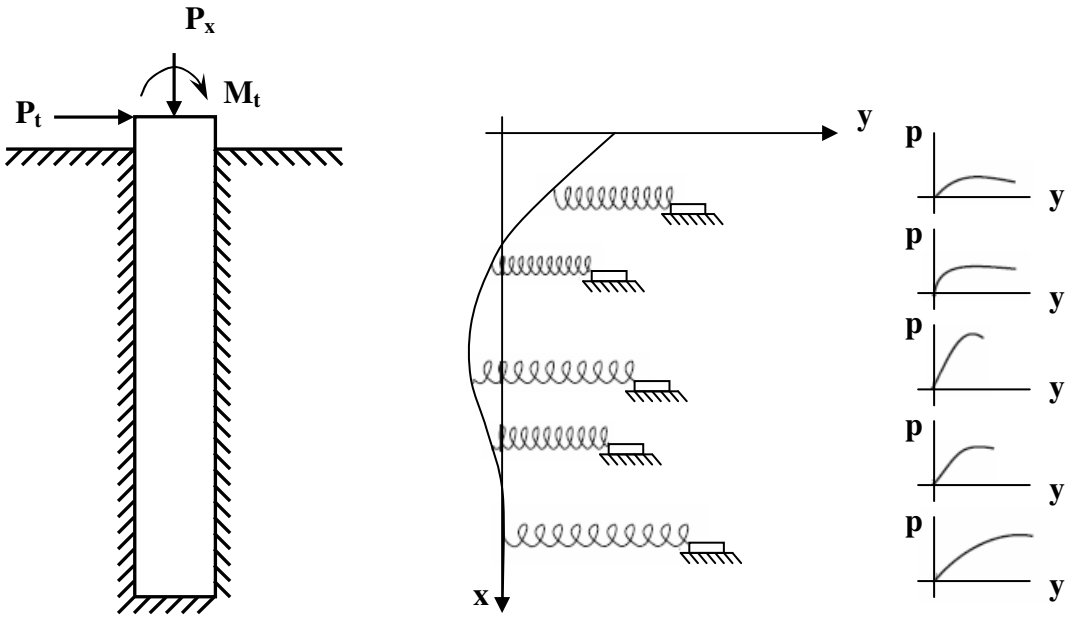

(a) (b) (c)

Figure 4.2. LPILE model of laterally loaded pile of soil response (a) Schematic profile of a pile embedded in soil, (b) Structural idealization for the pile-soil interaction, and (c) lateral spring force-displacement relationship (Ensoft, Inc. 2004)

The standard beam-column equation can be used to determine the deformation of a pile subjected to axial and lateral loads. This equation is expressed as

$$\frac{d^2}{dx^2}\left(E_p I_p \frac{d^2 y}{dx^2}\right) + P_x\left(\frac{d^2 y}{dx^2}\right) - p - W = 0 \qquad \text{(Eq. 4.1)}$$

where P_x = axial load on the pile (force),

y = lateral deflection of the pile at point x along the length of the pile (length),

p = soil resistance per unit length (force/length),

W = distributed load due to external loading along the length of the pile (force/length); and

$E_p I_p$ = flexural rigidity of the pile (force*length^2).

The soil resistance, p_i, at any location, i, along the pile depends on the state of the lateral displacement of the pile, y_i, through the following equation:

$$p_i = E_s y_i \qquad \text{(Eq. 4.2)}$$

where E_s = the soil modulus (force/length^2)

LPILE uses the finite difference method to develop a solution of the differential equation shown in Eq. 4.1. In the finite difference method, the pile is divided into several segments with equal lengths that are referred to as beam elements. Figure 4.2 shows an undeformed and deformed pile that is subdivided into segments. Eq. 4.1 can be expressed in the following form:

$$y_{m-2}R_{m-1} + y_{m-1}\left(-2R_{m-1} - 2R_m + Qh^2\right) + y_m\left(R_{m-1} + 4R_m + R_{m+1} - 2Qh^2 + k_m h^4\right) + y_{m+1}\left(-2R_m - 2R_{m+1} + Qh^2\right) + y_{m+2}R_{m+1} - W_m h^4 = 0 \qquad \text{(Eq. 4.3)}$$

where $R_m = E_m I_m$ (flexural rigidity of pile at point m); and

$k_m = E_{sm}$

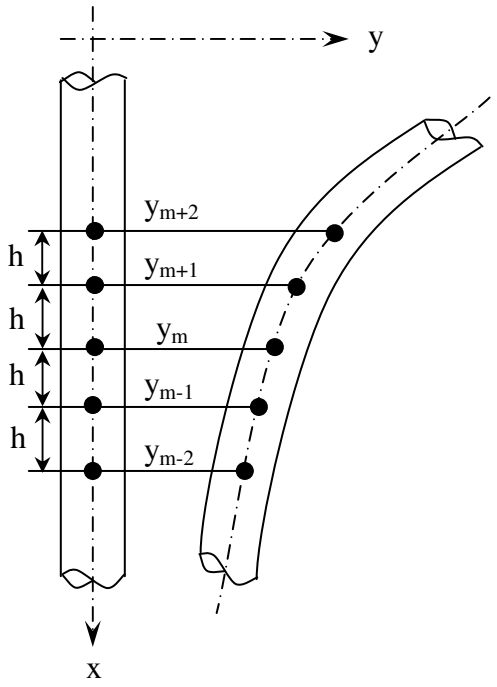

Figure 4.3. Subdivided pile model as used in LPILE for the finite difference solution

The relations needed to calculate the slope, curvature, shear, and load are shown below.

$$\frac{dy}{dx} = \frac{y_{m-1} + y_{m+1}}{2h} \qquad \text{(Eq. 4.4)}$$

$$\frac{d^2y}{dx^2} = \frac{y_{m-1} - 2y_m + y_{m+1}}{h^2} \qquad \text{(Eq. 4.5)}$$

$$\frac{d^3y}{dx^3} = \frac{-y_{m-2} + 2y_{m-1} - 2y_{m+1} + y_{m+2}}{2h^3} \qquad \text{(Eq. 4.6)}$$

$$\frac{d^4y}{dx^4} = \frac{y_{m-2} - 4y_{m-1} + 6y_m - 4y_{m+1} + y_{m+2}}{h^4} \qquad \text{(Eq. 4.7)}$$

To calculate the moment and shear within each element, the flexural rigidity, E_pI_p, is needed. However in concrete piles, the flexural rigidity changes according to the state of deformation within each element, thus inducing a non-linear effect on the pile. LPILE has the capabilities

to account for the non-linear behavior of each element according to a user-specified moment-curvature relationship.

For the above equations, LPILE uses the following steps to find the solution for a prescribed lateral load or displacement. A set of p-y curves are internally generated along the length of the pile for the selected soil profile. A linear relation is established between the soil resistance, *p*, to the deflection, *y*, with the slope of the line representing the soil modulus at the given *y*. The soil modulus values are established from each of the p-y curves that were generated along the pile length. In order to complete the computation, LPILE uses the computed values of the soil modulus and continues iterations on the deflection until the difference in the calculated deflections is less than a specified tolerance. Once the deflections have been computed, the derivatives of deflections equation can be utilized to compute the rotation, bending moment, shear, and soil reaction as presented in Eqs. 4.3, 4.4, 4.5, and 4.6.

4.5.2 Features of LPILE

To accomplish the completion of a typical analysis required in the current study, the following input are needed: selection of the analysis type, identification of the pile properties, selection of the loading type, selection of the boundary conditions, and selection of the soil surrounding the pile. In addition, a brief list of LPILE features relevant to the lateral analysis of piles and how these features were used in the current study are presented below.

- As previously noted, a user defined moment-curvature response can be defined for the pile section, thereby enabling accurate representation of confinement effects in the analysis. This was achieved by running moment-curvature analyses of the pile

sections using OpenSees (see Section 3.3.2) and defining EI as M/ϕ, where M is the moment output and ϕ is the corresponding section curvature.

- Five sets of boundary conditions are available to model the pile head. Depending on the boundary conditions, the pile-head loading may consist of a lateral load, a bending moment, a specific lateral displacement, or a specific pile-head rotation. The boundary conditions of interest for this study were a pinned connection, a fixed connection, and a partially fixed connection. By keeping the moment value zero and incrementally changing the displacement, a pinned connection at the pile head was established. By keeping the pile-head rotation zero and incrementally changing the lateral displacement, a fixed connection at the pile head was established. To represent a partially fixed condition, the slope values that were obtained at the pile top in the pinned condition were divided by a factor of two to define the partially fixed head condition until reaching the yield limit state. For displacements occurring after the yield limit state, there was no further increments to the slope value. Upon selecting the boundary condition, ten different incremental displacement steps may be applied at the pile head for a single analytical run. This enables observation of the pile behavior when subjected to a specific set of boundary conditions.
- If provided with basic soil properties, soil-resistance (i.e., p-y curves) curves can be internally generated by the program for 11 different types of soil: Soft Clay (Matlock, 1970), Stiff Clay with Free Water (Reese, 1975), Stiff Clay without Free Water (Reese, 1975), Sand (as recommended by Reese et al., 1974), Vuggy Limestone (Strong Rock), Silt (with cohesion and internal friction angle), API Sand (as recommended by API, 1997), Weak Rock (Reese, 1997), Liquefiable Sand (as

recommended by Rollins, 2003), and Stiff Clay without free water with specified initial k. In addition, any user-specified p-y curve may be utilized to represent the soil in LPILE. For the current study, the Soft Clay (Matlock, 1970) and the API Sand (as recommended by API, 1997) were used after consultation with Earth Mechanics, Inc., while varying the effective unit weight, the average undrained shear strength, the 50 percent strain for the clay and varying effective unit weight, the friction angle, and the initial modulus of subgrade reaction for the sand. In varying the parameters used to define the soft clay model by Matlock (1970), medium clay, stiff clay, very stiff clay, and hard clay can also be modeled from the Matlock curves. In varying the parameters used to define the API sand model (1997), loose sand, medium sand, dense sand, and very dense sand can modeled. Consultation with Earth Mechanics, Inc., provided the soil types and the corresponding parameter values that were established as the potential soil types. Table 4.1 gives the parameters s_u, ε_{50}, k, and γ_{dry}, of the clay models to be used in LPLIE, while Table 4.2 gives blow count, ϕ, k (saturated), k (dry), and γ_{dry} for the sand chosen for the LPILE analysis, where

- s_u = average undrained shear strength,
- ε_{50} = strain at 50% of the strength;
- k = initial modulus of subgrade reaction, either saturated or dry;
- γ_{dry} = effective unit weight,
- ϕ = internal friction angle

The soil conditions that are highlighted in these tables represent those analyzed in this study. These soil conditions were selected with the intention that the range of displacement limits would be tighter in a stiffer clay or denser sand rather than soft clay or loose sand. Generally

in practice, the Matlock Soft Clay Model is used for both the soft clay model and the stiff clay model, but reduces the value of ε_{50} for the stiff clay, as Reese Stiff Clay Model is not as widely accepted (Arulmoli, 2007).

Table 4.1. Parameters selected for clay soil used in LPILE

Soil Type / p-y Model	s_u	ε_{50}	k	γ_{dry}
soft clay (Matlock)	250-500 psf 12-24 KPa	0.02	NA	
medium clay (Matlock)	500-1000 psf 24-48 KPa	0.01	NA	73-93 lb/ft^3
stiff clay (Matlock)	1000-2000 psf 48-96 KPa	0.01	NA	
very stiff clay (Matlock)	2000-4000 psf 96-192 KPa	0	NA	
hard clay (Matlock)	4000-8000 psf 192-383 KPa	0	NA	108 lb/ft^3

Table 4.2. Parameters selected for sand used in LPILE

Soil Type / p-y Model	Blowcount per foot	Friction Angle (ϕ°)	k (Saturated) pci	k (Dry) pci	γ_{dry}
loose sand (API Sand)	<10	28-30	10-30	10-45	80-90 lb/ft^3
medium sand (API Sand)	10-30	31-35	40-80	60-135	90-100 lb/ft^3
dense sand (API Sand)	30-50	36-40	95-135	160-230	100-110 lb/ft^3
very dense sand (API Sand)	>50	41-42	145-160	240-270	110-120 lb/ft^3

4.6 Analyses and Results

To establish the permissible lateral displacement limits for precast, prestressed piles in different soil conditions using LPILE analyses, three different boundary conditions at the pile head were investigated: 1) fixed head; 2) pinned head; and 3) partially fixed head. The

L{ILE analyses were conducted for selected 16-inch octagonal piles. Table 4.3 represents the ultimate curvatures that were established for the 16-inch octagonal prestressed pile sections with the newly developed equation. In this table, Pile 1 through Pile 7 represents the maximum and the minimum curvature capacities are identified, with f_{pc}, $f_c^{'}$, and axial load ratios. Given that these piles represent the boundaries of the curvature capacities, only these 16-inch octagonal prestressed piles were analyzed in five different soil conditions, identified in Section 4.5.2. This was necessary to reduce the number of LPILE analyses needed to establish the displacement limits. Displacement limits for other pile types are established and reported elsewhere (Fanous et al., 2007)

Table 4.3. Ultimate curvature values of 16-inch octagonal prestressed piles using confinement reinforcement based on the newly developed equation

	Axial Load Ratio						
	0.2	**0.25**	**0.3**	**0.35**	**0.4**	**0.45**	**0.5**
16-inch Octagonal Pile with f'$_c$ = 6000 psi							
fpc-700	0.00363 (Pile 1)	0.00338	0.00320	0.00305	0.00292	0.00280	0.00269 (Pile 7)
fpc-900	0.00356	0.00335	0.00317	0.00301	0.00288	0.00276	
fpc-1100	0.00348	0.00328	0.00311	0.00298	0.00287	0.00277	
fpc-1200	0.00340	0.00357	0.00310	0.00297	0.00287	0.00276 (Pile 4)	
16-inch Octagonal Pile with f'$_c$ = 8000 psi							
fpc-700	0.00364 (Pile 2)	0.00337	0.00318	0.00302	0.00288	0.00275	
fpc-1000	0.00273	0.00335	0.00316	0.00299	0.00285	0.00273	
fpc-1300	0.00343	0.00344	0.00309	0.00295	0.00282	0.00271	
fpc-1600	0.00334	0.00317	0.00303	0.00291	0.00280	0.0027 (Pile 5)	
16-inch Octagonal Pile with f'$_c$ = 10000 psi							
fpc-700	0.00364 (Pile 3)	0.00336	0.00316	0.00299	0.00284	0.00272	
fpc-1200	0.00348	0.00327	0.00310	0.00295	0.00282	0.00270	
fpc-1600	0.00339	0.00320	0.00304	0.00291	0.00279	0.00268 (Pile 6)	
fpc-2000	0.00333	0.00316	0.00301	0.00288	0.00277		

4.6.1 Sample Analysis

This section provides a sample LPILE analysis of fixed-headed Pile 1 embedded in very stiff clay. The properties of this pile are as follows:

- $f_c^{'}$ = 6000 psi;
- f_{pc} = 700 psi;
- $P_e / f_c^{'} A_g$ = 0.2;
- length = 30 feet;
- moment of inertia = 3952 in.^{4}; and
- modulus of elasticity = 4415 ksi.

The moment versus curvature response of this pile section was obtained using OpenSees, which comprised of 250 data points. This 250 data set was then condensed to approximately 20 data points, which were input in the form of M vs. EI in LPILE. Figure 4.3 plots the complete moment versus curvature response with that based on the condensed number of data points. The comparison between the two curves ensures that the moment-curvature response of the pile was accurately represented in the LPILE analyses.

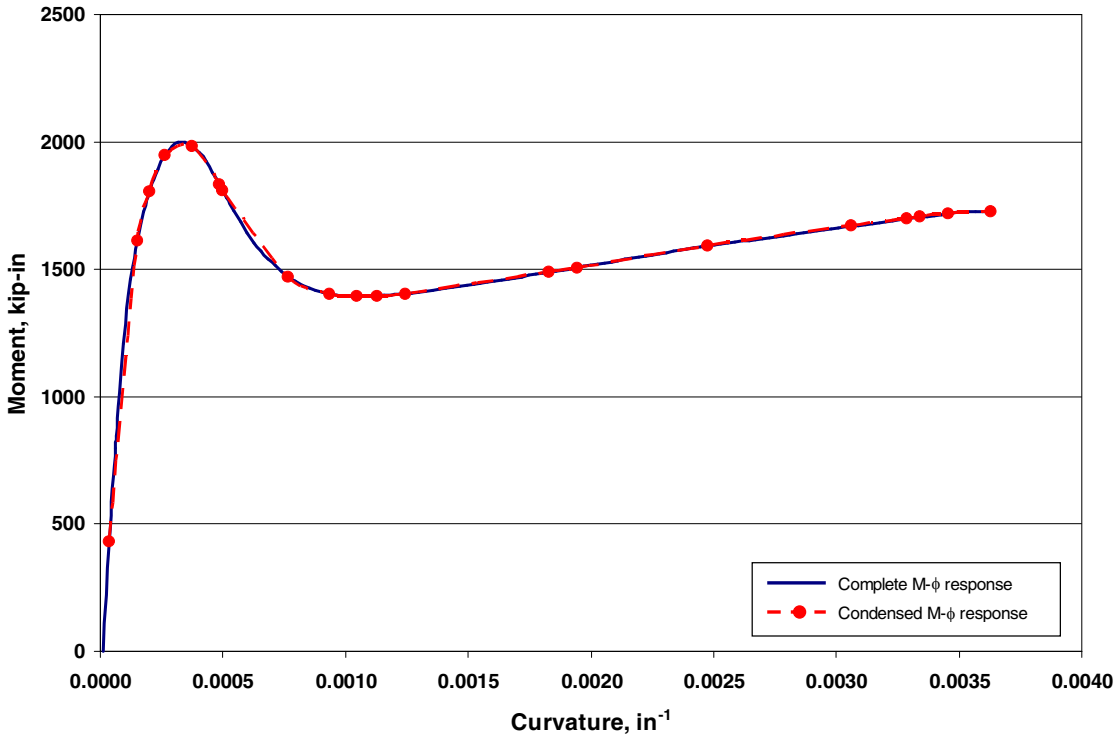

Figure 4.4. Complete moment versus curvature response from OpenSees with the condensed moment versus curvature relationship input in LPILE

Upon entering the pile properties as well as the moment versus curvature relationship, the soil type was defined. The following values were used to compose the very stiff clay:

- $\gamma = 0.0625$ lb/in^3;
- undrained cohesion, $c = 20.83$ lb/in^2; and

- strain factor, $\varepsilon_{50} = 0.004$.

The final step in the analysis was to enter the boundary conditions. Being a fixed head pile, the pile head was maintained at zero slope, while the lateral displacement of the pile at this location was progressively increased. Figure 4.4 depicts the boundary condition input for this particular case, where condition 1 represents the lateral displacement at the pile head, while condition 2 represents the slope at the pile head.

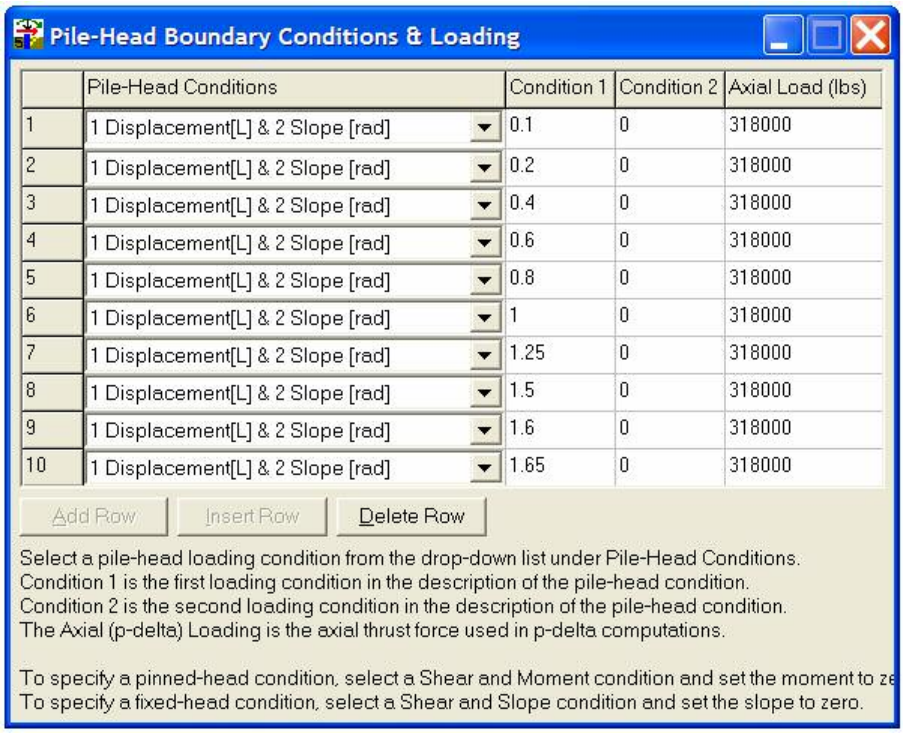

Figure 4.5. Boundary conditions input in LPILE

Once the boundary conditions are entered in LPILE, the execution of the analysis followed. With the completion of running the analysis, LPILE provides an output along the length of the pile for each target lateral displacement. The LPILE output along the pile length includes:

- deflection (in.);

- moment (lbs.-in.);
- shear (lbs.);
- slope (rad.);
- total stress (lbs./in.2);
- flexural rigidity (lbs.-in.2); and
- soil resistance (lbs./in.).

To assure that LPILE was utilizing the moment versus curvature relationship provided as an input to define the pile characteristics, the maximum curvature that the pile sustained was determined at lateral displacement step, and then they were compared with the input data. Figure 4.5 shows this comparison in graphical form, which is satisfactory.

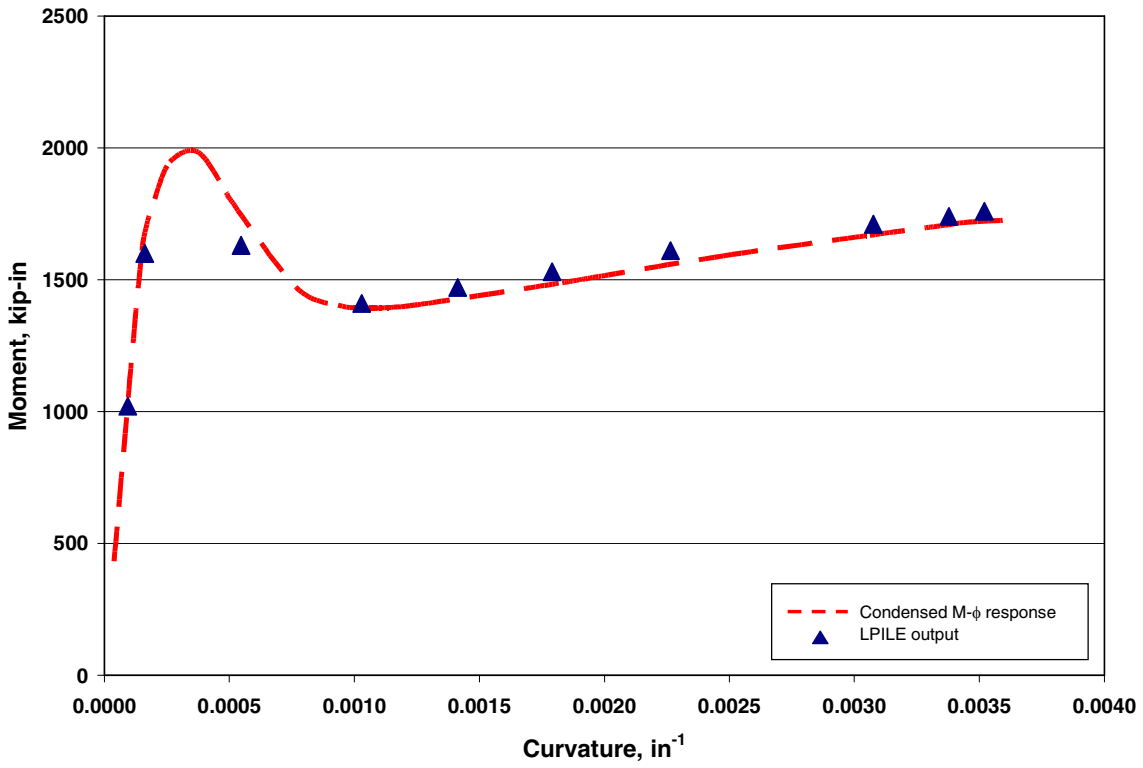

Figure 4.6. Comparison of LPILE output against the moment versus curvature response used as the input in LPILE for Pile 1

The maximum lateral displacement that the 16-inch octagonal pile embedded in very stiff clay was 1.65 inches, attained when the curvature corresponding to the maximum moment reached the ultimate curvature. Figure 4.7 compares the displacement, shear, and moment profiles obtained for this analysis case, at lateral displacements of 0.1 inches and 1.65 inches.

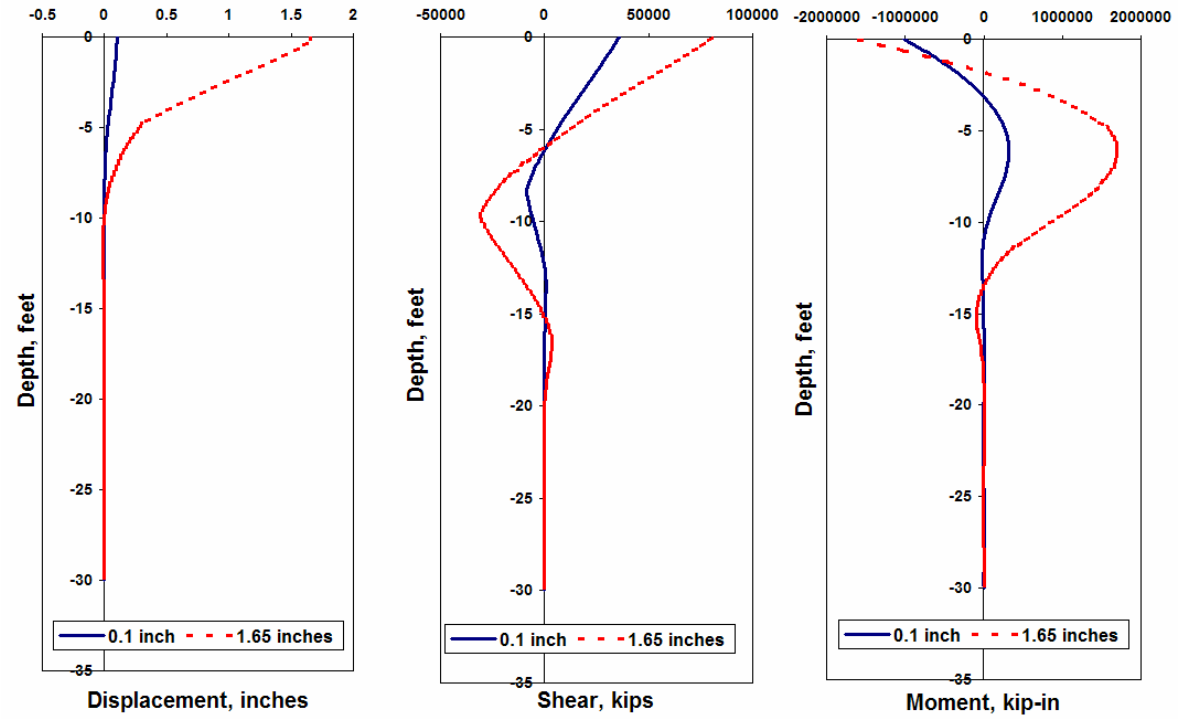

(a) (b) (c)

Figure 4.7 (a) Displacement, (b) Shear, and (c) Moment profiles of a 16-inch octagonal prestressed fixed-head pile in a very stiff clay at a small and ultimate displacements

According to this analysis, this pile should have a permissible displacement limit of 1.65 inches if installed in very stiff clay with a fixed boundary condition at the pile head. If the target displacement for this pile is less than 1.65 inches, the confinement reinforcement can be reduced. Similarly, if a designer chooses a target displacement greater than 1.65 inches,

an appropriate confinement beyond that prescribed in Eq. 3.28 should be provided. In all cases, the target pile displacements should be included when defining the system ductility of the structure as demonstrated in Figure 4.1.

4.6.2 Results

A summary of the results obtained for the LPILE analysis of the seven piles are presented in this section. Table 4.5 provides a summary of the compressive strength of the unconfined concrete, $f_c^{'}$, the compressive stress in the concrete at the centroid of the cross section due to prestress (after losses), f_{pc}, and the axial load ratio used in the LPILE analysis. Tables 4.6, 4.7, and 4.8 provide the permissible displacement limits that were established for each of the piles analyzed with a fixed pile head, pinned pile head, and partially fixed pile head, respectively. Table 4.8 shows a small set of selected piles that were analyzed with a partially fixed head. These were selected simply to ensure that the permissible limits of lateral displacements of the partially fixed head pile were between the lateral displacements established for the fixed pile head and the pinned pile head.

Table 4.5. 16-inch octagonal pile material properties analyzed in LPILE

Pile Number	f'_c (psi)	f_{pc} (psi)	Axial Load Ratio P/f'_cA_g
1	6000	700	0.2
2	8000	700	0.2
3	10000	700	0.2
4	6000	1200	0.45
5	8000	1600	0.45
6	10000	1600	0.45
7	6000	700	0.5

Table 4.6. Permissible displacement limits established for a 16-inch octagonal prestressed pile with a fixed-head condition in different types

Pile Number	Very Dense Sand	Dense Sand	Hard Clay	Very Stiff Clay	Stiff Clay
1	2.1	2.35	1.2	1.65	2.45
2	2	2.2	1.35	1.9	2.6
3	2.1	2.65	1.45	2	2.9
4	1.6	1.85	1	1.4	2
5	2	2.6	1.1	1.6	2.8
6	1.9	2.4	1.1	1.55	2.35
7	1.2	1.4	0.9	1.15	1.6

Table 4.7. Permissible displacement limits established for a 16-inch octagonal prestressed pile with a pinned-head condition in different soil types

Pile Number	Very Dense Sand	Dense Sand	Hard Clay	Very Stiff Clay	Stiff Clay
1	3	4.2	1.75	2.5	2.7
2	3	3	1.8	2.3	3.25
3	3.2	3.25	2	2.9	3.5
4	5	5	3	4	5
5	5	6	3.5	4.25	6
6	4.5	4.75	3.2	4	5.6
7	1.9	1.9	1.25	1.6	2

Table 4.8. Permissible displacement limits established for a 16-inch octagonal prestressed pile with a partially fixed-head condition in different soil types

Pile Number	Very Dense Sand	Dense Sand	Hard Clay	Very Stiff Clay	Stiff Clay
1	2.4	x	x	x	2.7
2	x	2.5	x	x	x
3	x	x	1.75	x	x
4	3	x	x	1.8	x
5	x	3	x	x	4
6	x	x	1.5	x	x
7	x	x	x	1.4	x

From the results presented in Tables 4.6, 4.7, and 4.8, the following observations can be made:

- a pile with a pinned-head will experience a larger lateral displacement at the pile head than that with a fixed-head, while embedded in the same soil type;
- a pile with a partially-fixed-head will experience a lateral displacement at the pile head that is bounded by the lateral displacements experienced by a pinned-head or fixed-head pile;
- the lateral displacements associated with fixed-head or pinned-head piles embedded in clay decreases as the undrained shear strength increases;
- the lateral displacements associated with fixed-head or pinned-head piles embedded in sand decreases as the friction angle, the initial modulus of subgrade reaction, and the effective unit weight increases;
- permissible limits were established for prestressed piles, confined by the newly developed equation, embedded in different soil types. These permissible limits can be summarized as:

- for a fixed-head pile and pinned-head pile embedded in sand, the minimum permissible displacements are 1.2 inches and 0.9 inches, respectively; and
- for a fixed-head pile and pinned-head pile embedded in clay, the minimum permissible displacements are 1.9 inches and 1.25 inches, respectively.

CHAPTER 5. SUMMARY, CONCLUSIONS AND RECOMMENDATIONS

5.1 Introduction

The research of the development of rational design methodology for spiral reinforcement in prestressed concrete piles in regions of high seismicity was motivated by the lack of conformity among various US codes and specifications regarding the requirements for spiral reinforcement in potential plastic hinge regions. Though there are several design equations available, none are satisfactorily applicable to designing confinement reinforcement for prestressed concrete piles. Thus, the objective of this research was to develop a simple design equation that will determine the minimum quantity of Grade 60 spiral reinforcement necessary to achieve a minimum target ductility over a given range of axial loads in prestressed concrete piles. The sections to follow provide a summary of the completed work, conclusions of the project, as well as recommendations that have developed throughout the analysis of the project.

5.2 Summary

The project began with an overall introduction of pile types, narrowing in on precast, prestressed concrete piles. Specific details were provided for the seismic design approach for piles supporting bridges, buildings, and wharfs in high seismic regions. Several codes were investigated and the scope of research was defined.

An extensive literature review was completed, aiming to gain knowledge of the curvature ductility demands expected for precast, prestressed piles. The currently adopted seismic design practice for precast, prestressed concrete piles was discussed. Previous analytical work and case studies were investigated in order to quantify the maximum possible curvature demand and/or capacity for different soil and boundary conditions. The transverse reinforcement requirements from several codes and standards were considered in this study and were discussed in detail.

A rationale approach for designing transverse reinforcement for confinement purposes was developed. The definition of yield, nominal, and ultimate conditions for precast, prestressed piles were presented. A design equation, known as the ISU equation, was developed and analytically tested with over 200 moment-curvature analyses. The finalized developed ISU equation is presented below.

LPILE analyses were performed to establish permissible limits on the lateral displacement of precast, prestressed piles in different soil conditions prior to reaching the curvature capacity of piles that used the confinement reinforcement as per the ISU equation. A design process that connects the lateral displacements of piles to the required amount of transverse reinforcement was developed and presented.

5.3 Conclusions

The following conclusions were drawn based on the completed study, presented in this report:

- An upper bound curvature demand of 0.00152 $in.^{-1}$ was established through the literature review.

- Though several equations exist for quantifying the volumetric ratio of transverse reinforcement, there is no agreement between the equations in computing the amount of transverse reinforcement necessary for a given axial load.
- To simplify the design of precast, prestressed piles, guidelines to idealize actual moment-curvature responses for these piles were developed. These guidelines are useful, as no guidelines for the idealization of moment-curvature responses of precast, prestressed piles existed prior to the commencement of this project and can be summarized as:
  - First yield moment: determined to occur at ec = 0.002 in./in.
  - Nominal moment: average of largest moment and smallest moment after first yield moment occurs
  - Ultimate moment: first occurrence of 1) 80% of the ultimate capacity, 2) ultimate strain in the strand of 0.004 in./in., or 3) ultimate strain in the concrete as defined by Eq. 2.4.
- The newly developed equation for the volumetric ratio of transverse reinforcement provides an ultimate curvature capacity of at least 0.00194, approximately 27% greater than the curvature demands established from the literature review.
- The newly developed equation for the volumetric ratio of transverse reinforcement contains a curvature ductility demand term that ensures a curvature ductility capacity of the value selected for μ_ϕ.
- Axial load ratios should be limited to 0.4 for a 16-inch octagonal pile, 0.45 for a 24-inch octagonal pile, and 0.2 for a 14-inch square pile. Axial load ratios that are

higher than these may result in additional piles required to support the superstructure loads.

- The moment-curvature relationship developed in this study for piles embedded in different soil types provide a useful tool for the designer, while accounting for the non-linear behavior of precast, prestressed concrete piles. The non-linear behavior has not been considered in previous published design methodologies.
- The permissible limits on the lateral displacement for a fixed-head pile and pinned-head pile, embedded in sand, ranges from 1.2 inches to 2.65 inches and 1.9 inches to 6 inches, respectively.
- For a fixed-head pile and pinned-head pile, embedded in clay, the permissible limits on the lateral displacement ranges from 0.9 inches to 2.9 inches and 1.25 inches to 6 inches, respectively.
- The upper limit of 6 inches for a pinned-head pile embedded in sand and clay, respectively, seems excessive. Therefore, the designer must consider serviceability limits in these cases.

5.4 Recommendations

Through the duration of this project, significant discrepancies were noticed between the several available equations for determining the volumetric ratio of transverse reinforcement in relation to precast, prestressed piles. This motivated the author to develop an equation specifically for the transverse reinforcement in precast, prestressed piles. The newly developed equation calculates the volumetric ratio of transverse reinforcement that is required for a specific curvature ductility capacity. This equation was confirmed through

analytical techniques. Through the performed analyses, the following recommendations are established:

- to gain more confidence in the developed equation, laboratory testing and experimental field testing are required;
- the strength drop in the square section is of concern as it is a widely used section in the precast, prestressed pile industry. Therefore, it is recommended that the square pile be investigated further;
- octagonal piles subjected to axial load ratios higher than 0.4 can be examined, as well as square piles subjected to axial load ratios higher than 0.2; and
- piles embedded into different soil conditions can be studied to establish other permissible limits.

REFERENCES

ACI Committee 318. *Building Code Requirements for Structural Concrete (ACI 318-05) and Commentary (318R-05)*, American Concrete Institute, Farmington Hills, Michigan, 2005.

American Association of State Highway and Transportation Officials. *AASHTO LRFD Bridge Design Specifications,* American Association of State Highway and Transportation Officials, Washington, D.C., Third Edition, 2004.

American Petroleum Institute. *Recommended Practice for Planning, Designing and Constructing Fixed Offshore Platforms, API Recommended Practice 2A (RP 2A)*, American Petroleum Institute, Seventeenth Edition, April 1, 1987.

American Society of Civil Engineers. *ASCE-7 Minimum Design Loads for Buildings and Other Structures*. American Society of Civil Engineers, 2005.

Arulmoli, Arul. Earth Mechanics, Inc. Consultation Interview. 2006-2007.

ATC-3-06, *Tentative Provisions for the Development of Seismic Regulations for Buildings,* Applied Technology Council, Redwood City, California, 1978.

ATC-32, *Improved Seismic Design Criteria for California Bridges: Provisional Recommendations*, Applied Technology Council, Redwood City, California, 1996.

Banerjee, S., F. Stanton, and N. Hawkins. "Seismic Performance of Precast Prestressed Concrete Piles," *Journal of Structural Engineering*, ASCE, V. 113, No. 2, February, 1987, pp. 381-396.

Birdy, J. and L. Dodd. "Design of Wharves for Seismic Regions," *Concrete International*, Farmington Hills, Michigan: American Concrete Institute, 1999, pp. 28-32.

Bowles, J. E. *Foundation Analysis and Design*, New York: The McGraw-Hill Companies, Inc., 1996.

Building Center of Japan. *The Building Standard Law of Japan*. Building Center of Japan, Japan, 2004.

California Department of Transportation. *CALTRANS Seismic Design Criteria*. California Department of Transportation, California, 2006.

Canadian Standard Association. *Canadian Highway Bridge Design Code*. Canadian Standard Association, Canada, 1998.

Das, B. M. *Principles of Foundation Engineering*. California: Thomson Brooks/Cole, 2004.

Dowell, R. K., 2002. *ANDRIANNA: Moment-Curvature Analysis of Reinforced and Prestressed Concrete Structures for Any General Section—User's Guide*, Dowell-Holombo Engineering, Inc., San Diego, CA.

Ensoft, Inc. *LPILE Plus 5.0*. Ensoft, Inc., 2004.

Fanous, A., S. Sritharan, M. Suleiman, and A. Arulmoli. "Development of Rational Design Methodology for Spiral Reinforcement in Prestressed Concrete Piles in Regions of High Seismicity," *Not yet published*, Expected publication 2007.

ICC, *International Building Code*, International Code Council, Falls Church, Virginia, 2000.

ICC. *Uniform Building Code (International Building Code)*, International Code Council, Falls Church Virginia. 1997.

Japan Road Association. *Specifications for Highway Bridges*. Japan Road Association, Japan, 1996.

Joen, Pam H. and Park, R., "Flexural Strength and Ductility Analysis of Spirally Reinforced Prestressed Concrete Piles," *PCI Journal*, V. 35, No. 4, July-August 1990, pp 64-83.

Joen, Pam H. and Park, R., "Simulated Seismic Load Tests on Prestressed Concrete Piles and Pile-Pile Cap Connections," *PCI Journal*, V. 35, No. 6, November-December 1990, pp 42-61.

Koyamada, K., Y. Miyamoto, and K. Tokimatsu. "Field Investigation and Analysis Study of Damaged Pile Foundation During the 2003 Tokachi-Oki Earthquake," *Proceedings of Seismic Performance and Simulation of Pile Foundations in Liquefied and Laterally Spreading Ground*, GSP, No. 145, March 2005, pp. 97-108.

Lin, S., Y. Tseng, C. Chiang, and C. Hung. "Damage of Piles Caused by Lateral Spreading – Back Study of Three Cases," *Proceedings of Seismic Performance and Simulation of Pile Foundations in Liquefied and Laterally Spreading Ground*, Davis, California, 2005, pp.121-133.

Mander, J.B., M.J.N. Priestley, and R. Park, "Observed Stress-Strain Behavior of Confined Concrete," *Journal of the Structural Division,* ASCE, Vol. 114, No. 8, August 1988, pp. 1827-1849.

Chang, G.A., and Mander, J.B., "Seismic Energy Based Fatigue Damage Analysis of Bridge Columns: Part 1 –Evaluation of Seismic Capacity," *NCEER Technical Report* No. NCEER-94-0006, State University of New York, Buffalo, N.Y., 1994.

Margason, E., "Earthquake Effects on Embedded Pile Foundations," Pile Talk Seminar, San Francisco, Calif., Mar., 1977. Also, Margason, E., and Holloway, D.M., "Pile Bending During Earthquakes," *Proceedings 6th World Conference on Earthquake Engineering*, Vol. 4, New Delhi, India, 1977, pp. 233.

Marine Facilities Division. *MOTEMS*. Marine Oil Terminal Engineering and Maintenance Standards. California, 2006.

Matlock, H. "Correlations for Design of Laterally Loaded Piles in Soft Clay," *Proceedings*, Offshore Technology Conference, Vol. I, No. 1204, April 1970, pp. 577-594.

Mazzoni, S., F. McKenna, M.H. Scott, and G.L. Fenves. "Open System for Earthquake Engineering Simulation," *Pacific Earthquake Engineering Research Center*, University of California, Berkeley California, Ver. 1.6., 2004.

Meyersohn, W.D. *Pile Response to Liquefaction-Induced Lateral Spread*. Doctorate Dissertation, Cornell University, NY, USA, 1994.

Naaman, A. *Prestressed Concrete Analysis and Design*. Michigan: Techno Press 3000, 2004.

NBCC. *National Building Code of Canada 2005*, Institute for Research in Construction, National Research Council of Canada, Ottawa, Ont., 2005.

NBCC. *User's Guide – Structural Commentaries (Part 4 of Division B) – NBC 2005*, National Research Council of Canada, Ottawa, Ont., 2005.

NZS 3101 – *The Design of Concrete Structures – Part 1: Practice* and *The Design of Concrete Structures –Part 2: Commentary*, Standards Association of New Zealand, Wellington, New Zealand, 1982.

NZS 3101 – *The Design of Concrete Structures – Part 1: Practice* and *The Design of Concrete Structures –Part 2: Commentary*, Standards Association of New Zealand, Wellington, New Zealand, 1995 with Amendments through 1998.

NZS 3101 – *The Design of Concrete Structures – Part 1: Practice* and *The Design of Concrete Structures –Part 2: Commentary*, Standards Association of New Zealand, Wellington, New Zealand, 2006.

Park, R. and Falconer, T.J., "Ductility of Prestressed Concrete Piles Subjected to Simulated Seismic Loading," *PCI Journal*, V. 28, No. 5, September-October 1983, pp. 112-144.

Paulay, T. and Priestley M. J. N. *Seismic Design of Reinforced Concrete and Masonry Buildings*, New York: John Wiley & Sons, 1992.

PCI Committee on Prestressed Concrete Piling, "Recommended Practice for Design, Manufacture and Installation of Prestressed Concrete Piling," *PCI Journal*, V. 38, No. 2, March-April 1993, pp. 64-83.

PCI Industry Handbook Committee, *PCI Design Handbook*. Precast/Prestressed Concrete Institute, Chicago, Illinois, 5th Edition, 1999.

Port of Los Angeles. Code for Seismic Design, Upgrade, and Repair of Container Wharves." *POLA Code*. Los Angeles, California, 2004.

Portland Cement Association. *Notes on ACI 318-05 Building Code Requirements for Structural Concrete*. Skokie, Illinois: Portland Cement Association, 2005.

Prakash, S. and H. Sharma. *Pile Foundations in Engineering Practice*. New York: John Wiley & Sons, 1990.

Priestley, M.J.N., Park, R., and Potangaroa, R.T., "Ductility of Spirally-Confined Concrete Columns," *Journal of Structural Division*, Proceedings ASCE, V. 107, No. ST1, January 1981, pp. 181-202.

Priestley, M.J.N.; Seible, F.; and Calvi, M. *Seismic Design and Retrofit of Bridges*, New York: John Wiley & Sons, 1996.

Priestley, M.J.N., Seible, F., and Chai, Y.H., "Design Guidelines for Assessment Retrofit and Repair of Bridges for Seismic Performance," University of California, San Diego, August, 1992.

Reese, L., W. Cox. and F. Koop, "Analysis of Laterally Loaded Piles in Sand," *Proceedings to the 5th Annual Offshore Technology Conference.*, No. OTC 2080, 1975, pp. 473–485.

Reese, L., "Analysis of Piles in Weak Rock," *Journal of the Geotechnical and Geoenvironmental Engineering Division*, ASCE, Vol. 123, no. 11, Nov. 1997, pp. 1010-1017.

Rollins, K., T. Gerber, J. Lane, and S. Ashford, "Lateral Resistance of a Full-Scale Pile Group in Liquefied Sand," *submitted to Journal of the Geotechnical and Geoenvironmental Engineering Division*, American Society of Civil Engineers, 2003 (under review).

Sheppard, D.A., "Seismic Design of Prestressed Concrete Piling," *PCI Journal*, V. 28, No. 2, March-April, 1983, pp. 20-49

Song, S., Chai, Y., and Hale, T. "Limit State Analysis of Fixed-Head Concrete Piles under Lateral Load," *Proceedings 13th World Conference on Earthquake Engineering*, WCEE Paper No. 971, August, 2004.

South Carolina Department of Transportation. *SCDOT Seismic Design Specifications*. South Carolina Department of Transportation, 2006.

Tomlinson, M.J. *Pile Design and Construction Practice*. London: E & FN Spon, 1994.

Watson, S., Zahn, F.A., and Park, R.. "Confining Reinforcement for Concrete Columns," *Journal of Structural Engineering*, ASCE, V. 120, No. 6, June, 1994, pp. 1798-1823.

Waugh, Jon. Ph.D. Dissertation, Iowa State University, *in progress*. 2007.

APPENDIX A. DEFINITION OF AN ORDINARY BRIDGE

A.1 Caltrans (2001)

The Seismic Design Criteria (SDC) published by the California Department of Transportation (Caltrans), defines an ordinary standard bridge as a bridge that is required to meet all of the following requirements:

- span length less than 300 feet;
- constructed with normal weight concrete girder, and column or pier elements;
- horizontal members are either rigidly connected, pin connected, or supported on conventional bearings on the substructure. (Isolation bearings and dampers are considered nonstandard components);
- dropped bent caps or integral bent caps terminating inside the exterior girder, C-bents, outrigger bents, and offset columns are nonstandard components;
- foundations supported on spread footing, pile cap with piles, or pile shafts; and
- soil that is not susceptible to liquefaction, lateral spreading, or scour.

The components of an ordinary standard bridge consist of a superstructure and a substructure, the latter of which includes the foundations and abutments.

A.2 South Carolina DOT (2001)

The South Carolina DOT (SCDOT, 2001) Seismic Design Specifications include minimum requirements for the selection of an analysis method that are determined by the "regularity" of the bridge. The "regularity" of a bridge is a function of the number of spans and the distribution of weight and stiffness. Regular bridges in South Carolina are defined as

Having less than seven spans, no abrupt or unusual changes in weight, stiffness, or geometry, and no larger changes in these parameters from span-to-span or support-to-support.

A.3 Washington State

In the state of Washington, the seismic design criteria adhere to the AASHTO LRFD Bridge Design Specifications (AASHTO, 2004). For precast, prestressed piles in high seismic activity, the foundation should be designed in accordance with Section 5.13.4.4 of the AASHTO Specifications. Regardless of the pile cross section, the minimum pile dimensions must abide by the following standards:

- when the pile foundation is not exposed to salt water, the gross-sectional area must not be less than 140 in^2; and
- when the pile foundation is exposed to salt water the gross-sectional area increases to 220 in^2.

For both instances, the concrete compressive strength shall not be less than 5.0 ksi. The prestressing strands within a precast, prestressed pile foundation should be spaced and stressed in order to provide a uniform compressive stress of 0.7 ksi or greater on the cross-section of the pile after all losses have occurred.

APPENDIX B. SPECIFICATIONS REGARDING STRUCTURE'S CAPABILITIES IN SPECIFIC SEISMIC RISK LEVELS

B.1 ACI 318 Building Code (2005)

In the ACI code, seismic risk levels are defined as low, moderate, and high. The code respectively provides specifications regarding these risk levels such that the structures will:

1. resist earthquakes of minor intensity without damage – a structure would be expected to resist such frequent but minor shocks within its elastic range of stresses;
2. resist moderate earthquakes with negligible structural damage and some nonstructural damage – with proper design and construction, it is expected that structural damage due to the majority of earthquakes will be repairable; and
3. resist major catastrophic earthquakes without collapse – some structural and nonstructural damage is expected.

B.2 ASCE 7 (2005)

The ASCE 7 includes basic requirements for the design of building structures in high seismic regions. These requirements begin with an inclusive statement of the structure's capabilities within high seismic regions: "*the building structure shall include complete lateral and vertical force-resisting systems capable of providing adequate strength, stiffness,*

and energy dissipation capacity to withstand the design ground motions within the prescribed limits of deformation and strength demand" (ASCE 7, 2005).

APPENDIX C SAMPLE OPENSEES INPUT

C.1 Sample Input for a 16-Inch Octagonal Pile

OpenSees is the program that was selected for the completion of the moment-curvature responses pertaining to this project. In this Appendix, a sample of the input for OpenSees is provided. The input on the following pages is for a 16-inch octagonal section with the following properties:

- $f_c^{'}$ = 10,000 psi
- f_{pc} = 1600 psi
- $\frac{P_e}{f_c^{'} A_g}$ = 0.45

```
set 1y 0.00
set 1z 5.8125
set 2y 2.2243
set 2z 5.37
set 3y 3.3137
set 3z 8.00
set 4y 0.00
set 4z 8.00
set 5y 4.1101
set 5z 4.1101
set 6y 5.37
set 6z 2.2243
set 7y 8.00
set 7z 3.3137
set 8y 5.6569
set 8z 5.6569
set 9y 5.8125
set 9z 0.00
set 10y 5.37
set 10z -2.2243
set 11y 8.00
set 11z -3.3137
set 12y 8.00
set 12z 0.00
set 13y 4.1101
set 13z -4.1101
set 14y 2.2243
set 14z -5.37
set 15y 3.3137
set 15z -8.00
set 16y 5.6569
set 16z -5.6569
set 17y 0.00
set 17z -5.8125
set 18y -2.2243
set 18z -5.37
set 19y -3.3137
set 19z -8.00
set 20y 0.00
```

```
set 20z -8.00
set 21y -4.1101
set 21z -4.1101
set 22y -5.37
set 22z -2.2243
set 23y -8.00
set 23z -3.3137
set 24y -5.6569
set 24z -5.6569
set 25y -5.8125
set 25z 0.00
set 26y -5.37
set 26z 2.2243
set 27y -8.00
set 27z 3.3137
set 28y -8.00
set 28z 0.00
set 29y -4.1101
set 29z 4.1101
set 30y -2.2243
set 30z 5.37
set 31y -3.3137
set 31z 8.00
set 32y -5.6569
set 32z 5.6569

# ---------------- #
# Model Definition

model basic -ndm 2 -ndf 3

# Create Nodes for model
node 1 0.0 0.0
node 2 0.0 0.0

# Apply Boundary Conditions
fix 1 1 1 1
fix 2 0 1 0
```

```
# Create Material Models for analysis of sections
# Confined concrete material models
uniaxialMaterial Concrete06 1 -16.567 -0.010709 7069.544 .75 .000256 2 30 1.909

# Unconfined concrete maerial model
uniaxialMaterial Concrete06 2 -10.00 -0.0025 5850.214 .75 .000256 2 2.3 11.43

## Prestressing steel material model.
uniaxialMaterial ElasticPP 3 28000 0.00850 -0.00850 -.00714
uniaxialMaterial ElasticPPGap 4 700 1000 .00136
uniaxialMaterial Parallel 5 3 4

section Fiber 1 {
      # Confined Concrete Fibers
      patch circ 1 122 20 0.00 0.00 0.00 5.8125 0 360

      # Unconfined Concrete FIbers
      patch quad 2 8 10 $1y $1z $2y $2z $3y $3z $4y $4z
      patch quad 2 8 10 $2y $2z $5y $5z $8y $8z $3y $3z
      patch quad 2 8 10 $5y $5z $6y $6z $7y $7z $8y $8z
      patch quad 2 8 10 $6y $6z $9y $9z $12y $12z $7y $7z
      patch quad 2 8 10 $9y $9z $10y $10z $11y $11z $12y $12z
      patch quad 2 8 10 $10y $10z $13y $13z $16y $16z $11y $11z
      patch quad 2 8 10 $13y $13z $14y $14z $15y $15z $16y $16z
      patch quad 2 8 10 $14y $14z $17y $17z $20y $20z $15y $15z
      patch quad 2 8 10 $17y $17z $18y $18z $19y $19z $20y $20z
      patch quad 2 8 10 $18y $18z $21y $21z $24y $24z $19y $19z
      patch quad 2 8 10 $21y $21z $22y $22z $23y $23z $24y $24z
      patch quad 2 8 10 $22y $22z $25y $25z $28y $28z $23y $23z
      patch quad 2 8 10 $25y $25z $26y $26z $27y $27z $28y $28z
      patch quad 2 8 10 $26y $26z $29y $29z $32y $32z $27y $27z
      patch quad 2 8 10 $29y $29z $30y $30z $31y $31z $32y $32z
      patch quad 2 8 10 $30y $30z $1y $1z $4y $4z $31y $31z

      # Prestress strand fibers
      layer circ 5 12 .153 0.0 0.0 5.375 0 360}


# Define element
```

```
element zeroLengthSection 1 1 2 1

# Create recorder
recorder Node -file Annie.out -time -node 2 -dof 3 disp
recorder Element -file StrandStrain.out -time -ele 1 section fiber -5.375 0.00 5 stressStrain
recorder Element -file ConcStrain1.out -time -ele 1 section fiber 8.0 0 2 stressStrain
recorder Element -file ConcStrain2.out -time -ele 1 section fiber 0.0 0.0 1 stressStrain
recorder Element -file ConcStrain3.out -time -ele 1 section fiber -8.0 0 2 stressStrain
recorder Element -file Forces.out -time -ele 1 section force

# Define constant axial load
set LR 0.00;#0.65
set GA 212
set fc -10.00
set P -954;#[expr $LR*$GA*$fc]
pattern Plain 1 "Constant" {
 load 2 $P 0.0 0.0
}

# Define analysis parameters
integrator LoadControl 0 1 0 0
system SparseGeneral -piv
test NormDispIncr 1.0e-8 100 0
numberer Plain
constraints Plain
algorithm KrylovNewton
analysis Static

# Do one analysis for constant axial load
analyze 1

# Define reference moment
pattern Plain 2 "Linear" {
 load 2 0.0 0.0 1.0
}

# Maximum curvature
set maxK .007
set numIncr 250
```

```
set dK [expr $maxK/$numIncr]

# Use displacement control at node 2 for section analysis
integrator DisplacementControl 2 3 $dK

# Perform the section analysis
analyze $numIn
```

ACKNOWLEDGEMENTS

The research described herein was completed due to the combined efforts of Iowa State University Civil, Construction, and Environmental Engineering (CCEE) department, PCI, the members of the PCI Advisory Committee, and Arul Arulmoli.

The author would first and foremost like to thank her Lord and Savior, Jesus Christ. She has learned what it means to truly depend on Him in all things and has learned time and time again the meaning behind Philippians 4:13, "I can do all things through Christ who gives me strength." The author is grateful for the constant reminder from Isaiah 40:31, "but those who hope in the LORD will renew their strength. They will soar on wings like eagles; they will run and not grow weary, they will walk and not be faint."

The author would like to recognize Dr. Sri Sritharan and Dr. Muhannad Suleiman for the opportunity to work on this project. Their commitment to the success of this project was greatly appreciated.

The author would like to thank her parents, sister, brother, and friends for their prayers and support through the duration of this project. The author is blessed to be surrounded by such an amazing group of prayer warriors and knows that this experience is one that will always be remembered.